Title
Evaluation And Analysis Of Automated Highway System Concepts And Architectures

Author
Ioannou, Petros

Publication Date
1998

CALIFORNIA PATH PROGRAM
INSTITUTE OF TRANSPORTATION STUDIES
UNIVERSITY OF CALIFORNIA, BERKELEY

Evaluation and Analysis of Automated Highway System Concepts and Architectures

Petros Ioannou
University of Southern California

California PATH Research Report
UCB-ITS-PRR-98-12

This work was performed as part of the California PATH Program of the University of California, in cooperation with the State of California Business, Transportation, and Housing Agency, Department of Transportation; and the United States Department of Transportation, Federal Highway Administration.

Report for MOU 235

March 1998

ISSN 1055-1425

Abstract

This is the final report for the project entitled "Evaluation and Analysis of Automated Highway System Concepts and Architectures" in response to the contractual requirements of the Memorandum of Understanding MOU# 235, between the Partners of Advanced Transit and Highways (PATH) and the University of Southern California, administered at the University of California at Berkeley.

The purpose of this project was to select, evaluate and analyze a number of promising Automated Highway System (AHS) operational concepts based on previous work. The evaluation and analysis includes headway distributions for vehicle following and lane changing, capacity calculations and the modeling, analysis and control of the resulting traffic flow. The design, analysis and simulation parts of the project were performed at the Center of Advanced Transportation Technologies at the University of Southern California. The work performed under this project is presented in the form of five reports presented in part I, II, III, IV, and V of this final report. In addition to these reports floppy disks containing the "Inter Vehicle Spacing Software Tool" is included.

Keywords: Automated Highway Systems, Vehicle Following, Vehicle Spacing, Highway Capacity, Highway Safety, Accident Avoidance, Collision Avoidance, Braking Scenarios, Brake Performance, Lane Changing, Merging, Macroscopic Models, Traffic Flow, Hybrid Systems, Roadway Controller.

Executive Summary

This is the final report for the project entitled "Evaluation and Analysis of Automated Highway System Concepts and Architectures" in response to the contractual requirements of the Memorandum of Understanding MOU# 235, between the Partners of Advanced Transit and Highways (PATH) and the University of Southern California, administered at the University of California at Berkeley.

The purpose of this project was to select, evaluate and analyze a number of promising Automated Highway System (AHS) operational concepts based on previous work. The evaluation and analysis includes headway distributions for vehicle following and lane changing, capacity calculations and the modeling, analysis and control of the resulting traffic flow. The design, analysis and simulation parts of the project were performed at the Center of Advanced Transportation Technologies at the University of Southern California. The work performed under this project is presented in the form of five reports presented in part I, II, III, IV, and V of this final report. In addition to these reports floppy disks containing the "Inter Vehicle Spacing Software Tool" is included.

In part I entitled "Spacing and Capacity Evaluations for different AHS Concepts" six different AHS operational concepts are identified and discussed. For each particular AHS operating concept we calculate the minimum safety intervehicle spacing that could be applied in order to achieve collision-free longitudinal vehicle following under different road conditions. In addition to collision-free environments, for AHS architectures involving platoons, we also apply the alternative constraint of bounded energy collisions to calculate the minimum spacing that could be applied if wanted to allow collisions at a specific limit of relative velocity. In every case, the minimum spacing is used to calculate the maximum achievable capacity for each operational concept, thus opening the way for safety, risk, cost and performance tradeoff analysis of different AHS concepts.

Part II of this report entitled "Inter Vehicle Spacing: User's Manual" is the User's Manual for the Inter Vehicle Spacing (IVS) software tool. The IVS software tool is a user friendly interactive interface which, by using the analysis presented in part I of this report, allows the user to perform the

following:

- Calculate the minimum initial spacing between two vehicles (moving in the longitudinal direction) with specified deceleration profiles, initial velocities, friction coefficient between the tires and the road and reaction times such that no collision will occur and/or for collisions to occur with a relative speed less than a given bound.

- Calculate the possibility and severity of collision between two vehicles, given their initial intervehicle spacing and deceleration profiles, friction coefficients and reaction times.

- Visualize the motion of the two vehicles in the longitudinal direction during braking maneuvers for different deceleration profiles and initial intervehicle spacing.

- Calculate the highway capacity given the velocity, intervehicle spacing, interplatoon spacing, vehicle size and platoon size.

Using the IVS software tool, we can easily evaluate the performance and limitations of any AHS operational concept and obtain results that can be useful in ranking the relative merits of the different candidate AHS operational concepts.

In part III entitled "Strategies and Spacing Requirements for Lane Changing and Merging in Automated Highway Systems", we extend the results obtained for the pure longitudinal case in parts I and II to the case where the vehicles are allowed to perform lane changing and merging maneuvers. Similarly to part I, we analyze the problem of minimum spacing for collision-free merging and lane changing. We examine various alternative scenaria for merging and lane changing and we present an algorithm for calculating the *Minimum Safety Spacing for Lane Changing (MSSLC)*, that is, we calculate the spacings that the vehicles should have during a merging or lane changing maneuver so that, in the case where one of the vehicles enters in an emergency braking maneuver, the rest of the vehicles have enough time and space to stop without any collision taking place. The calculation of the MSSLC's for merging or lane changing maneuver is more complicated than the calculation of the Minimum Safety Spacing for longitudinal vehicle following, since, in the former case we have to take into account the particular

lane changing policy of the merging vehicle as well as the effect of combined lateral/longitudinal motion during the lane changing maneuver. The braking profiles of the vehicles involved in an emergency scenario during lane changing maneuver depend on the particular AHS operational concept, i.e., on the degree of communication between the vehicles and between the vehicles and the infrastructure. We consider six different AHS operational concepts; we present the braking profiles of the vehicles for each operational concept and we investigate the effects of the particular operational concept to the MSSLC.

While part I, II, III of the report concentrate on the microscopic aspect of calculating the minimum safety intervehicle spacing, part IV and V deal with the macrospopic aspect of the system. In part IV entitled "Macroscopic Modeling and Analysis of Traffic Flow of Automated Vehicles" a macroscopic traffic flow model of automated vehicles is developed by using the microscopic control laws that govern the longitudinal motion of individual vehicles together with the dynamics of the interconnection with other vehicles. The model is a very general one and is applicable to a wide range of concepts associated with automated highway systems (AHS). The developed model is used to analyze the steady state behavior of traffic flow for different operating conditions. The analysis indicates that some of the proposed modes of AHS which operate without a traffic flow controller may not be effective in avoiding traffic congestion problems resulting from traffic flow disturbances. The model also predicts the existence of shock waves in extreme cases for the same modes of AHS. The results of this analysis can be used as guidelines for designing macroscopic as well as microscopic control laws.

The analysis of the macroscopic model of automated traffic flow in part IV, indicates that there are operating conditions in which such a system can end up in undesirable steady states and that these undesirable effects can be sufficiently attenuated by introducing some kind of cooperation between vehicles. This analysis strongly suggests the presence of a high level controller, called roadway controller, to provide the necessary coordination between the automated vehicles. In part V of the report entitled "Roadway Controller Design using Spatio-Temporal Control Technique" the design of a roadway controller is presented to guarantee global asymptotic convergence of the system states to the desired ones. The design is based on a spatio-temporal control (STC) technique. This particular choice is dictated by the macro-

scopic traffic flow model, which describes its states in spatial and temporal coordinates. The control input is derived by feedback linearizing the model with the help of a two dimensional virtual control inputs. The actual control input is obtained in the second step by inverting the dynamics related between the virtual and actual control input. The control design guarantees closed loop stability and achieves the desired performance.

SPACING AND CAPACITY EVALUATIONS FOR DIFFERENT AHS CONCEPTS

Alexander Kanaris, Petros Ioannou, Fu-Sheng Ho

Center for Advanced Transportation Technologies
University of Southern California
3740 McClintock Ave. EEB-200
Los Angeles, CA 90089 - 2562

ABSTRACT

In Automated Highway Systems (AHS), vehicles will be able to follow each other automatically by using their own sensing and control systems, effectively reducing the role of the human driver in the operation of the vehicle. Such systems are therefore capable of reducing one source of error, human error, that diminishes the potential capacity of the highways and in the worst case becomes the cause of accidents. The inter-vehicle separation during vehicle following is one of the most critical parameters of the AHS system, as it affects both safety and highway capacity. To achieve the goal of improved highway capacity, the inter-vehicle separation should be as small as possible. On the other hand, to achieve the goal of improved safety and elimination of rear end collisions, the inter-vehicle separation should be large enough that even under a worst case stopping scenario, no vehicle collisions will take place. These two requirements demand diametrically opposing solutions and they have to be traded off. Since safety cannot be compromised for the sake of capacity, it becomes a serious constraint in most AHS design decisions. The trade-off between capacity and safety gives rise to a variety of different AHS concepts and architectures.

In this study we consider a family of six AHS operational concepts. For each concept we calculate the minimum inter-vehicle spacing that could be used for collision-free vehicle following, under different road conditions. For architectures involving platoons we also use the alternative constraint of bounded energy collisions to calculate the minimum spacing that can be applied if we allowed collisions at a limited relative velocity in case of emergency stopping. The minimum spacing is used to calculate the maximum possible capacity that could be achieved for each operational concept.

1 INTRODUCTION

Urban highways in many major cities are congested and need additional capacity. Historically, capacity has been added by building additional lanes and new highways. Scarcity of land and escalating construction costs make it increasingly difficult to add capacity this way. One possible way to improve capacity is to use current highways more efficiently. The concept of Automated Highway Systems (AHS) was introduced to improve the capacity of the current transportation systems by using automation and intelligence.

Highway capacity depends on two variables: The velocity of the vehicles and the distance between them. Clearly, the higher the velocity of the vehicles, the higher the number of vehicles per lane per hour will be. But the vehicles need to maintain a certain amount of "safety distance" between them, to accommodate for the case that the flow of vehicles has to be slowed down or stopped, by applying the brakes. The moment that each vehicle starts applying its brakes typically involves a couple of seconds of delay in relation to the onset of braking of the vehicle in front, due to the fact that the human drivers need some time to process the information they perceive [22], plus an additional time delay to react and a delay for the mechanical and hydraulic systems of the vehicle to respond. During this time, the vehicle continues moving forward at practically the same speed and if there is not sufficient space between the leading and the following vehicle at the moment the leading vehicle applies the brakes and begins to decelerate, a collision would be inevitable. Even if the follower begins to apply its brakes at exactly the same time as the leader, the deceleration of the leading and the following vehicle may not match [9,10] and this generates the need for additional inter-vehicle distance during the cruising stage in order to accommodate for the difference in braking performance.

Heavy vehicles travel a significantly longer distance from the moment they apply their brakes until they come to a complete stop. This has to be accommodated for by allowing a significantly larger inter-vehicle spacing. On the other hand, when a light vehicle follows a heavy vehicle, the braking distance is not the limiting factor because typically the light vehicle will be able to come to a stop in a much shorter time and distance. In this case, the limiting factors are the initial conditions and the total delay between the time that the leader starts decelerating and the time that the follower starts decelerating at the maximum possible deceleration.

The delay in detecting and in reacting to the leading vehicle's deceleration can be reduced significantly, by taking the human driver out of the "control loop" [1,12,13,16]. With advances in technology and vehicle electronics, systems that were previously considered impossible to implement or too costly are becoming feasible and available. One such system is a functional extension of the classic cruise control [12]. The cruise control which is widely available on luxury cars today, is a controller that controls a throttle actuator in order to maintain constant vehicle speed. The next step in functionality, is a controller that uses a sensor to measure the relative distance and the relative speed to any vehicle ahead and

controls a throttle and a brake actuator in order to follow at the same speed and maintain a fixed relative distance [12,14,15]. Such vehicles can follow each other in the same lane automatically by relying on their own sensors and controls. Vehicles that rely on their own sensors, controls and intelligence to operate in a highway environment are referred to as autonomous vehicles.

Advances in communications made it possible for vehicles to communicate with each other exchanging information about braking intentions and capabilities, acceleration, lane changing etc. The infrastructure may also support vehicle following and maneuvers by providing desired speed and spacing commands in addition to traveler information. This distribution of intelligence gives rise to the operating concept referred to as infrastructure supported free agent.

When the infrastructure becomes actively involved by sending braking commands for emergency stops and lane changing maneuvers, we have an operating concept referred to as infrastructure managed free agent.

Another concept is to organize vehicles in platoons of a certain size where the intra-platoon spacing is very small and the inter-platoon spacing could be larger for safety purposes. In this case each platoon appears to the infrastructure as a single unit and therefore can be managed more efficiently. Each platoon is now responsible for the control of its vehicles.

If the inter-vehicle separation becomes very small, the laws of physics dictate that collisions between vehicles may be inevitable. In the interest of safety and avoidance of vehicle damage it will be of paramount importance that the energy dissipated during the collision be constrained. Since safety cannot be compromised for the sake of capacity, it becomes a serious constraint in most AHS design decisions.

In this study we consider a family of AHS platooning concepts. For each concept we calculate the minimum inter-vehicle spacing that would be required to guarantee either collision free following or bounded energy dissipation in the event of a collision. We will be assuming that if the collisions are relatively rare events, are always very minor and cause no permanent damage to the vehicles, the public might be willing to accept the fact that collisions may happen. Allowing for collisions to happen can reduce the minimum headway requirements for a platoon based AHS architecture.

Finally, in a slightly different operational concept, a high level of synchronization is introduced where each vehicle is allocated a slot in time and space. The infrastructure manages the slot distribution by issuing the appropriate commands for each vehicle.

The degree of infrastructure involvement and distribution of intelligence lead to different operational concepts and architectures for AHS. The purpose of this section is to study the Minimum Safety Spacing (MSS) for a number of different AHS concepts and architectures and to obtain capacity estimates.

2 SAFE INTERVEHICLE SPACING ANALYSIS

Inter-vehicle spacing during vehicle following is a very critical parameter of highway traffic. Insufficient spacing is usually the cause of rear-end collisions. In principle, the possibility of having a rear-end collision can be reduced by increasing the inter-vehicle spacing. However, the spacing that guarantees collision-free vehicle following can be characterized only when the braking scenario is known and well defined.

A braking scenario, which describes exactly how the vehicles brake, is usually specified by the deceleration profiles of the vehicles as a function of time. For each scenario there is a minimum spacing which must be maintained during steady state traffic flow, if collision-free vehicle following must be guaranteed. In this section we develop the basic equations that can be used to calculate the minimum spacing for collision free vehicle following, given the deceleration response information for both the leading and the following vehicle.

2.1 Minimum spacing for collision avoidance

Consider two vehicles following each other, as shown in figure 1. Assume that at t = 0 the leading vehicle begins to brake according to the deceleration profile defined by $a_l(t)$ and the following vehicle brakes according to the deceleration profile defined by $a_f(t)$. Assume that L_l and L_f are the lengths of the leading and following vehicles respectively. At t=0 the leading vehicle has a velocity $V_l(0)=V_{l0}$ and a position $S_l(0)=S_{l0}$ and the following vehicle has a velocity $V_f(0)=V_{f0}$ and a position $S_f(0)=S_{f0}$. If the spacing between the two vehicles at t=0, $S_r(0) = S_{l0} - S_{f0} - L_l$ is large enough, then there would be no collision during braking maneuvers.

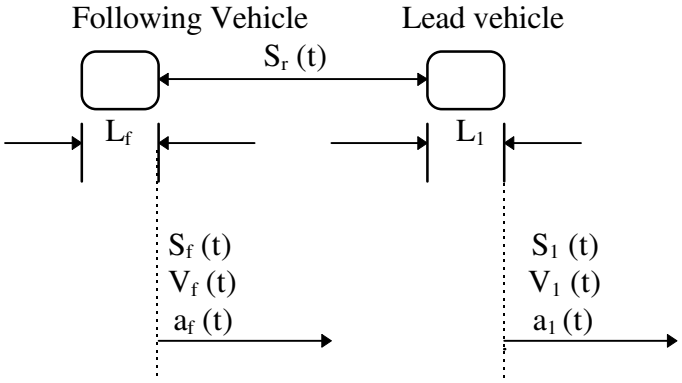

Figure 1: Vehicle Following

For a given braking scenario we would like to calculate the minimum value of the initial intervehicle spacing $S_r(0)$ for which there will be no collision. We refer to this value as the Minimum Safety Spacing, (*MSS*).

The spacing between the two vehicles measured from the front of the following vehicle to the rear of the lead vehicle is given by

$$S_r(t) = S_l(t) - L_l - S_f(t) \tag{1}$$

where

$$S_l(t) = S_l(0) + \int_0^t V_l(\tau) d(\tau) \tag{2}$$

$$S_f(t) = S_f(0) + \int_0^t V_f(\tau) d\tau \tag{3}$$

and

$$V_l(t) = V_l(0) + \int_0^t a_l(\tau) d\tau \tag{4}$$

$$V_f(t) = V_f(0) + \int_0^t a_f(\tau) d\tau \tag{5}$$

If the decelerations $a_l(t)$ and $a_f(t)$ and initial positions and velocities are specified, the MSS can be calculated as follows:

Assume that the two vehicles travel in the same direction but in two separate lanes and that $S_r(0) = 0$ as shown in figure 2.

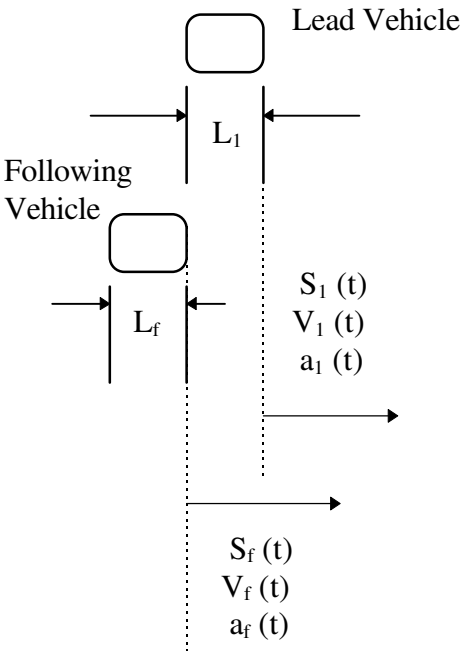

Figure 2: Hypothetical vehicle motion

Let t_s be the stopping time of the following vehicle. Then

$$V_f(0) + \int_0^{t_s} a_f(\tau)d(\tau) = 0 \tag{6}$$

$$S_f(t) = S_f(0) + \int_0^t V_f(\tau)d(\tau),\ \forall t \le t_s \tag{7}$$

and

$$S_f(t) = S_f(t_s), \forall t > t_s \tag{8}$$

The position of the leading vehicle at each time t is given by

$$S_l(t) = S_l(0) + \int_0^t V_l(\tau)d(\tau),\ \forall t \le t_s \tag{9}$$

The relative spacing at each time t is given by

$$S_r(t) = S_l(t) - L_l - S_f(t) \tag{10}$$

If both the leading and following vehicle are in the same lane, then $S_r(t) > 0$ for all $t \in (0,t_s]$ will imply no collision, whereas $S_r(t) < 0$ at some $t = t_c \in (0,t_s]$ will imply collision.

The MSS value denoted by S_{min} is given as $S_{min} = - \min [S_r(t),0] \ \forall \ t \in (0,t_s]$.

In other words S_{min} is equal to the maximum distance by which the following vehicle would overtake the leading vehicle at any time t in the interval $[0,t_s]$ in the scenario shown in figure 2 which assumes $S_r(0) = 0$. In the general case where $S_r(0) \neq 0$, the MSS is given by $S_{min} = - \min [S_r(t),0] + S_r(0) \ \forall \ t \in (0,t_s]$.

Based on the above analysis, we adopt a numerical method to calculate S_{min}. Assume that the following vehicle brakes and it does so by following the given deceleration profile, and comes to a full stop at $t=t_s$. We divide the interval $[0,t_s]$ into small time steps and consider the time instants $t = 0, T_s, 2T_s, \ldots, kT_s$ where T_s is the length of the time step and k is an integer with the property $kT_s \leq (k+1)T_s$. The method of calculation of S_{min} is shown in the flowchart of figure 3.

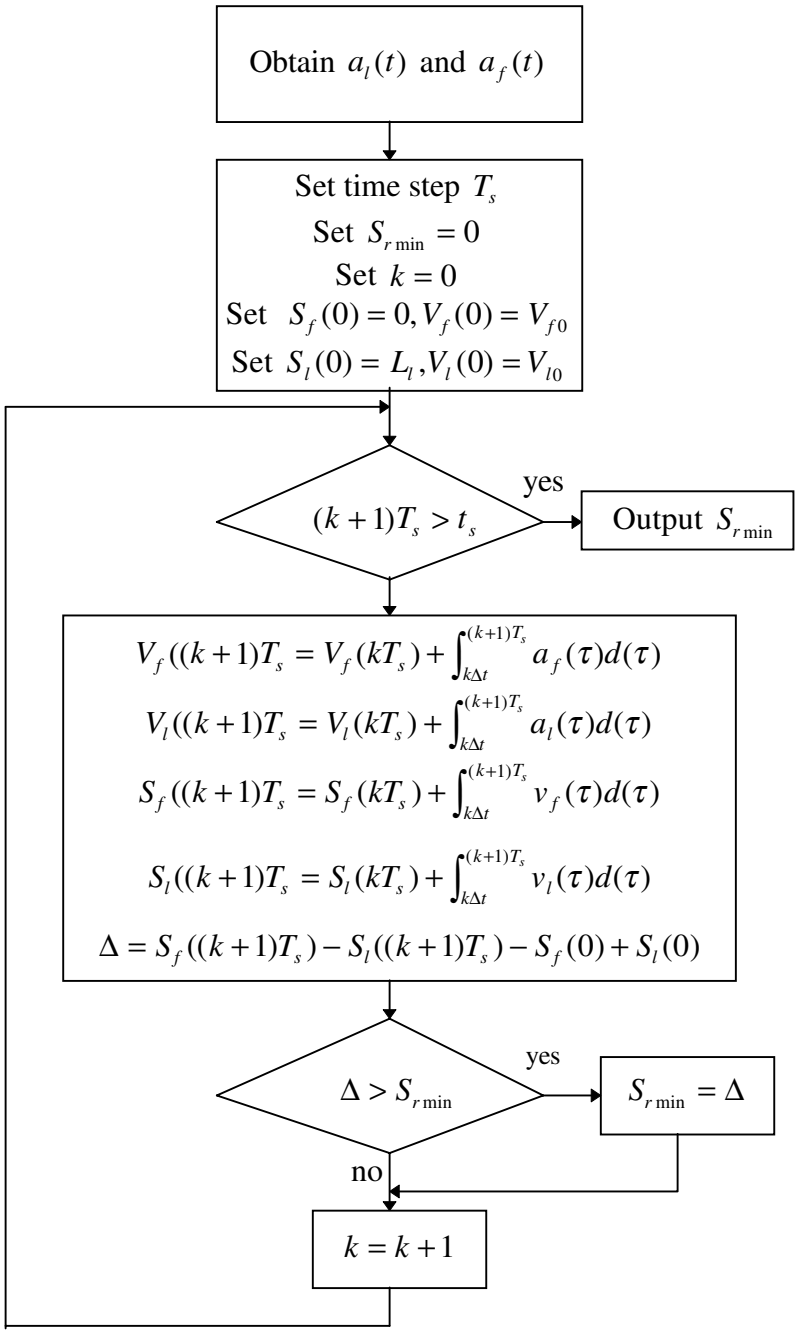

Figure 3. Flowchart for MSS calculation

2.2 Minimum spacing for low impact collisions

The relative velocity at impact is the most significant factor determining the severity of the collision and the extent of property damage and the possibility of passenger injury[4]. In vehicle following situations, the relative velocity between the leader and the follower is determined by differences in deceleration rate and by the time differential of the onset of braking. Assuming the leader and the follower had been traveling at approximately the same speed, the inter-vehicle spacing becomes the critical parameter. In principle, the possibility of having a rear-end collision can be reduced by increasing the inter-vehicle spacing. However, the spacing that theoretically guarantees collision-free vehicle following can be characterized only when the braking scenario is known and well defined and the parameters are not subject to variations. Furthermore, the amount of spacing required in order to provide a guarantee at a 100% confidence level that collisions will never happen, might be surprisingly large, much larger than the spacing we are used to seeing with manual driving. Hence, it might be very hard or impossible to guarantee a collision free environment. The dynamics and effects of inter-vehicle collisions should therefore be analyzed and understood.

Accepting the fact that inter-vehicle collisions may occasionally happen, requires that we carefully study the effects of such collisions to the vehicles involved. The conservation of momentum theorem states that after the collision of two objects the vector sum of the momentum before the collision will be equal to the vector sum of the momentum after the collision. If the two objects have mass *m1* and *m2* respectively and velocities *u1* and *u2* respectively before the collision, they will have velocities *v1* and *v2* respectively after the collision, such that:

$$m_1 u_1 + m_2 u_2 = m_1 v_1 + m_2 v_2 \tag{11}$$

The collision coefficient *cc* has been defined to be the scalar:

$$cc = \frac{v_2 - v_1}{u_1 - u_2} = -\frac{\Delta v}{\Delta u} \tag{12}$$

The collision coefficient is the ratio of the relative velocity at which the two objects separate after a collision over the relative velocity that the two objects approached each other before the collision. When *cc = 1* we have what we call “elastic” impact. When *cc = 0* we have what we call “plastic” impact. In the former case the two objects bounce off each other at a relative velocity equal to their relative velocity before the impact. In the latter case the two objects essentially “stick” to each other and keep moving as one. Real world objects rarely behave like any of these extremes, so the collision coefficient will be assuming values between 0 and 1.

In this section we develop the basic equations that can be used to calculate the minimum spacing for vehicle following, given the deceleration response information for both the leading and the following vehicle parameterized in terms of the value of the collision coefficient.

2.3 Bounded Collision Energy Analysis

In recent literature Glimm and Fenton [3] expressed the accident severity index *(S^2)* for a platoon of (n+1) vehicles that collide as

$$S^2 = \sum_{i=1}^{n} \Delta V_{i+1,i}^2 (t_{ci})$$

where $\Delta V_{i+1,i}^2 (t_{ci})$ denotes the relative speed at impact between vehicle (*i*) and and (*I+1*), at time t_{ci}, the moment of the collision.

When only two vehicles are involved, the severity index is simply

$$S^2 = \Delta V^2 (t_c) = [V_f (t_c) - V_l (t_c)]^2$$

where t_c is the time of the collision.

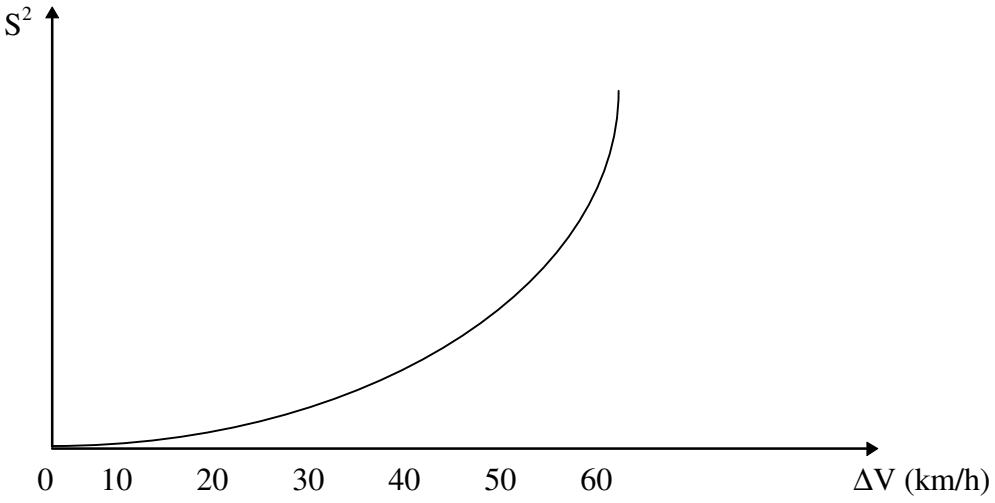

Figure 4: The Severity (impact energy) versus relative velocity at impact.

Consider two vehicles following each other, as shown in figure 1. Assume that at t = 0 the leading vehicle begins to brake according to the deceleration profile defined by $a_l(t)$ and the following vehicle brakes according to the deceleration profile defined by $a_f(t)$. Assume

that L_l and L_f are the lengths of the leading and following vehicles respectively. At t=0 the leading vehicle has a velocity $V_l(0)=V_{l0}$ and a position $S_l(0)=S_{l0}$ and the following vehicle has a velocity $V_f(0)=V_{f0}$ and a position $S_f(0)=S_{f0}$. We want to determine the necessary spacing between the two vehicles at t=0, $S_r(0) = S_{l0} - S_{f0} - L_l$ such that if there is a collision during braking maneuvers, the impact will happen at a relative velocity bounded by a preset upper limit, ΔV_s that gives a low accident severity index S^2.

For a given braking scenario we would like to calculate the minimum value of the initial intervehicle spacing $S_r(0)$ that will lead to collisions at relative velocities smaller than ΔV_s. We will refer to this value as the Minimum Impact Spacing, (*MIS*).

The spacing between the two vehicles measured from the front of the following vehicle to the rear of the lead vehicle is given by

$$S_r(t) = S_l(t) - L_l - S_f(t) \tag{13}$$

where

$$S_l(t) = S_l(0) + \int_0^t V_l(\tau)d(\tau) \tag{14}$$

$$S_f(t) = S_f(0) + \int_0^t V_f(\tau)d\tau \tag{15}$$

and

$$V_l(t) = V_l(0) + \int_0^t a_l(\tau)d\tau \tag{16}$$

$$V_f(t) = V_f(0) + \int_0^t a_f(\tau)d\tau \tag{17}$$

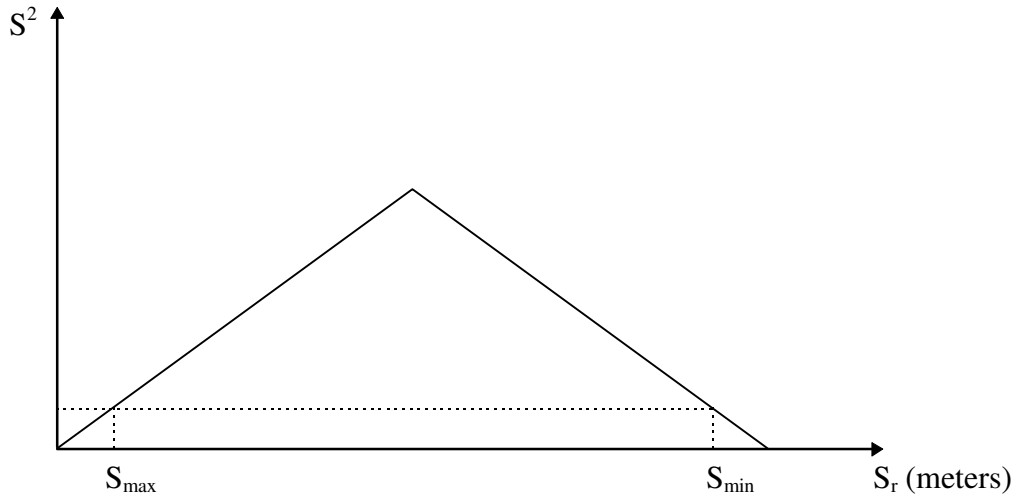

Figure 5: The Severity (impact energy) versus initial intervehicle spacing.

If the decelerations $a_l(t)$ and $a_f(t)$ and initial positions and velocities are specified, the MIS can be calculated in a way very similar to the method used earlier. Let's assume that we want to bound the energy of the collision by limiting the relative velocity just before the collision to less than ΔV.

Let's also assume the existence of energy absorbing bumpers that can absorb and dissipate the energy of the collision, thus guaranteeing a perfectly plastic collision. (cc = 0). The diagram of figure 5 indicates that there are two ways to limit the relative velocity before the collision.

Assuming initial conditions where the leading and the following vehicle travel at approximately the same speed, we can guarantee that there is not enough time for a velocity differential to develop by limiting the relative spacing between vehicles to a very small distance. This leads to one possible vehicle following scenario, where in the event of an emergency the vehicles will always collide with each other and with the assumption of plastic collisions they will continue traveling as a single body until they come to a full stop.

The second likely braking scenario assumes that there is sufficient headway between vehicles but somewhat less than what would be required to guarantee no collisions in the event of emergency braking. We can apply the same methodology we used earlier to determine the minimum headway between vehicles that guarantees collisions with relative velocity less than a preselected ΔV. Assume that the two vehicles travel in the same direction but in two separate lanes. The position of the vehicles at time t = 0 is shown in figure 2.

Let t_{sl} be the time needed by the leading and the following vehicle to slow down from their initial velocities V_{lo} and V_{fo} to velocities V_{lsl} and V_{fsl} such that $V_{fsl} - V_{lsl} < \Delta V$. This

condition may occur more than once, from the moment the leading vehicle applied deceleration until the moment the following vehicle comes to a full stop. Therefore we are interested in computing the headway for the two boundary cases. The case where the vehicles have first developed a sufficient ΔV and the case where the vehicles are at the end of the braking trajectory, the leader may have already stopped, but the follower is still moving and there is still a ΔV between them. The equations are practically the same as before. We have:

$$V_f(0) + \int_0^{t_s} a_f(\tau) d(\tau) = 0 \tag{18}$$

$$S_f(t) = S_f(0) + \int_0^t V_f(\tau) d(\tau), \ \forall t \le t_{sl} \tag{19}$$

and

$$S_f(t) = S_f(t_s), \forall t > t_{sl} \tag{20}$$

The position of the leading vehicle at each time t is given by

$$S_l(t) = S_l(0) + \int_0^t V_l(\tau) d(\tau), \ \forall t \le t_{sl} \tag{21}$$

The relative spacing at each time t is given by

$$S_r(t) = S_l(t) - L_l - S_f(t) \tag{22}$$

and the relative speed at each time t is given by

$$-\Delta V(t) = V_l(0) + \int_0^t a_l(\tau) d\tau - V_f(0) + \int_0^t a_f(\tau) d\tau \tag{23}$$

In this case we have to determine the time instances t_{c1} and t_{c2} where the relative velocity is equal to the desired threshold. Having determined t_{c1} and t_{c2} we can then determine the relative spacing between the two vehicles. Therefore the Minimum Impact Spacing, MIS

has a minimum value and a maximum value. To limit the impact of the first collision at t_{c1}, we must allow for a maximum headway of $S_{max} = - max\ S_r(t),\ \forall\ t \in (0,t_{c1}]$.

To limit the impact of the last collision at t_{c2}, we must allow for a minimum headway of $S_{min} = - min\ [S_r(t),0],\ \forall\ t \in [t_{c1},t_{c2}]$.

From this description it becomes clear that the required headway must be either less than S_{max} or greater than $S_{min.}$ (see figure 5).

The two limits, S_{max} and S_{min}, are equal to the distance by which the following vehicle would have overtaken the leading vehicle at the time instances t_{c1} and t_{c2} respectively, which corresponds to the time instances when their relative velocity is equal to ΔV, assuming the initial conditions shown in figure 2. Based on the above analysis, we use numerical methods to calculate S_{max} and S_{min}.

3 VEHICLE FOLLOWING CONCEPTS

With advances in technology and in particular in vehicle electronics, systems that were previously considered impossible or too costly to implement are becoming feasible and available. One such system is a functional extension of the classic cruise control. It consists of a controller that uses a sensor to measure the relative distance and the relative speed to any vehicle ahead and controls a throttle and a brake actuator in order to follow at the same speed and maintain a desired relative distance. The relative distance may be characterized in terms of a constant length or it may be a function of the speed. If the majority of vehicles have such a controller on board, we can have an environment where vehicles follow each other automatically, in the same highway lane, without any other kind of interaction such as communication between them. The highway may provide a level of support to the vehicles by transmitting information about road conditions, congestion, routing suggestions and possibly recommended speeds. If the vehicles do not communicate and do not require any infrastructure support they are said to operate autonomously. A system like that, may provide a capacity increase by smoothing out traffic flow and eliminating the mistake that human drivers tend to do, that is to follow at short and unsafe distances and then overcorrecting by slowing down too much when a vehicle ahead starts to decelerate.

A further functionality enhancement comes by allowing the vehicles to communicate and notify each other about their braking intentions. Also the infrastructure may become involved in setting the desired velocity for each section of the highway, communicating to vehicles about the need for emergency braking and coordinating the flow of the traffic. Such systems may achieve significant improvements in flow rates and capacity increases of the existing highways. By adding more equipment and intelligence to the vehicle-infrastructure system we can come up with more advanced concepts that have the potential for bigger benefits. In this section we describe a number of operating AHS concepts for automatic vehicle following.

3.1 Autonomous Vehicles

A possible AHS concept is one where the vehicles operate independently i.e., autonomously, using their own sensors. Each vehicle senses its environment, including lane position, adjacent vehicles and obstacles. The infrastructure may provide basic traveler information services, i.e., road conditions and routing information. The infrastructure may also provide some means to assist the vehicle in sensing its lane position. Many different systems have been proposed to help the vehicle sense its position, such as implanted magnetic nails, magnetic stripes, radar reflective stripes, Radio Frequency cables, or GPS satellites [23].

In an autonomous environment, the vehicle does not rely on communications with other vehicles or the infrastructure in order to make vehicle following decisions. Each autonomous vehicle maintains a safe distance from the vehicle it is following or if a vehicle is not present within the sensing distance it travels at a constant speed in accordance with the posted speed limits and regional safety regulations and of course road conditions. In other words, if there is no vehicle ahead within the maximum safety distance, the vehicle travels at the speed limit or at a lower speed depending on the road conditions.

Since there is no communication between vehicles, each vehicle senses the relative spacing and speed to the vehicle ahead and selects a headway based on its own braking capabilities and by assuming that the vehicle in front may brake with the 'worst' possible deceleration. The technology that allows the vehicle to sense the relative position and speed to the vehicle ahead can also be adapted to allow the vehicle to estimate the size and indirectly the vehicle class and braking capabilities of the vehicle ahead. This knowledge will allow a less conservative assumption about the braking capabilities of the leading vehicle that will lead to a more accurate selection of intervehicle spacing. In the case where mixing of vehicles classes in the same lane is allowed, distinguishing whether the vehicle ahead is a truck, bus or a passenger vehicle will have a significant effect on the selection of spacing and therefore on capacity.

3.2 Free Agent Vehicles - Infrastructure Supported

A vehicle is considered a 'Free Agent' if it has the capability to operate autonomously but it is also able to receive communications from other vehicles and from the infrastructure. This implies that the infrastructure may get involved in a supporting role, by issuing warnings and recommendations for desired speed and headways but the infrastructure will not have the authority to issue direct control commands. Therefore this concept has been referred to as "Infrastructure Supported". The fundamental difference between this concept and that described in subsection 3.1 is that there is vehicle to vehicle and vehicle to infrastructure communication. Each vehicle communicates to the vehicle behind its braking capabilities and its braking intentions. This allows the vehicle behind to choose its headway. For example a shorter headway can be selected by a passenger vehicle if the vehicle ahead is a heavy truck or a bus. A larger headway must be selected by a heavy

vehicle if the vehicle ahead is a passenger vehicle. A free agent vehicle uses its own sensors to sense its position and environment, including lane position, adjacent vehicles and obstacles.

With this concept the MSS between vehicles is expected to be smaller than that on conventional highways because of the intelligent longitudinal control system and vehicle to vehicle and infrastructure to vehicle communications. Each vehicle senses the relative spacing and speed to the vehicle ahead and decides and selects a headway based on its own braking capability, the braking capability of the vehicle ahead and the road surface conditions which are either sensed by the vehicle or are broadcasted from the infrastructure. When a vehicle starts to brake, it notifies the vehicle behind about the magnitude of its braking force. Even if we assumed a relatively primitive form of communication between vehicles like a line of sight communication that transmits the applied braking force, we can achieve better separation control as we eliminate the delay in deciding if the vehicle ahead is performing emergency braking or routine braking.

3.3 Free Agent Vehicles - Infrastructure Managed

The concept of Free Agent vehicles with Infrastructure Management is based on the assumption that the traffic is composed of vehicles acting as free agents while the infrastructure assumes a more active and more complex role in the coordination of the traffic flow and control of vehicles. Each vehicle is able to operate autonomously and uses its own sensors to sense its position and environment, including lane position, adjacent vehicles and obstacles. The difference in this centrally managed architecture is that the infrastructure has the ability to send commands to individual vehicles.

This is envisioned to be a "request-response" type architecture, in which individual vehicles ask permission from the infrastructure to perform certain activities and the infrastructure responds by sending commands back to the requesting vehicle and to other vehicles in the neighborhood.

It is expected and assumed that the infrastructure is able to detect emergency situations and whenever it detects such emergency, the infrastructure will have the responsibility to send an emergency braking command to all vehicles affected. This concept minimizes the delay in performing emergency braking. This allows for some further reduction of the minimum headway, compared to the concepts presented so far. On the other side, the accurate timing of the emergency and stopping commands for each vehicle that must be issued by the infrastructure, requires accurate tracking of individual vehicles as well as extensive and frequent communications between individual vehicles and the infrastructure.

3.4 Platooning without coordinated braking

This concept represents the possibility that the safest and possibly most cost-effective way of achieving maximum capacity is by making platoons of vehicles the basic controlling

unit. This will boost road capacity by expanding on the concept of infrastructure managed control [17,18,19].

Platoons are clusters of vehicles with short spacing between individual vehicles in each group and longer spacing between platoons. The characterizing differentiation is that the platoon is to be treated by the infrastructure as an "entity" thereby minimizing some of the need for communicating with and coordinating individual vehicles. The infrastructure does not attempt to control any individual vehicle under normal circumstances, keeping the cost and necessary bandwidth low. The infrastructure is expected to be an intelligent agent which monitors and coordinates the operation of the platoons.

Tight coordination is required within the platoon in order to maintain a close spacing and this requires that the vehicles must be communicating with each other, constantly. The significantly longer inter-platoon spacing is required to guarantee no inter-platoon collisions.

Each vehicle is expected to be equipped with the sensors and intelligence to maintain its lane position, sense its immediate surroundings, and perform the functions of merging into and splitting off a platoon. It is not expected to accomplish lane changes, or merging and splitting without the infrastructure's or the platoon entity's help.

The main mode of operation of the infrastructure would be of a request-response type. Each platoon’s and/or vehicle's request is processed and appropriate commands are sent to the appropriate vehicles/platoons to respond to that request. The infrastructure takes a more pro-active role in monitoring traffic flow, broadcasting traffic flow messages, advising lane changes to individual vehicles and platoons in addition to the usual information provider functions.

Once a vehicle has merged into a platoon, the headway maintenance controller must take into account the braking capabilities of the vehicle ahead in the platoon in order to set an appropriate separation distance that minimizes the possibility of collision. The platoon leader may also provide corrections to the individual intra-platoon headways in order to reduce the possibility of a rear-end collision between two vehicles propagating to the other members of the platoon.

Mixing of vehicle classes, although an implicit feature of the present highway system, creates a major complication because of the dissimilar braking characteristics of each vehicle class. Therefore it makes sense to form platoons of vehicles belonging to the same class, exclusively. In this concept we assume that no coordination of the braking sequence takes place within a platoon in order to distinguish it from the next one where coordinated braking is employed.

3.5 Platooning with coordinated braking

The platooning concept with coordinated braking is based on the concept of maximizing capacity by carefully coordinating the timing and degree of braking among the vehicles participating in a platoon entity. This allows the minimization of the spacing between vehicles without compromising safety. For example, during a braking maneuver the platoon leader may dictate a braking sequence to be followed by each vehicle so that the maneuver is performed without any intra-platoon collision. Such a sequence may require the last vehicle to brake first followed by the second last vehicle etc. The distinguishing feature of this concept is the minimization of intra-platoon spacing and the promise of higher capacity.

3.6 Infrastructure Managed Slotting

Under the Infrastructure Managed Slotting concept, an infrastructure based control system creates and maintains vehicle "slots" in space and time. Slots can be thought of as moving roadway segments, each of which holds at most one vehicle at any time. The vehicles are identified and managed only by association with these slots. For simplicity in management i.e., to achieve slots of uniform length, vehicles that need more space may be assigned multiple slots. Heavy loaded light trucks may be assigned two slots, unloaded semis may be assigned three slots, loaded heavy trucks may be assigned four slots etc.

In the basic slotting concept the slots should be of fixed length. The virtual leading edge of each slot can be thought of as a moving point that the vehicle assigned to the slot has to follow. Thus the controller on the vehicle is assigned to follow this virtual moving point, not another vehicle. In essence this relieves the requirement of using headway sensors on the vehicle and of sensing the relative distance and speed to any other vehicle. Under no circumstances is a vehicle allowed to violate the edges of its assigned slot.

The distinguishing feature of this concept is that the sensing requirements are theoretically simplified. At least, the vehicle does not need to sense the relative position and speed of other vehicles. Yet the vehicle must be able to sense its position relative to the edge of the slot and the virtual point it tries to follow. A global and accurate longitudinal position sensing system is required.

In terms of separation policy, the slotting method is bounded by the limitations of the inherently "synchronous" architecture. This means that the size of each slot must be sufficient such that the spacing between individual vehicles occupying a single slot is sufficient to avoid collisions under the worst case scenario. Thus the weakest link in the chain is the vehicle with the worst braking performance that the system tries to accommodate in a single slot. Once the spacing is set to accommodate such a vehicle, every other vehicle which has better braking performance will not be able to utilize this capability to shorten the spacing to the vehicle in front. There will be "dead space" in between them. Similarly, a vehicle that does not meet the minimum braking requirement to

occupy a single slot will be assigned two (or more) consecutive slots, with the resulting inefficiency of wasting even more space than is really needed.

By comparison, an architecture where each vehicle optimizes the headway between itself and the vehicle in front based only on the braking capabilities of the two vehicles involved is inherently an "asynchronous" architecture, which results in true minimization of the unused space between vehicles.

The relative merits of a "synchronous" versus "asynchronous" architecture have been intriguing the designers of computers and communications systems ever since digital systems became a reality. The typical tradeoff is complexity versus performance. It has been well established through extensive research in other fields that asynchronous architectures provide the potential for maximizing performance at the cost of increased complexity [24]. It is almost obvious that the same is true on the subject of the AHS separation policy architecture.

4 SPACING AND CAPACITY EVALUATIONS

In this section we present briefly the fundamental factors that affect traction during vehicle acceleration and braking. Traction is what ultimately defines the braking capabilities of any kind of vehicle, under any kind of whether and road conditions. Then we develop likely emergency stopping scenarios for each AHS concept under consideration which we then use to calculate intervehicle spacing and capacity.

4.1 Adhesion and Friction

The friction force between two surfaces is defined as the force opposing the relative displacement of the two surfaces when a force is applied as shown in figure 6. In the context of vehicle traction this force is referred to as adhesion. Adhesion (attraction between two surfaces) and friction (resistance to relative motion of adjacent surfaces) are very complex physical phenomena. But for practical purposes it is common to use the approximation that the magnitude of the friction force F depends on two factors only: The normal force G between the two surfaces and a dimension-less coefficient of friction *m*, such that:

$$F = \mu G \tag{24}$$

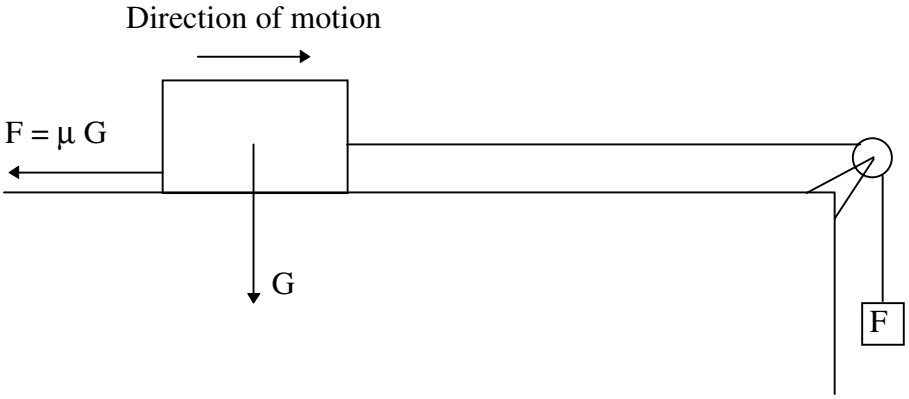

Figure 6: Physical representation of friction force F.

The value of the coefficient of friction μ depends on the characteristics of the two surfaces, primarily their smoothness and their hardness, and on the relative speed V_r between them. For most surfaces, as V_r increases, μ decreases. When the two surfaces do not move μ assumes a considerably higher value, referred to as the static friction coefficient.

Applying the general concept to the problem of vehicle traction, it is clear that the maximum Tractive or Braking Effort (TE_{max}) which can be utilized is limited by the tire to road surface adhesion.

$$TE_{max} = \mu G_a \tag{25}$$

where G_a is the weight on the wheels which apply the force. For propulsion G_a is the weight on the powered axle while for braking G_a represents the total vehicle weight G since the brakes act on all wheels. The actual weight distribution between front and rear axles depends on vehicle design and furthermore varies as a function of the actual deceleration due to the mass transfer phenomenon.

The change of μ with speed is very important in traction and friction. It makes braking at high speeds more difficult than at low speeds because it increases the possibility of skidding. Any spinning or skidding of the wheels results in a rapid increase of the relative speed V_r between the wheels and the road surface and therefore a sudden reduction of μ. As a result, traction is lost. To restore the friction coefficient spinning or skidding must be terminated by reducing the tractive or braking effort. This is the principle of operation of the so called Antilock Braking Systems (ABS).

The value of μ for vehicles depends on the type and condition of the road surface, the vehicle speed and the condition of the tires. A range of values of μ for most types of vehicles is shown in figure 7 [8].

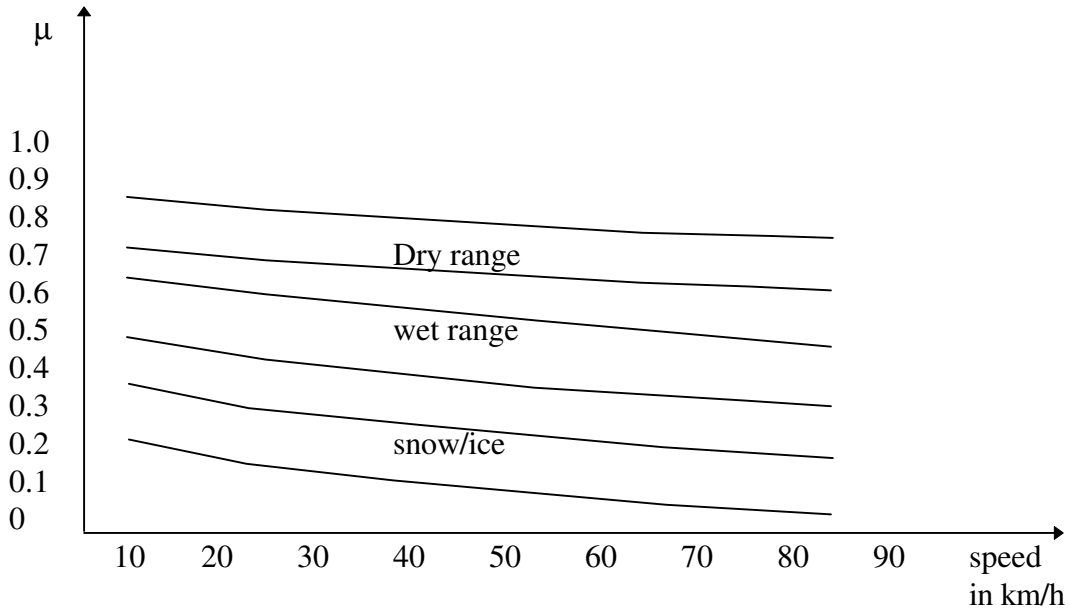

Figure 7: Friction coefficient of vehicles with rubber tires.

The braking ability of all vehicles is best on dry pavement. It degrades substantially on wet pavement and braking ability is virtually lost on snow.

In our analysis, we use data from vehicle tests performed by established authorities. For passenger vehicles, we use information from the "Consumer Reports" publication [9] and the consumer oriented "Road and Track" magazine [10]. For heavy vehicles like buses and trucks, we obtained information from actual tests [11]. Based on these data, we have estimated the braking capabilities of a range of passenger and heavy vehicles on dry, wet and snowed road pavement. In a more or less expected fashion, we found that sports cars can achieve the best braking distances (highest deceleration), followed by middle and upper class medium size vehicles (such as in the "sports sedan" category), followed by small or economy class vehicles. The last finding is a little counter intuitive, based on the fact that small vehicles are light weight thus require less energy dissipation to achieve braking and are less demanding of good tire performance. Yet there is an obvious trend for auto manufacturers to try to match the braking capabilities with the acceleration capabilities of a given vehicle. We found that the trend is to offer approximately double the deceleration (in g's) to the available acceleration (also in g's) in low gear. This is a ball park figure, of course, and deviations do exist.

The braking capability of any vehicle degrades on wet pavement by a factor determined by the texture of the pavement and the type of tires used. We represent that as a change in the friction coefficient μ. The data collected give a quantitative estimate of the friction coefficient on dry, wet and snowed pavement. The numbers of course vary depending on the vehicle, its tires and the presence of ABS. A typical vehicle that can achieve 0.8g

deceleration on dry pavement can go down to 0.55g in wet conditions and to as low as 0.15g in snow conditions. The collected braking test results are presented in Appendix A.

In our study, we simplified somewhat our assumptions regarding the friction coefficient μ. Instead of assuming a maximum deceleration of 1 g and scaling it by the typical value of μ, i.e., 0.8 for passenger vehicles, we used the value 0.8 g for maximum deceleration and assumed that μ is 1.0. This does not affect the results for braking on dry road pavement. Then for wet road conditions we assumed a worst case scenario where the friction coefficient becomes half, i.e., μ becomes 0.5 while the maximum deceleration remains at 0.8 g for passenger vehicles. Similarly, instead of assuming different values of μ for buses and for heavy trucks, we used the same value for all of them, but we used a different value of maximum deceleration for each class. We used 0.4 g maximum deceleration for buses and 0.3 g maximum deceleration for heavy trucks. These numbers are based on measurements on actual vehicles, and the data can be found in Appendix A.

The maximum deceleration that each vehicle can achieve depends on many factors and therefore it cannot be predicted exactly. It depends mostly on the tires of course, like the quality and type of tread, hardness, temperature, inflation pressure and the age of the tire. It also depends on the size and type of friction materials in the brakes, the mass distribution of the vehicle, the presence of ABS and many other factors. In our analysis we simplify these complex dependencies by using the abstraction of uniform value of μ and assuming appropriate values for maximum deceleration for different classes of vehicles, without affecting the accuracy of the results.

During the emergency braking phase the jerk is not intentionally limited and the maximum deceleration is allowed to be as large as the vehicle can achieve. The jerk clearly depends on the mass of the vehicle first and on the hydraulic brake system second. It clearly depends on the rate of change of the force that the driver applies on the brake pedal in the case of manually driven vehicles. For automated vehicles it will depend on the dynamics of the brake actuator. It would simply be inversely proportional to the mass of the vehicle if all the vehicles had exactly the same actuators and hydraulic systems, but this is certainly not going to be the case.

Based on our experience with an actual brake system which is in use in a prototype automated passenger class vehicle, we made an educated guess for other classes of vehicles. We assumed that the maximum jerk is limited to 50 *meters/sec*^{3} for passenger vehicles, 40 *meters/sec*^{3} for buses and 30 *meters/sec*^{3} for heavy loaded trucks.

4.2 Uniform versus non-uniform braking.

For a realistic estimation of the theoretical capacity, we have assumed a "typical" maximum deceleration level for each class of vehicles, based on actual test data. Since discrepancies of 10% or more can be clearly seen in the braking capabilities among vehicles of the same class, we have made the assumption of a 10% discrepancy in maximum deceleration between the leader and the follower in the sense that the follower

has inferior maximum deceleration capability, an assumption which inevitably generates the need for more spacing.

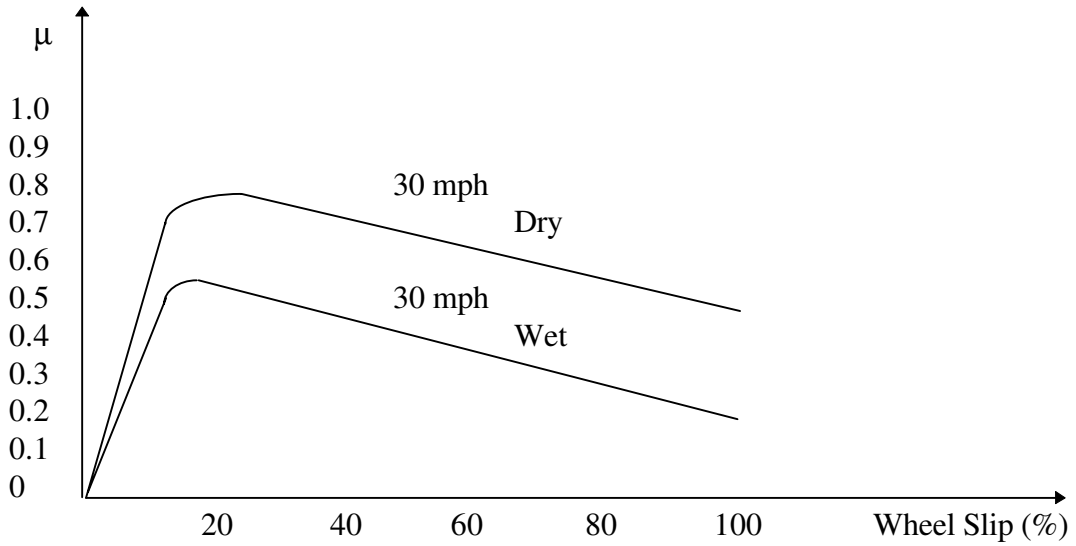

Figure 8: Braking coefficient versus slip.

To be realistic, this discrepancy exists mostly at the limit of the braking capability of the vehicles, when braking occurs in the unstable region where the slope of μ versus wheel slip is negative as seen in figure 8 [7]. At that point, demanding slightly higher deceleration results in skidding of the tires and in a sharp reduction in the μ and in overall deceleration. In our effort to represent a realistic worst case scenario, we assumed 10% deviation from the maximum braking capability for the following vehicle in all cases of unrestricted braking, i.e., when the traction of the tires is pushed to the limits. On the other hand, braking by applying less than the maximum deceleration is easier because we can stay away from the unstable region of the μ curve. This can be used to our benefit if we impose a limit in deceleration for all vehicles. This limit is a common denominator that all vehicles should be able to meet by a proper design of their control system. This is the definition of the concept we will henceforth call "uniform braking". By staying away from the unstable braking region we can almost guarantee a better control of the magnitude of the deceleration. This justifies using only 5% deviation from the nominal braking capability for the follower in the case of uniform braking. Uniform braking is more crucial in platooning where, in the interest of efficiency, vehicles within each platoon have to have similar performance. For completeness and for the sake of comparison, we analyzed the effects of uniform braking both in platooning and non-platooning environments.

The concept that all vehicles should be restricted to a closely matched (i.e. uniform) degree of deceleration is clearly an architectural decision. We assumed that the braking deceleration on a dry road can be restricted to 0.5g for all passenger vehicles, 0.3g for all buses and 0.2g for all heavy trucks. The idea here is to use a number that every vehicle in

its respective class can comfortably achieve. This helps guarantee that the deviation from one vehicle to another will be less than 5% in the worst case. So we used a 5% discrepancy in the deceleration of the leading and following vehicle to represent the worst case mismatch in the case of uniform braking.

4.3 Mixing of vehicle classes

The mixing of different classes of vehicles on the same AHS will affect capacity due to the different braking capabilities of the different classes of vehicles. In out analysis we consider three different vehicle classes, possessing fundamentally different characteristics: Passenger vehicles (P), buses (B) and heavy trucks (T).

This leads to the following possible combinations:

(a) PP: A Passenger vehicle leading a Passenger vehicle

(b) PB: A Passenger vehicle leading a Bus

(c) PT: A Passenger vehicle leading a Truck

(d) BP: A Bus leading a Passenger vehicle

(e) BB: A Bus leading a Bus

(f) BT: A Bus leading a Truck

(g) TP: A Truck leading a Passenger vehicle

(h) TB: A Truck leading a Bus

(i) TT: A Truck leading a Truck

We made the following distinctions in mixing possibilities:

a) No mixing.

Traffic consists of passenger vehicles only, i.e. we have 0% mixing. In this case, the passenger vehicle to passenger vehicle (PP) minimum headway was assumed between all vehicles.

b) Allowed mixing of vehicle classes.

All cases of mixing assume uniform mixing, i.e., the minority vehicles are uniformly distributed among the population of passenger cars. This is a realistic assumption as long as the percentage of mixing is fairly low.

Case 1:

Traffic consisting of passenger vehicles with 5% mixing of buses. In this case, the passenger vehicle to passenger vehicle (PP) minimum headway was assumed between 90% of the vehicles, passenger vehicle to bus (PB) minimum headway between 5% of the vehicles and bus to passenger vehicle (BP) between 5% of the vehicles.

Case 2:

Traffic consisting of passenger vehicles with 5% mixing of trucks. In this case, the passenger vehicle to passenger vehicle (PP) minimum headway was assumed between 90% of the vehicles, passenger vehicle to truck (PT) minimum headway between 5% of the vehicles and truck to passenger vehicle (TP) between 5% of the vehicles.

Case 3:

Traffic consisting of passenger vehicles with 2.5% mixing of buses and 2.5% mixing of trucks. In this case, the passenger vehicle to passenger vehicle (PP) minimum headway was assumed between 90% of the vehicles, passenger vehicle to bus (PB) minimum headway between 2.5% of the vehicles passenger vehicle to truck (PT) minimum headway between 2.5% of the vehicles bus to passenger vehicle (BP) between 2.5% of the vehicles. and truck to passenger vehicle (TP) between 2.5% of the vehicles.

Case 4:

Traffic consisting of passenger vehicles with 5% mixing of buses. and 5% mixing of trucks. In this case, the passenger vehicle to passenger vehicle (PP) minimum headway was assumed between 80% of the vehicles, passenger vehicle to bus (PB) minimum headway between 5% of the vehicles passenger vehicle to truck (PT) minimum headway between 5% of the vehicles bus to passenger vehicle (BP) between 5% of the vehicles. and truck to passenger vehicle (TP) between 5% of the vehicles.

4.4 Autonomous Vehicles

In the case of autonomous vehicles, each vehicle relies on its own sensors to determine the motion intentions of the leading vehicle. Since there is no vehicle to vehicle communication, each vehicle has to use relative speed and spacing measurements to determine the intentions of the vehicle ahead. Therefore, in calculating a safe intervehicle spacing we consider the following worst case stopping scenario.

The acceleration (actually deceleration) profile of the leading and following vehicles involved in a braking maneuver is assumed to follow the trajectories shown in figure 9.

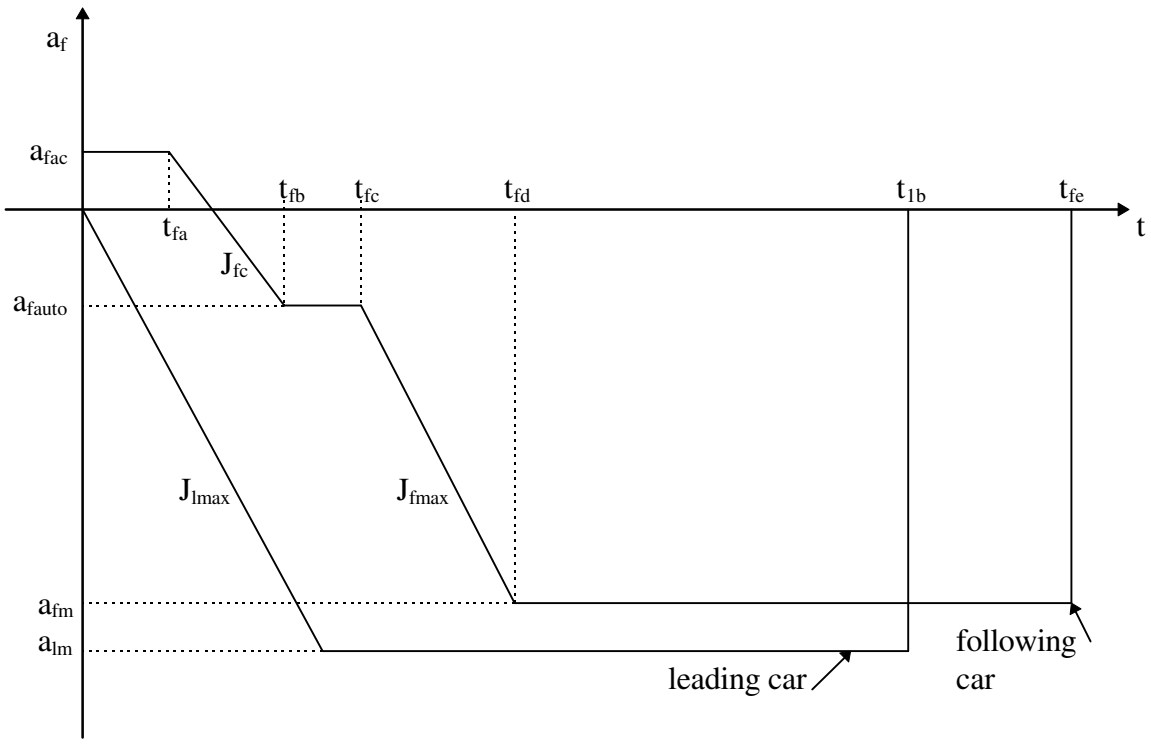

Figure 9: Autonomous vehicles.

The leading vehicle performs emergency braking at time t = 0, at a maximum rate of change (jerk) equal to J_{lmax} until it reaches a maximum deceleration of a_{lm}. The follower, which might have been accelerating initially, at a_{fac} starts decelerating after a detection and brake actuation delay equal to t_{fa} in an effort to maintain the desired spacing. Since initially the follower is not aware that the leader is performing emergency braking, it limits its jerk and deceleration to J_{fc} and a_{fauto} respectively, in an effort to meet the vehicle control objective and at the same time maintain passenger comfort. The follower detects and initiates emergency braking at $t = t_{fc}$. At this time passenger comfort is no longer a crucial issue and braking is done with maximum jerk J_{fmax} and maximum deceleration a_{fm}.

In this section we use the above stopping scenario to calculate the minimum time headway for collision free vehicle following by substituting appropriate numerical values for all the above parameters.

In evaluating the above scenario we adopted a set of likely initial conditions at the onset of braking. The assumptions regarding the initial conditions are the following: The leader has been traveling at a speed of 60 miles per hour while the follower has an instantaneous velocity 5% higher, i.e. 63 miles per hour and an instantaneous acceleration $a_{fac} = 0.15g$. These conditions represent the realistic scenario that the follower had been performing a position adjustment as in trying to catch up with the leader. Therefore the vehicle is accelerating just before it has to start braking. When the vehicle detects that the leader is

braking (which involves a 0.1 sec delay for detection and a 0.1 sec delay in the actuator) it starts braking until it reaches the maximum allowable deceleration a_{fauto} = -0.1g for passenger comfort.

The vehicle initially applies a limited amount of braking because at the onset of braking it is not known if the leader is simply slowing down or performing emergency braking. If the follower applies emergency braking every time it detects the leader slowing down it would be detrimental to the stability of the traffic flow. Therefore the follower applies limited braking at first, with the objective of not upsetting the quality of the ride of the passengers or the position and velocity error of any vehicles behind. For this reason, the Jerk is limited to 5 meters/sec^3 during this phase.

Eventually, the follower will detect that the headway is diminishing rapidly and therefore the leader is performing an emergency braking maneuver. We assumed that the detection of emergency braking involves 0.3 seconds of delay.

Using these parameter values, we computed the necessary headways for different road conditions and levels of mixing of classes of vehicles using the algorithm presented in section 2.1. The spacing results are presented in Table 1 for the case of dry road surface. The spacing results for the case of wet road surface are presented in Table 2.

The spacing calculations in tables 1 and 2 are based on the assumption that vehicles can brake with maximum possible deceleration depending on their capabilities. Another possible scenario is to use the concept of uniform braking that limits the maximum deceleration and maximum jerk to values that could be met and used by all vehicles of the same class. These limits will make the braking performance of the vehicles very similar. Using this scenario we calculated spacings based on the vehicle values shown in Table 3. In this case due to uniformity we assume 5% deviation between decelerations of vehicles of the same class. This 5% deviation accounts for inaccuracies in measuring acceleration/deceleration and maintaining the desired one using the on board vehicle controller.

Based on the above spacings the maximum possible throughput referred to as the capacity C measured as the number of vehicles per hour per lane is given by the formula

$$C = (360000V)[(100-2W_T-2W_B)(L_P+h_{PP}V) + W_T(L_P+h_{PT}V+h_{TP}V+L_T) + W_B(L_P+h_{PB}V+h_{BP}V+L_B)]^{-1} \quad (26)$$

where V is the speed of flow measured in meters/sec, L_p is the length of passenger cars, L_B is the length of buses and L_T is the length of trucks with trailers, in meters. The parameter h_{PP} is the minimum time headway between passenger cars, h_{PT} is the minimum time headway between a passenger car and a truck that follows it, h_{TP} is the minimum time headway between a truck and a passenger car that follows it, h_{PB} is the minimum time

headway between a passenger car and a bus that follows it and h_{BP} is the minimum time headway between a bus and a passenger car that follows it, in seconds. W_B is the percentage of buses and W_T is the percentage of trucks in the mix. We use eq. (26) and the numerical results of tables 1, 2 and 3 to calculate the capacity values which are presented in Table 4a.

In eq.26 we assumed that a bus or a truck is always between two passenger vehicles and the passenger vehicle recognizes when its leader is a truck or a bus. This is a reasonable assumption because the radar sensors used for ranging measurements can be designed to be able to distinguish different classes of vehicles. Without this assumption each vehicle has to assume the worst possible situation which is the one where each vehicle treats its leader as a passenger vehicle i.e., a vehicle with the highest possible braking capability. In this case eq. 26 is modified to

$$C = (360000V)[(100-2W_T-2W_B)(L_P+h_{PP}V) + W_T(L_P+h_{PT}V+h_{PP}V+L_T) + W_B(L_P+h_{PB}V+h_{PP}V+L_B)]^{-1} \quad (27)$$

The capacity results for this case are listed in Table 4b.

4.5 Free Agent Vehicles - Infrastructure Supported

In the case of Free Agent Vehicles we assumed the braking scenario shown in figure 10. The use of vehicle to vehicle communication simplifies the task of determining when the leading vehicle is performing emergency braking. The leader at t = 0 starts performing emergency braking. At t = 0 it communicates its intention to the following vehicle. The following vehicle receives the information from the leader and verifies using its own sensors that it has to perform an emergency braking as well.

The assumptions regarding the initial conditions are the same as in the previous case: We assume the leader has been traveling at a speed of 60 miles per hour while the follower has an instantaneous velocity of 63 miles per hour and an instantaneous acceleration of 0.15g, as if the follower had been trying to catch up with the leader.

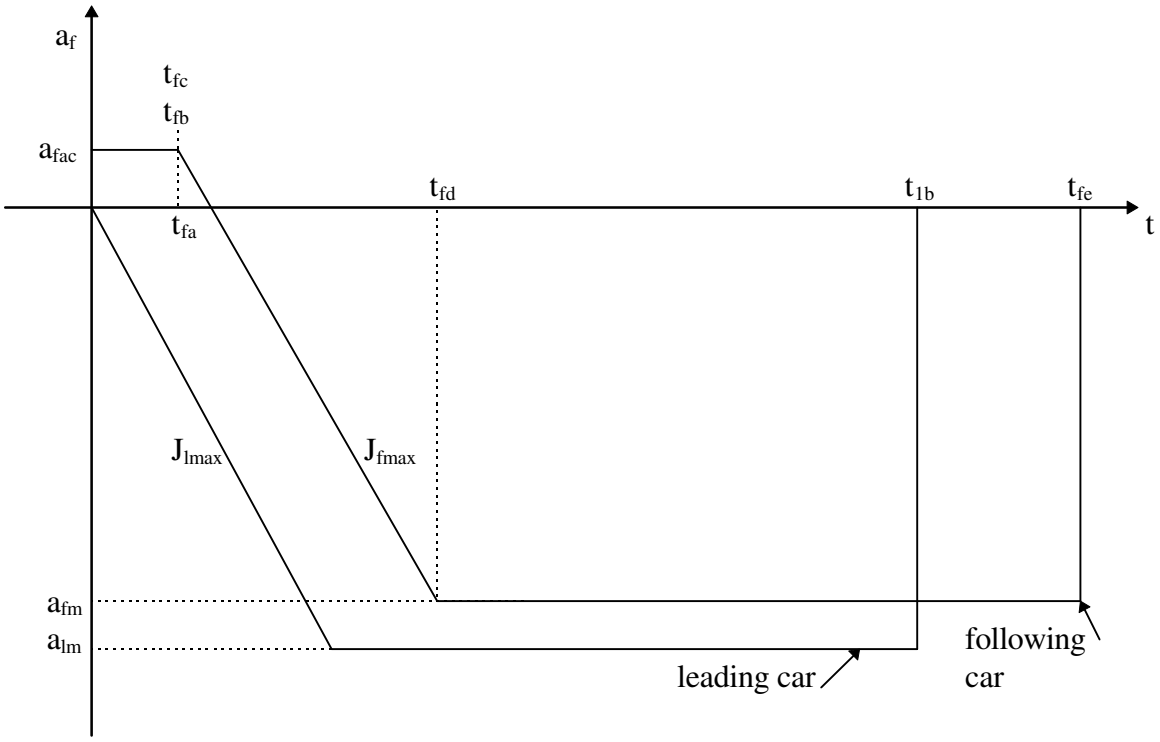

Figure 10: Infrastructure Supported Free Agent vehicles.

When the vehicle detects the leader is braking and at the same time receives the information that this is emergency braking, it bypasses the limited jerk / limited braking stage shown in figure 9 in the previous section. In figure 10, we have clustered the detection and the actuation delay into a single 0.1 seconds delay before the follower applies emergency braking. In effect, the actuation delay is compensated for by the fact that the vehicle knows in advance it will have to apply the brakes, and the brake actuator may be pre-loaded. Therefore in figure 10 we assume $t_{fa} = t_{fc} = 0.1$ sec. The minimum headway results together with the numerical values of the variables shown in figure 10 are presented in tables 5, 6 and 7. Equation (27) is used to calculate capacity for different levels of mixing of different classes of vehicles. The results are shown in Table 8.

4.6 Free Agent Vehicles - Infrastructure Managed

In the case of Free Agent Vehicles with infrastructure management we have assumed that the infrastructure has the primary responsibility of detecting the presence of emergencies and synchronizing the onset of emergency braking of all vehicles involved. This results in the most favorable timing for braking delays.

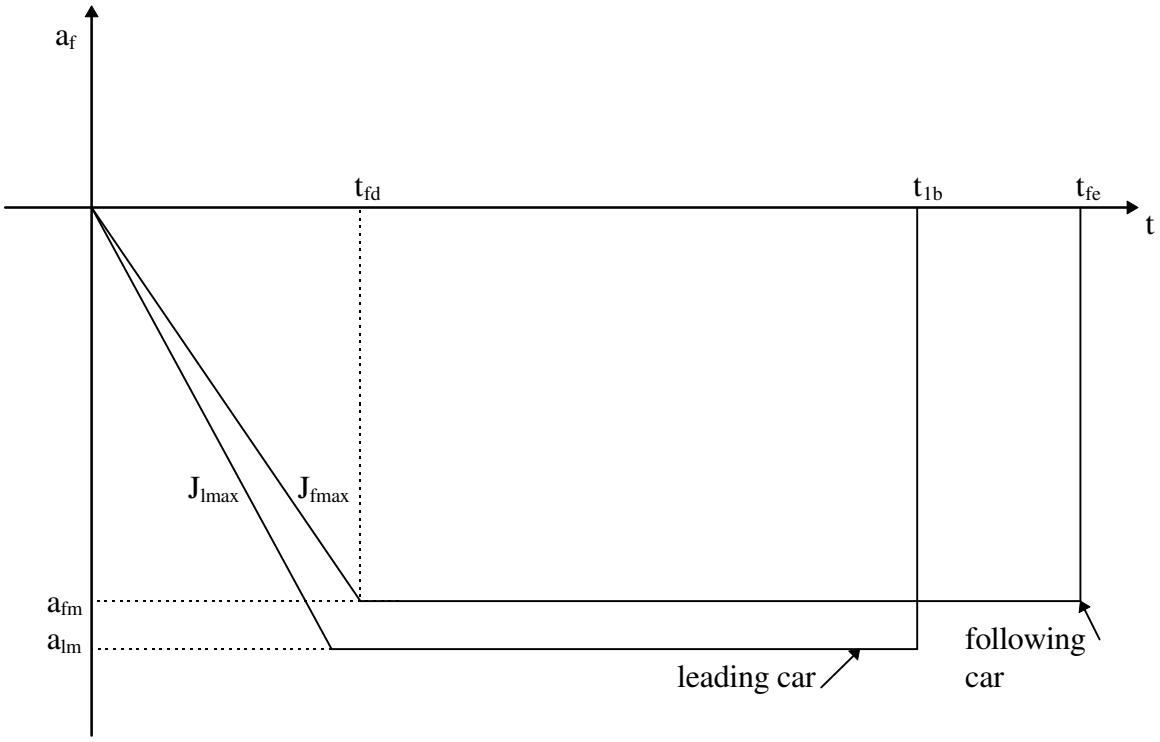

Figure 11: Infrastructure Managed Free Agent vehicles.

The infrastructure may simply issue the command "Begin emergency braking now" and all vehicles receiving this will have to apply maximum braking without further delay. This, not only simplifies the task of determining when the leading vehicle is performing emergency braking but also minimizes the relative delay in propagating the onset of emergency braking from each vehicle to the vehicle behind, effectively down to zero.

We have listed the actuation delay as a single 0.1 seconds delay before each vehicle applies emergency braking, but since all the vehicles receive the command at the same time the relative delay is zero and this is reflected in the value of the parameter t_{fc}. The time t_{fc} represents the total delay between the onset of emergency braking between the leader and the follower and in this case $t_{fc} = 0$.

The assumptions regarding the initial conditions are the same as before: The leader has been traveling at a speed of 60 miles per hour while the follower has an instantaneous velocity of 63 miles per hour and an instantaneous acceleration of 0.15g, as if the follower had been trying to catch up with the leader. The minimum headway results together with the numerical values of the variables shown in figure 11 are presented in tables 9, 10 and 11. Equation (27) is used to calculate capacity for different levels of mixing of different classes of vehicles. The results are shown in Table 12.

4.7 Vehicles Platoons without coordinated braking

In the platooning without coordinated braking case, we have assumed that each vehicle notifies the vehicle behind about its braking capabilities and the magnitude and timing of the braking force used.

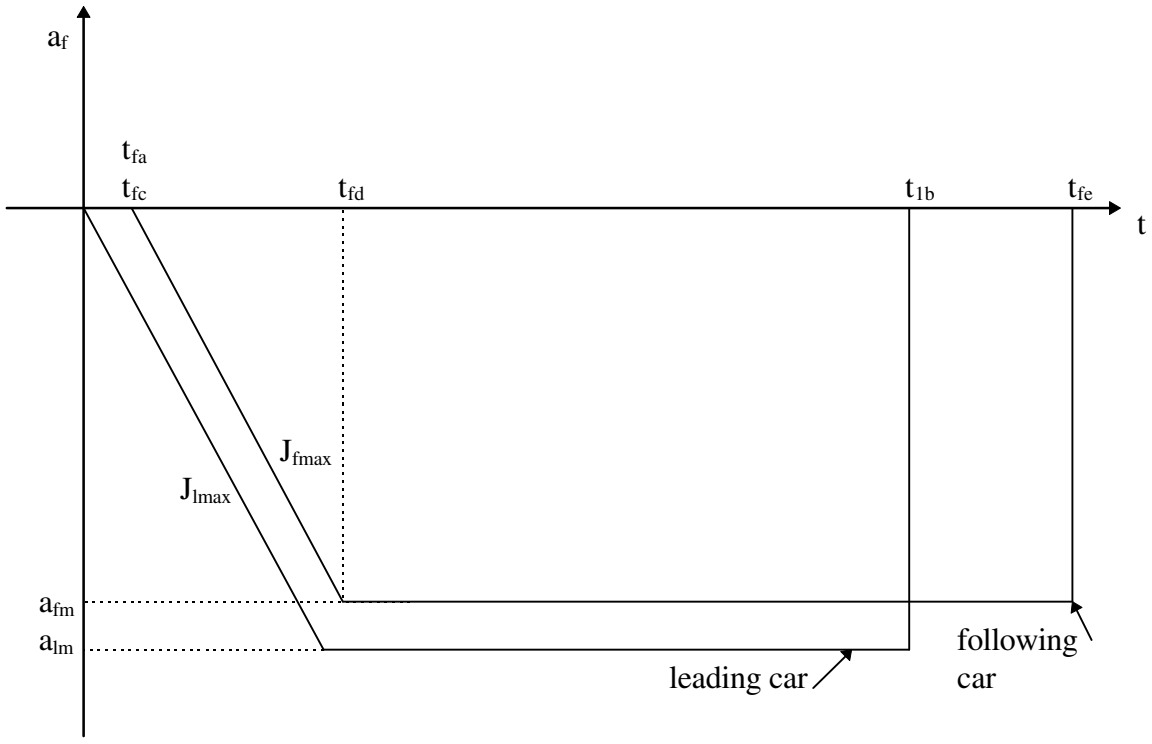

Figure 12: Platoons without coordinated braking.

When the platoon leader detects an emergency, it immediately notifies the vehicle that follows. There will be a delay while the message propagates from each vehicle to the vehicle behind, as well as an actuation delay. But the actuation delay is not affecting the scenario as long as it is approximately the same for each vehicle. We have assumed that the total delay is 0.1 seconds for every vehicle and it is represented by the parameter t_{fa}. Therefore we have accounted for only a 0.1 seconds total delay in propagating the message from each vehicle to the vehicle behind and this becomes the value of the parameter t_{fc}, which represents the delay of the onset of emergency braking.

The assumptions regarding initial conditions are as follows: The leader has been traveling at a speed of 60 miles per hour while the follower has an instantaneous velocity of 61.5 miles per hour. Since the platoon protocol involves a much tighter control of individual vehicle velocity than in the case of free agents, only a 2.5% difference is assumed in the initial vehicle velocities. The instantaneous acceleration was also taken to be 0g as it would be impossible for a vehicle in a platoon to be accelerating while the vehicle ahead is

maintaining constant speed. Both the velocities and the accelerations of vehicles in platoons are expected to be closely coordinated. In addition, for reasons explained earlier we assumed no mixing of vehicle classes.

The inter-platoon spacing depends on the concept used for platoon following. We compared three different concepts.

a) Autonomous platoons, where platoons do not communicate with each other and each platoon relies on its own sensors to detect the motion of a leading platoon. In this case, the inter-platoon spacing is calculated as in the case of autonomous vehicles. Therefore, each vehicle assumes $t_{fc} = 0.1$ seconds and each platoon entity assumes the parameters of autonomous vehicles: $t_{fc} = 0.3$ seconds for 10 car platoons and again $t_{fc} = 0.3$ seconds for 20 car platoons.

b) Free agent platoons supported by the infrastructure where the inter-platoon spacing is calculated as in the case of free agent vehicles with infrastructure support. Each vehicle in the platoon assumes $t_{fc} = 0.1$ seconds. Each platoon entity assumes the parameters of free agent infrastructure supported vehicles: $t_{fc} = 0.1$ seconds for 10 car platoons and $t_{fc} = 0.1$ seconds for 20 car platoons.

c) Free agent platoons managed by the infrastructure where the inter-platoon spacing is calculated as in the case of free agent vehicles with infrastructure management. Each vehicle in the platoon assumes $t_{fc} = 0.1$ seconds. Each platoon entity assumes the parameters of free agent infrastructure managed vehicles: $t_{fc} = 0$ seconds for 10 car platoons and $t_{fc} = 0$ seconds for 20 car platoons.

The capacity is calculated in each case using the equation:

$$C = (3600\ V\ N) / ((h_{pp}\ V + L_p)\ (N-1) + H_{pp}\ V + L_p) \qquad (28)$$

where L_p is the length of each vehicle in the platoon (we have assumed vehicles of same length), h_{pp} is the intra-platoon time headway, H_{pp} is the inter-platoon time headway and N is the number of vehicles in the platoon. The resulting intra-platoon spacing for platoons without coordinated braking can be found in Table 13. Allowing intervehicle collisions at up to 5 miles per hour yields the results of Table 13a. The capacity results with and without intervehicle collisions are presented in Table 14.

4.8 Vehicle Platoons with coordinated braking and no delay

In platooning with coordinated braking we assume that the vehicle in the platoon leader position assumes the primary responsibility of detecting emergencies and notifying each and every vehicle in the platoon. This notification takes place through a network style vehicle to vehicle communications system that minimizes the communication delays. The platoon leader notifies all the vehicle in the platoon about the magnitude of the braking

force that is to be applied and also the exact time this is to be applied. This architecture, not only eliminates the need for each vehicle to detect the magnitude of braking and if the braking should be limited or emergency braking, but also can adjust the onset of emergency braking for an effective 0 seconds relative delay, or even to an artificial negative relative delay.

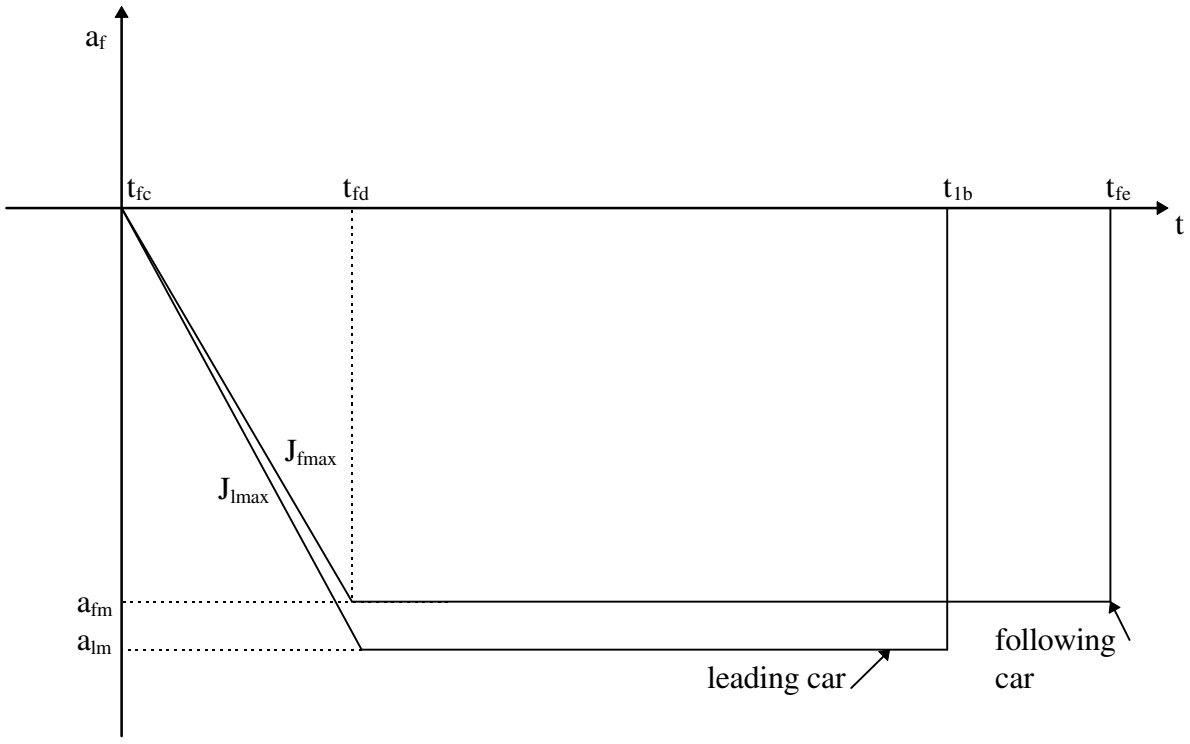

Figure 13: Platoons with coordinated braking and no delay.

The brake actuation delay can be completely compensated for and it is not affecting the scenario as long as it is approximately the same for each vehicle. We have assumed it is 0.1 seconds on every vehicle. Therefore we have made the assumption of exactly 0 seconds total delay for the onset of braking for each vehicle in the platoon and this is the value of the parameter t_{fc} which represents this delay.

The other assumptions regarding the initial conditions are the same as in all architectures involving platoons. The leader has been traveling at a speed of 60 miles per hour while the follower has an instantaneous velocity of 61.5 miles per hour. The instantaneous acceleration was also take to be 0g as it would be impossible for a vehicle in a platoon to be accelerating while the vehicle ahead is maintaining constant speed. Both the velocities and the accelerations of vehicles in platoons are expected to be closely coordinated.

For the inter-platoon spacing we used and compared three different concepts.

a) Autonomous platoons where the inter-platoon spacing is calculated as in the case of autonomous vehicles. Therefore, each vehicle assumes t_{fc} = 0 seconds and each platoon entity assumes the parameters of autonomous vehicles: t_{fc} = 0.3 seconds for 10 car platoons and again t_{fc} = 0.3 seconds for 20 car platoons.

b) Free agent platoons supported by the infrastructure where the inter-platoon spacing is calculated as in the case of free agent vehicles with infrastructure support. Each vehicle in the platoon assumes t_{fc} = 0 seconds. Each platoon entity assumes the parameters of free agent infrastructure supported vehicles: t_{fc} = 0.1 seconds for 10 car platoons and t_{fc} = 0.1 seconds for 20 car platoons.

c) Free agent platoons managed by the infrastructure where the inter-platoon spacing is calculated as in the case of free agent vehicles with infrastructure management. Each vehicle in the platoon assumes t_{fc} = 0 seconds. Each platoon entity assumes the parameters of free agent infrastructure managed vehicles: t_{fc} = 0 seconds for 10 car platoons and t_{fc} = 0 seconds for 20 car platoons.

The inter-platoon spacing results for platoons with coordinated braking are calculated using equation (28), based on the intra-platoon spacings presented in Table 15. Allowing intervehicle collisions at up to 5 miles per hour yields the results of Table 15a. The capacity results with and without intervehicle collisions are presented in Table 16.

4.9 Vehicle Platoons with coordinated braking and staggered timing

This case is identical to the previous one except for the purposeful timing of the onset of emergency braking. In the platooning with coordinated braking case we have assumed the vehicle in the platoon leader position assumes the primary responsibility of detecting emergencies and notifying each and every vehicle in the platoon. This notification takes place through a network style vehicle to vehicle communications system that minimizes the communication delays. The platoon leader notifies all the vehicles in the platoon about the magnitude of the braking force that is to be applied and also the exact time this is to be applied. This architecture, not only eliminates the need for each vehicle to detect the magnitude of braking and if the braking should be limited or emergency braking, but also can adjust the onset of emergency braking to an artificial negative relative delay.

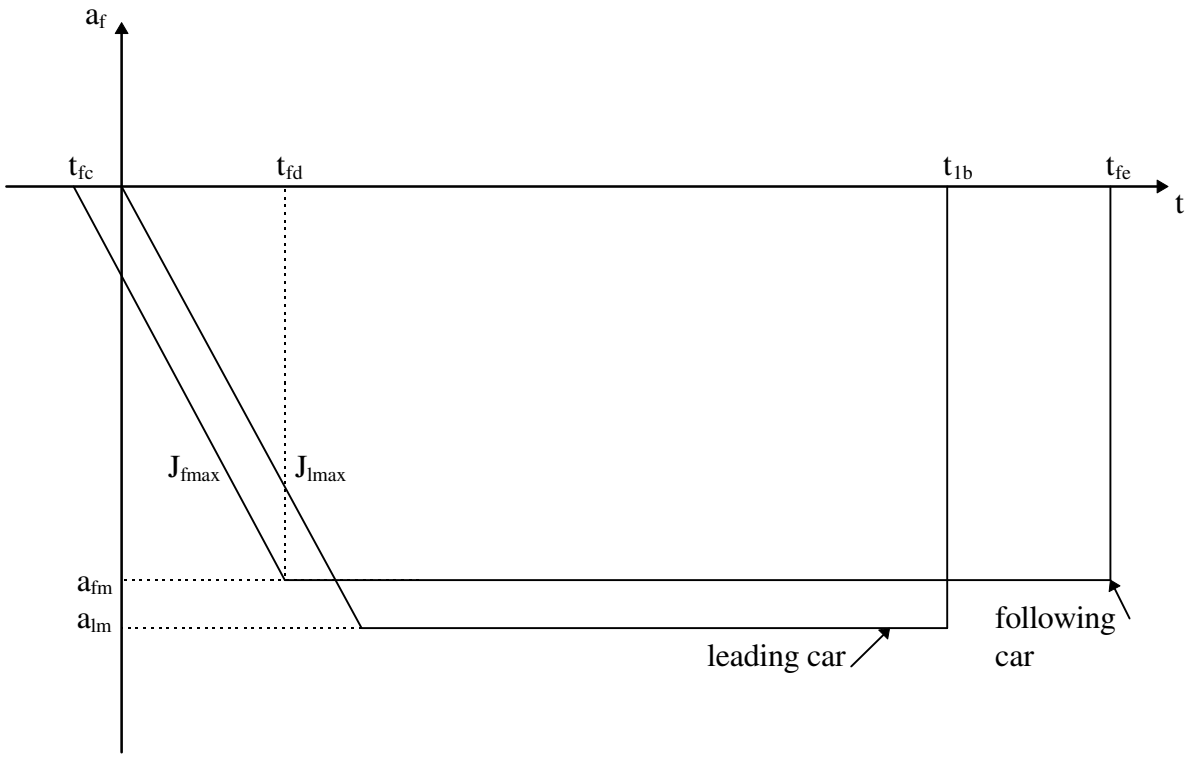

Figure 14: Platoons with coordinated braking with staggered delay.

Therefore we have made the choice of using a 0.1 seconds total delay for the onset of braking for each vehicle in the platoon going from the tail to the head, in the sense that the tail of the platoon is requested to brake first, then the vehicle ahead after a delay of 0.1 seconds, until the command to begin braking becomes effective for the platoon leader. Therefore we used a negative value, -0.1 seconds, as the value of the parameter t_{fc} which represents the relative delay for two consecutive vehicles within the platoon..

We cannot omit mentioning the fact that the platoon leader which detects the presence of emergency is subsequently restrained from braking until every other vehicle in the platoon has begun braking. Therefore, while this architecture allows us to minimize the necessary spacing between vehicles in the platoon, it increases the inter-platoon spacing requirement.

The other assumptions regarding the initial conditions are the same for all architectures involving platoons. For the inter-platoon spacing we used and compared several different concepts.

a) Autonomous platoons where the inter-platoon spacing is calculated as the sum of the inter-vehicle spacing used in the case of autonomous vehicles and the product of the coordinated braking delay with the number of vehicles in a platoon. Each vehicle in the

platoon assumes t_{fc} = -0.1 seconds. Each platoon entity assumes t_{fc} = 1.3 seconds for 10 car platoons and t_{fc} = 2.3 seconds for 20 car platoons.

b) Free agent platoons supported by the infrastructure where the inter-platoon spacing is calculated as the sum of the inter-vehicle spacing used in the case of free agent vehicles with infrastructure support and the product of the coordinated braking delay with the number of vehicles in a platoon. Each vehicle in the platoon assumes t_{fc} = -0.1 seconds. Each platoon entity assumes t_{fc} = 1.1 seconds for 10 car platoons and t_{fc} = 2.1 seconds for 20 car platoons.

c) Free agent platoons managed by the infrastructure where the inter-platoon spacing is calculated as the sum of the inter-vehicle spacing used in the case of free agent vehicles with infrastructure management and the product of the coordinated braking delay with the number of vehicles in a platoon. Each vehicle in the platoon assumes t_{fc} = -0.1 seconds.

Each platoon entity assumes t_{fc} = 1.0 seconds for 10 car platoons and t_{fc} = 2.0 seconds for 20 car platoons.

The capacity is calculated using the following formula:

$$C = (3600\ V\ N) / [(h_{pp}\ V + L_p)\ (N-1) + L_p + (H_{pp} + N\ t_b)\ V]$$

where L_p is the length of each vehicle in the platoon (we have assumed vehicles of same length), h_{pp} is the intra-platoon time headway, H_{pp} is the inter-platoon time headway, N is the number of vehicles in the platoon and t_b is the coordinated braking delay. The spacing is calculated using equation (29) based on the intra-platoon spacings given in Table 17. Allowing intervehicle collisions at up to 5 miles per hour yields the results of Table 17a. The capacity results with and without intervehicle collisions are presented in Table 18.

4.10 Infrastructure Managed Slotting

The infrastructure managed slotting concept involves a different set of assumptions and parameters. We have not presented it in detail in the tables, except one table which shows capacity estimates under this architecture concept. We used the spacing data for passenger cars by assuming a doubling of all communication delays with an additional 3 meters to account for position inaccuracy, due to the inability to utilize space effectively by using the exact slot size for each vehicle. We also assumed that the follower has no initial acceleration. The capacities computed under these assumptions can be found in Table 19.

5 DISCUSSION AND CONCLUSIONS.

The capacity estimates for each concept considered are summarized in Table 20. These results indicate that the capacity is reduced by 30% to 40% by going from dry road to wet road conditions under each concept. The capacity is also reduced by about 10% if all vehicles are required to use lower but similar braking force during emergency stopping. Mixing of different classes of vehicles reduces capacity by about 11% in the case of mixing 2.5% buses and 2.5% trucks with passenger vehicles and by about 23% for 5% buses and 5% trucks. Platooning with coordinated braking gives the highest capacity. Infrastructure managed slotting gives the lowest. The use of vehicle to vehicle communication for notifying vehicles about the onset of braking used in the Free Agent and Platooning based concepts helps increase capacity considerably.

The results developed are based on several assumptions regarding braking capabilities, worst case stopping scenarios etc. We tried to make these assumptions as realistic as possible, by using braking data from actual experiments and by considering a wide class of concepts that cover a wide range of AHS configurations. Despite this effort there are still a lot of uncertainties in the choice of intervehicle spacing that need to be addressed. The level of conservatism is one of them and is related to the trade off between safety and capacity. The frequency of failures on AHS operations that lead to the need for emergency braking is another uncertainty that depends on how AHS will be designed and operated. The results of this chapter are therefore qualitative in nature and can be used to compare the requirements and benefits of different AHS concepts.

ACKNOWLEDGMENT

This work was performed as part of the California PATH Program of the University of California, in cooperation with the State of California Business, Transportation and Housing Agency, Department of Transportation; and the United States Department of Transportation, Federal Highway Administration.

The contents of this chapter reflect the views of the authors who are responsible for the facts and the accuracy of the data presented herein. The contents do not necessarily reflect the official views or policies of the State of California. This chapter does not constitute a standard, specification, or regulation.

The authors would like to thank Steve Shladover, Jacob Tsao, Datta Godbole, and Jim Misener of PATH for many useful discussions on the subject of intervehicle spacing.

REFERENCES

[1] C. C. Chien Intelligent Vehicle Highway System (IVHS): "Advanced vehicle Control Systems." *Doctoral Dissertation*, University of Southern California, 1994.

[2] Y. Sun and P. Ioannou "A Handbook for Inter-Vehicle Spacing in Vehicle Following." *California PATH Research Report* UCB-ITS-PRR-95-1, University of Southern California, 1995.

[3] J. Glimm and R. Fenton "Dynamic Behavior of Strings of Automated Transit Vehicles." *SAE Paper Series,* No. 770288, 1977.

[4] W. L. Calson "Crash Injury Loss: The Effect of Speed, Weight and Crash Configuration. Accident Analysis and Prevention." 1977.

[5] M. Lenard, "Safety Consideration for a High Density Automated Vehicle System." General Electric Company, Erie, Pennsylvania, 1969.

[6] A. Rahimi *et al*. "Safety Analysis for Automated Transportation Systems." *Transportation Science, Page~1-17,* 1971.

[7] T. D. Gillespie. "Fundamentals of Vehicle Dynamics", Published by the SAE, 1992

[8] V. R. Vuchic. "Urban Public Transportation, Systems and Technology", Prentice-Hall, 1981

[9] *Consumer Reports magazine,* March to September 1995

[10] *Road and Track magazine,* April 1989 and October 1995

[11] NHTSA. "Heavy duty vehicle brake research program report no. 1. Stopping capability of air braked vehicles volume 1." Technical Report no. DOT HS 806 738, April 1985

[12] C.C. Chien and P. Ioannou. "Automatic vehicle following." *Proc. American Control Conference,* 1992

[13] J.K. Hedric, D. McMahon, V. Narendran, D. Swaroop. "Longitudinal vehicle controller design for IVHS systems." *Proc. American Control Conference,* pages 3107-3112, 1991

[14] P. Ioannou, F. Ahmed-Zaid, D. Wuh. "A time headway autonomous intelligent cruise controller: Design and simulation." Technical Report, USC-SCT 92-11-01, 1992

[15] P. Ioannou and C.C. Chien. "Autonomous intelligent cruise control." *IEEE Transactions on Vehicular Technology,* 42:657-672, Nov. 1993

[16] U. Karaslan, P. Varaiya, J. Walrand. "Two proposals to improve freeway traffic flow." Preprint, 1990

[17] B.S.Y. Rao, P. Varaiya, F. Eskafi. "Investigations into achievable capacities and stream stability with coordinated intelligent vehicles." PATH Technical Report, 1992

[18] S. Sheikholeslam, C.A. Desoer "A system level study of the longitudinal control of a platoon of vehicles." *ASME Journal of Dynamic System, Measurement and Control,* 1991

[19] S.E. Shladover. "Longitudinal control of automotive vehicles in close-formation platoons." *ASME Journal of Dynamic Systems, Measurement and Control,* 113:231-241, 1991

[20] A. Stotsky, C.C. Chien, P. Ioannou. "Robust platoon-stable controller design for autonomous intelligent vehicles." *Proceedings of the 33rd Conference on Decision and Control,* Florida, December 1994

[21] S. Swaroop, C.C. Chien, P. Ioannou, J.K. Hedrick. "A comparison of spacing and headway control laws for automatically controlled vehicles." *Journal of Vehicle System Dynamics,* 1993

[22] A. Sage, editor, "System Design for Human Interaction." IEEE Press, 1987

[23] S.E. Shladover, C.A. Desoer, J.K Hedrick, M. Tomizuka, J. Walrand, W.B. Zhang, D.McMahon, S. Sheikholeslam, "Automatic vehicle control developments in the PATH program." *IEEE Transactions on Vehicular Technology,* 40:114-130, 1991

[24] B.W. Stuck, E. Arthurs "A Computer Communications Network Performance Analysis Primer", Prentice Hall, 1985

Appendix A: Vehicular data references

Table A.1

Braking performance comparisons of popular passenger vehicles on dry and wet roads. (from Consumer Reports, March 1995) (Family sedans)						
	DRY			WET		
	Initial Velocity	Stopping Distance	Deceler/n (avg. g)	Initial Velocity	Stopping Distance	Deceler/n (avg. g)
Chrysler Cirrus Lxi	60 mph	145 ft	0.83 g	60 mph	167 ft	0.72 g
Mercury Mystique LS	60 mph	140 ft	0.86 g	60 mph	165 ft	0.73 g
Ford Contour GL	60 mph	148 ft	0.81 g	60 mph	158 ft	0.76 g
Honda Accord LX	60 mph	143 ft	0.84 g	60 mph	175 ft	0.69 g

Braking performance comparisons on Dry and Wet roads of popular passenger vehicles (from Consumer Reports, May 1995) (Upscale sedans)						
	DRY			WET		
	Initial Velocity	Stopping Distance	Deceler/n (avg. g)	Initial Velocity	Stopping Distance	Deceler/n (avg. g)
Toyota Avalon XLS	60 mph	129 ft	0.93 g	60 mph	146 ft	0.82 g
Mazda Millenia S	60 mph	136 ft	0.88 g	60 mph	157 ft	0.77 g
Lexus ES300	60 mph	133 ft	0.90 g	60 mph	167 ft	0.72 g
Oldsmobile Aurora	60 mph	136 ft	0.88 g	60 mph	155 ft	0.78 g

Braking performance comparisons on Dry and Wet roads of popular passenger vehicles (from Consumer Reports, June 1995) (Low-Priced Sedans)						
	DRY			WET		
	Initial Velocity	Stopping Distance	Deceler/n (avg. g)	Initial Velocity	Stopping Distance	Deceler/n (avg. g)
Mazda Protege ES	60 mph	135 ft	0.89 g	60 mph	167 ft	0.72 g
Chevrolet Cavalier LS	60 mph	133 ft	0.90 g	60 mph	165 ft	0.73 g
Nissan Sentra GXE	60 mph	142 ft	0.85 g	60 mph	158 ft	0.76 g
Saturn SL2	60 mph	138 ft	0.87 g	60 mph	157 ft	0.77 g

Table A.2

Braking performance comparisons on Dry and Wet roads of popular passenger vehicles (from Consumer Reports, July 1995) (Mid-Sized Coupes)						
	DRY			WET		
	Initial Velocity	Stopping Distance	Deceler/n (avg. g)	Initial Velocity	Stopping Distance	Deceler/n (avg. g)
Dodge Avenger ES	60 mph	129 ft	0.93 g	60 mph	157 ft	0.77 g
Ford Thunderbird LX	60 mph	131 ft	0.92 g	60 mph	153 ft	0.79 g
Chevrolet Monte Carlo Z34	60 mph	139 ft	0.87 g	60 mph	165 ft	0.73 g
Buick Riviera	60 mph	133 ft	0.90 g	60 mph	147 ft	0.82 g

Braking performance comparisons on Dry and Wet roads of popular passenger vehicles (from Consumer Reports, August 1995) (Sport-utility vehicles)						
	DRY			WET		
	Initial Velocity	Stopping Distance	Deceler/n (avg. g)	Initial Velocity	Stopping Distance	Deceler/n (avg. g)
Ford Explorer	60 mph	148 ft	0.81 g	60 mph	181 ft	0.66 g
Jeep Grand Cherokee	60 mph	144 ft	0.84 g	60 mph	159 ft	0.76 g
Chevrolet Blazer	60 mph	156 ft	0.77 g	60 mph	172 ft	0.70 g
Land Rover Discovery	60 mph	143 ft	0.84 g	60 mph	202 ft	0.60 g

Braking performance comparisons on Dry and Wet roads of popular passenger vehicles (from Consumer Reports, September 1995) (Small, Cheap Cars)						
	DRY			WET		
	Initial Velocity	Stopping Distance	Deceler/n (avg. g)	Initial Velocity	Stopping Distance	Deceler/n (avg. g)
Hyundai Accent 4-door	60 mph	137 ft	0.88 g	60 mph	172 ft	0.70 g
Hyundai Accent 2-door L	60 mph	145 ft	0.83 g	60 mph	204 ft	0.59 g
Toyota Tercel 4-door DX	60 mph	156 ft	0.77 g	60 mph	195 ft	0.62 g
Toyota Tercel 2-door base	60 mph	153 ft	0.79 g	60 mph	193 ft	0.62 g
Geo Metro 4-door LSi	60 mph	151 ft	0.80 g	60 mph	172 ft	0.70 g
Geo Metro 2-door LSi	60 mph	152 ft	0.79 g	60 mph	199 ft	0.60 g

Table A.3

Braking performance comparisons of seven 4-wheel drive vehicles on dry roads and on snow. (from Road and Track, April 1989)						
		DRY			SNOW	
	Initial Velocity	Stopping Distance	Deceler/n (avg. g)	Initial Velocity	Stopping Distance	Deceler/n (avg. g)
BMW 325iX	60 mph	142 ft	0.85 g	20 mph	75 ft	0.18 g
Audi 90 Quatro	60 mph	143 ft	0.84 g	20 mph	99 ft	0.14 g
VW Quantum GL5	60 mph	145 ft	0.83 g	20 mph	59 ft	0.23 g
Toyota Celica All-Trac	60 mph	146 ft	0.82 g	20 mph	80 ft	0.17 g
Subaru Justy 4WD GL	60 mph	151 ft	0.80 g	20 mph	63 ft	0.21 g
Subaru XT6 4WD	60 mph	153 ft	0.79 g	20 mph	49 ft	0.27 g
Pontiac 6000 STE 4WD	60 mph	N/A	N/A	20 mph	56 ft	0.24 g

Braking performance comparisons on dry roads of passenger vehicles representing extremes (from Road and Track, October 1995)						
		DRY			DRY	
	Initial Velocity	Stopping Distance	Deceler/n (avg. g)	Initial Velocity	Stopping Distance	Deceler/n (avg. g)
BMW 325i	60 mph	126 ft	0.95 g	80 mph	212 ft	1.01 g
Chevrolet Corvette LT1	60 mph	123 ft	0.98 g	80 mph	225 ft	0.95 g
Ford Mustang Cobra	60 mph	123 ft	0.98 g	80 mph	214 ft	1.00 g
Toyota Supra Turbo	60 mph	122 ft	0.99 g	80 mph	208 ft	1.03 g
Porsche 911 Turbo	60 mph	116 ft	1.04 g	80 mph	199 ft	1.07 g
BMW 740i	60 mph	144 ft	0.84 g	80 mph	255 ft	0.84 g
Chevrolet Camaro V6	60 mph	162 ft	0.74 g	80 mph	282 ft	0.76 g
Mercury Villager	60 mph	178 ft	0.68 g	80 mph	293 ft	0.73 g
Toyota Corolla DX	60 mph	186 ft	0.65 g	80 mph	319 ft	0.67 g
VW Golf III GL	60 mph	175 ft	0.69 g	80 mph	301 ft	0.71 g

Braking performance comparisons on dry roads of air braked heavy duty vehicles (From NHTSA test data)						
	Initial Velocity	Stopping Distance	Deceler/n (avg. g)	Initial Velocity	Stopping Distance	Deceler/n (avg. g)
IH School Bus	20 mph	28 ft	0.48 g	60 mph	310 ft	0.34 g
Ford/IH Short School Bus	20 mph	36 ft	0.37 g	60 mph	375 ft	0.32 g
Thomas Transit Bus	20 mph	36 ft	0.37 g	60 mph	292 ft	0.41 g
Ford 4 by 2 Truck	20 mph	36 ft	0.37 g	60 mph	331 ft	0.36 g
GMC 6 by 4 Truck	20 mph	54 ft	0.25 g	60 mph	528 ft	0.23 g
Mack 6 by 4 Truck	20 mph	44 ft	0.30 g	60 mph	363 ft	0.33 g
Peterbilt 4 by 2 Tractor	20 mph	39 ft	0.34 g	60 mph	407 ft	0.30 g
Ford 4 by 2 Tractor	20 mph	30 ft	0.45 g	60 mph	289 ft	0.42 g
White 4 by 2 Tractor	20 mph	42 ft	0.32 g	60 mph	366 ft	0.33 g
IH 6 by 4 Tractor	20 mph	51 ft	0.26 g	60 mph	475 ft	0.25 g
Western Star 6 by 4 tractor	20 mph	46 ft	0.29 g	60 mph	431 ft	0.28 g
Stuart Conv. auto hauler	20 mph	43 ft	0.31 g	60 mph	434 ft	0.28 g
Stuart Stringer auto hauler	20 mph	39 ft	0.34 g	60 mph	354 ft	0.34 g

Appendix B: Tables of results

Table B.1 Symbols and Notation

PP: Passenger car leader, Passenger car follower
PB: Passenger car leader, Bus follower
PT: Passenger car leader, Truck follower

BP: Bus leader, Passenger car follower
BB: Bus leader, Bus follower
BT: Bus leader, Truck follower

TP: Truck leader, Passenger car follower
TB: Truck leader, Bus follower
TT: Truck leader, Truck follower

$L_{P:}$ Length of a passenger vehicle, in meters
$L_{B:}$ Length of a bus, in meters
$L_{T:}$ Length of a truck with trailer, in meters

$h_{PP:}$ Minimum time headway between Passenger car leader Passenger car follower, in sec.
$h_{PB:}$ Minimum time headway between Passenger car leader, Bus follower, in seconds
$h_{PT:}$ Minimum time headway between Passenger car leader, Truck follower, in seconds
$h_{BP:}$ Minimum time headway between Bus leader, Passenger car follower, in seconds
$h_{BB:}$ Minimum time headway between Bus leader, Bus follower, in seconds
$h_{BT:}$ Minimum time headway between Bus leader, Truck follower, in seconds
$h_{TP:}$ Minimum time headway between Truck leader, Passenger car follower, in seconds
$h_{TB:}$ Minimum time headway between Truck leader, Bus follower, in seconds
$h_{TT:}$ Minimum time headway between Truck leader, Truck follower, in seconds

V_{lo}: Leading Vehicle initial Velocity, in miles per hour.
V_{fo}: Following Vehicle initial Velocity, in miles per hour.
A_{lm}: The maximum achievable deceleration of the leading vehicle in g
A_{fm}: The maximum achievable deceleration of the leading vehicle in g
J_{lmax}: The maximum achievable jerk of the leading vehicle in meters/sec^3
J_{fmax}: The maximum achievable jerk of the following vehicle in meters/sec^3
μ_{lmax}: The maximum road-tire friction coefficient (dimensionless)
μ_{fmax}: The maximum road-tire friction coefficient (dimensionless)
A_{fauto}: The acceleration value under automatic brake control during soft braking, in g
A_{fac}: The initial acceleration value during vehicle following, in g
J_{fc}: The jerk value under automatic brake control during soft braking, in meters/sec^3
t_{fa} : Detection and brake actuation delay applicable to the following vehicle, in seconds.
t_{fc}: The time at which the following vehicle starts the emergency braking maneuver, in seconds

Table 1: Autonomous Vehicles, Dry road surface

		P P	**P B**	**P T**	**B P**	**B B**	**B T**	**T P**	**T B**	**T T**
V_{lo}	mph	60	60	60	60	60	60	60	60	60
V_{fo}	mph	63	63	63	63	63	63	63	63	63
A_{lmax}	g	0.8	0.8	0.8	0.4	0.4	0.4	0.3	0.3	0.3
A_{fmax}	g	0.72	0.36	0.27	0.72	0.36	0.27	0.72	0.36	0.27
J_{lmax}	m/s^3	50	50	50	40	40	40	30	30	30
J_{fmax}	m/s^3	50	40	30	50	40	30	50	40	30
μ_{lmax}		1	1	1	1	1	1	1	1	1
μ_{fmax}		1	1	1	1	1	1	1	1	1
A_{fauto}	g	0.1	0.1	0.1	0.1	0.1	0.1	0.1	0.1	0.1
A_{fac}	g	0.15	0.15	0.15	0.15	0.15	0.15	0.15	0.15	0.15
J_{fc}	m/s^3	5	5	5	5	5	5	5	5	5
t_{fa}	sec	0.2	0.2	0.2	0.2	0.2	0.2	0.2	0.2	0.2
t_{fc}	sec	0.3	0.3	0.3	0.3	0.3	0.3	0.3	0.3	0.3
min headway	sec	**0.66**	**2.63**	**3.97**	**0.063**	**1.04**	**2.37**	**0.045**	**0.171**	**1.28**
min headway	m	18.71	74.2	111.7	1.79	29.15	66.63	1.29	4.81	36.07

Table 2: Autonomous Vehicles, Wet road surface

		P P	**P B**	**P T**	**B P**	**B B**	**B T**	**T P**	**T B**	**T T**
V_{lo}	mph	60	60	60	60	60	60	60	60	60
V_{fo}	mph	63	63	63	63	63	63	63	63	63
A_{lmax}	g	0.8	0.8	0.8	0.4	0.4	0.4	0.3	0.3	0.3
A_{fmax}	g	0.72	0.36	0.27	0.72	0.36	0.27	0.72	0.36	0.27
J_{lmax}	m/s^3	50	50	50	40	40	40	30	30	30
J_{fmax}	m/s^3	50	40	30	50	40	30	50	40	30
μ_{lmax}		0.5	0.5	0.5	0.5	0.5	0.5	0.5	0.5	0.5
μ_{fmax}		0.5	0.5	0.5	0.5	0.5	0.5	0.5	0.5	0.5
A_{fauto}	g	0.1	0.1	0.1	0.1	0.1	0.1	0.1	0.1	0.1
A_{fac}	g	0.15	0.15	0.15	0.15	0.15	0.15	0.15	0.15	0.15
J_{fc}	m/s^3	5	5	5	5	5	5	5	5	5
t_{fa}	sec	0.2	0.2	0.2	0.2	0.2	0.2	0.2	0.2	0.2
t_{fc}	sec	0.3	0.3	0.3	0.3	0.3	0.3	0.3	0.3	0.3
min headway	sec	**1.03**	**4.99**	**7.65**	**0.065**	**1.77**	**4.43**	**0.049**	**0.211**	**2.26**
min headway	m	29.01	140.7	215.6	1.847	49.77	124.7	1.379	5.937	63.57

Table 3: Autonomous Vehicles - Uniform braking - Dry road

		P P	P B	P T	B P	B B	B T	T P	T B	T T
V_{lo}	mph	60	60	60	60	60	60	60	60	60
V_{fo}	mph	63	63	63	63	63	63	63	63	63
A_{lmax}	g	0.5	0.5	0.5	0.3	0.3	0.3	0.2	0.2	0.2
A_{fmax}	g	0.475	0.285	0.19	0.475	0.285	0.19	0.475	0.285	0.19
J_{lmax}	m/s^3	50	50	50	40	40	40	30	30	30
J_{fmax}	m/s^3	50	40	30	50	40	30	50	40	30
μ_{lmax}		1	1	1	1	1	1	1	1	1
μ_{fmax}		1	1	1	1	1	1	1	1	1
A_{fauto}	g	0.1	0.1	0.1	0.1	0.1	0.1	0.1	0.1	0.1
A_{fac}	g	0.15	0.15	0.15	0.15	0.15	0.15	0.15	0.15	0.15
J_{fc}	m/s^3	5	5	5	5	5	5	5	5	5
t_{fa}	sec	0.2	0.2	0.2	0.2	0.2	0.2	0.2	0.2	0.2
t_{fc}	sec	0.3	0.3	0.3	0.3	0.3	0.3	0.3	0.3	0.3
min headway	sec	**0.72**	**2.73**	**5.25**	**0.075**	**1.00**	**3.52**	**0.045**	**0.100**	**1.36**
min headway	m	20.33	76.83	147.7	2.112	28.27	99.15	1.290	2.833	38.19

Table 4: Autonomous Vehicles. Capacity Estimates under different road conditions, with and without detection ability.

a) With Identification of different vehicle classes	**Dry road surface**	**Wet road surface**	**Uniform braking**
0% mixing	4116	2860	3850
5% buses	3746	2516	3525
5% trucks	3458	2278	3096
2.5% buses + 2.5% trucks	3596	2391	3297
5% buses + 5% trucks	3193	2054	2882
b) No identification of different vehicle classes	**Dry road surface**	**Wet road surface**	**Uniform braking**
0% mixing	4116	2860	3850
5% buses	3631	2432	3416
5% trucks	3356	2207	3007
2.5% buses + 2.5% trucks	3488	2314	3198
5% buses + 5% trucks	3026	1943	2735

Table 5: Free Agent Vehicles - Infrastructure Supported - Dry road

		P P	**P B**	**P T**	**B P**	**B B**	**B T**	**T P**	**T B**	**T T**
V_{lo}	mph	60	60	60	60	60	60	60	60	60
V_{fo}	mph	63	63	63	63	63	63	63	63	63
A_{lmax}	g	0.8	0.8	0.8	0.4	0.4	0.4	0.3	0.3	0.3
A_{fmax}	g	0.72	0.36	0.27	0.72	0.36	0.27	0.72	0.36	0.27
J_{lmax}	m/s^3	50	50	50	40	40	40	30	30	30
J_{fmax}	m/s^3	50	40	30	50	40	30	50	40	30
μ_{lmax}		1	1	1	1	1	1	1	1	1
μ_{fmax}		1	1	1	1	1	1	1	1	1
A_{fauto}	g	0.1	0.1	0.1	0.1	0.1	0.1	0.1	0.1	0.1
A_{fac}	g	0.15	0.15	0.15	0.15	0.15	0.15	0.15	0.15	0.15
J_{fc}	m/s^3	10	10	10	10	10	10	10	10	10
t_{fa}	sec	0.1	0.1	0.1	0.1	0.1	0.1	0.1	0.1	0.1
t_{fc}	sec	0.1	0.1	0.1	0.1	0.1	0.1	0.1	0.1	0.1
min headway	sec	**0.463**	**2.432**	**3.762**	**0.027**	**0.832**	**2.162**	**0.021**	**0.088**	**1.077**
min headway	m	13.03	68.50	106.0	0.784	23.45	60.91	0.600	2.466	30.35

Table 6: Free Agent Vehicles - Infrastructure Supported - Wet road

		P P	**P B**	**P T**	**B P**	**B B**	**B T**	**T P**	**T B**	**T T**
V_{lo}	mph	60	60	60	60	60	60	60	60	60
V_{fo}	mph	63	63	63	63	63	63	63	63	63
A_{lmax}	g	0.8	0.8	0.8	0.4	0.4	0.4	0.3	0.3	0.3
A_{fmax}	g	0.72	0.36	0.27	0.72	0.36	0.27	0.72	0.36	0.27
J_{lmax}	m/s^3	50	50	50	40	40	40	30	30	30
J_{fmax}	m/s^3	50	40	30	50	40	30	50	40	30
μ_{lmax}		0.5	0.5	0.5	0.5	0.5	0.5	0.5	0.5	0.5
μ_{fmax}		0.5	0.5	0.5	0.5	0.5	0.5	0.5	0.5	0.5
A_{fauto}	g	0.1	0.1	0.1	0.1	0.1	0.1	0.1	0.1	0.1
A_{fac}	g	0.15	0.15	0.15	0.15	0.15	0.15	0.15	0.15	0.15
J_{fc}	m/s^3	10	10	10	10	10	10	10	10	10
t_{fa}	sec	0.1	0.1	0.1	0.1	0.1	0.1	0.1	0.1	0.1
t_{fc}	sec	0.1	0.1	0.1	0.1	0.1	0.1	0.1	0.1	0.1
min headway	sec	**0.828**	**4.792**	**7.451**	**0.037**	**1.564**	**4.224**	**0.028**	**0.140**	**2.054**
min headway	m	23.34	135.0	210.0	1.039	44.07	119.0	0.800	3.951	57.85

Table 7: Free Agent Vehicles - Infrastructure Supported - Uniform braking - Dry road

		P P	P B	P T	B P	B B	B T	T P	T B	T T
V_{lo}	mph	60	60	60	60	60	60	60	60	60
V_{fo}	mph	63	63	63	63	63	63	63	63	63
A_{lmax}	g	0.5	0.5	0.5	0.3	0.3	0.3	0.2	0.2	0.2
A_{fmax}	g	0.475	0.285	0.19	0.475	0.285	0.19	0.475	0.285	0.19
J_{lmax}	m/s^3	50	50	50	40	40	40	30	30	30
J_{fmax}	m/s^3	50	40	30	50	40	30	50	40	30
μ_{lmax}		1	1	1	1	1	1	1	1	1
μ_{fmax}		1	1	1	1	1	1	1	1	1
A_{fauto}	g	0.1	0.1	0.1	0.1	0.1	0.1	0.1	0.1	0.1
A_{fac}	g	0.15	0.15	0.15	0.15	0.15	0.15	0.15	0.15	0.15
J_{fc}	m/s^3	10	10	10	10	10	10	10	10	10
t_{fa}	sec	0.1	0.1	0.1	0.1	0.1	0.1	0.1	0.1	0.1
t_{fc}	sec	0.1	0.1	0.1	0.1	0.1	0.1	0.1	0.1	0.1
min headway	sec	**0.519**	**2.525**	**5.041**	**0.036**	**0.800**	**3.317**	**0.023**	**0.058**	**1.151**
min headway	m	14.64	71.11	142.0	1.030	22.55	93.44	0.668	1.638	32.43

Table 8: Free Agent Vehicles - Infrastructure Supported. Capacity Estimates

	Dry road surface	Wet road surface	Uniform braking
0% mixing	5400	3425	4942
5% buses	4730	2923	4377
5% trucks	4276	2605	3730
2.5% buses + 2.5% trucks	4492	2755	4025
5% buses + 5% trucks	3845	2304	3400

Table 9: Free Agent Vehicles - Infrastructure Managed - Dry road

		P P	P B	P T	B P	B B	B T	T P	T B	T T
V_{lo}	mph	60	60	60	60	60	60	60	60	60
V_{fo}	mph	63	63	63	63	63	63	63	63	63
A_{lmax}	g	0.8	0.8	0.8	0.4	0.4	0.4	0.3	0.3	0.3
A_{fmax}	g	0.72	0.36	0.27	0.72	0.36	0.27	0.72	0.36	0.27
J_{lmax}	m/s^3	50	50	50	40	40	40	30	30	30
J_{fmax}	m/s^3	50	40	30	50	40	30	50	40	30
μ_{lmax}		1	1	1	1	1	1	1	1	1
μ_{fmax}		1	1	1	1	1	1	1	1	1
A_{fauto}	g	0.1	0.1	0.1	0.1	0.1	0.1	0.1	0.1	0.1
A_{fac}	g	0.15	0.15	0.15	0.15	0.15	0.15	0.15	0.15	0.15
J_{fc}	m/s^3	20	20	20	20	20	20	20	20	20
t_{fa}	sec	0	0	0	0	0	0	0	0	0
t_{fc}	sec	0	0	0	0	0	0	0	0	0
min headway	sec	**0.36**	**2.327**	**3.655**	**0.014**	**0.73**	**2.056**	**0.012**	**0.054**	**0.971**
min headway	m	10.15	65.55	103.0	0.409	20.5	57.91	0.326	1.538	27.35

Table 10: Free Agent Vehicles - Infrastructure Managed - Wet road

		P P	P B	P T	B P	B B	B T	T P	T B	T T
V_{lo}	mph	60	60	60	60	60	60	60	60	60
V_{fo}	mph	63	63	63	63	63	63	63	63	63
A_{lmax}	g	0.8	0.8	0.8	0.4	0.4	0.4	0.3	0.3	0.3
A_{fmax}	g	0.72	0.36	0.27	0.72	0.36	0.27	0.72	0.36	0.27
J_{lmax}	m/s^3	50	50	50	40	40	40	30	30	30
J_{fmax}	m/s^3	50	40	30	50	40	30	50	40	30
μ_{lmax}		0.5	0.5	0.5	0.5	0.5	0.5	0.5	0.5	0.5
μ_{fmax}		0.5	0.5	0.5	0.5	0.5	0.5	0.5	0.5	0.5
A_{fauto}	g	0.1	0.1	0.1	0.1	0.1	0.1	0.1	0.1	0.1
A_{fac}	g	0.15	0.15	0.15	0.15	0.15	0.15	0.15	0.15	0.15
J_{fc}	m/s^3	20	20	20	20	20	20	20	20	20
t_{fa}	sec	0	0	0	0	0	0	0	0	0
t_{fc}	sec	0	0	0	0	0	0	0	0	0
min headway	sec	**0.726**	**4.687**	**7.344**	**0.025**	**1.460**	**4.117**	**0.019**	**0.109**	**1.947**
min headway	m	20.46	132.0	206.9	0.697	41.12	116.0	0.546	3.066	54.85

Table 11: Free Agent Vehicles - Infrastructure Managed - Uniform braking - Dry road

		P P	P B	P T	B P	B B	B T	T P	T B	T T
V_{lo}	mph	60	60	60	60	60	60	60	60	60
V_{fo}	mph	63	63	63	63	63	63	63	63	63
A_{lmax}	g	0.5	0.5	0.5	0.3	0.3	0.3	0.2	0.2	0.2
A_{fmax}	g	0.475	0.285	0.19	0.475	0.285	0.19	0.475	0.285	0.19
J_{lmax}	m/s^3	50	50	50	40	40	40	30	30	30
J_{fmax}	m/s^3	50	40	30	50	40	30	50	40	30
μ_{lmax}		1	1	1	1	1	1	1	1	1
μ_{fmax}		1	1	1	1	1	1	1	1	1
A_{fauto}	g	0.1	0.1	0.1	0.1	0.1	0.1	0.1	0.1	0.1
A_{fac}	g	0.15	0.15	0.15	0.15	0.15	0.15	0.15	0.15	0.15
J_{fc}	m/s^3	20	20	20	20	20	20	20	20	20
t_{fa}	sec	0	0	0	0	0	0	0	0	0
t_{fc}	sec	0	0	0	0	0	0	0	0	0
min headway	sec	**0.416**	**2.43**	**4.93**	**0.021**	**0.695**	**3.21**	**0.014**	**0.040**	**1.042**
min headway	m	11.72	68.13	138.9	0.602	19.56	90.36	0.404	1.123	29.36

Table 12: Free Agent Vehicles - Infrastructure Managed. Capacity Estimates

	Dry road surface	Wet road surface	Uniform braking
0% mixing	6437	3823	5810
5% buses	5472	3197	5018
5% trucks	4873	2820	4184
2.5% buses + 2.5% trucks	5155	2997	4563
5% buses + 5% trucks	4299	2464	3756

Table 13: Platoons without coordinated braking

		DRY	WET	UNIFORM
V_{lo}	mph	60	60	60
V_{fo}	mph	61.5	61.5	61.5
A_{lmax}	g	0.8	0.8	0.5
A_{fmax}	g	0.72	0.72	0.475
J_{lmax}	m/s^3	50	50	50
J_{fmax}	m/s^3	50	50	50
μ_{lmax}		1	0.5	1
μ_{fmax}		1	0.5	1
A_{fauto}	g	0	0	0
A_{fac}	g	0	0	0
J_{fc}	m/s^3	20	20	20
t_{fa}	sec	0.1	0.1	0.1
t_{fc}	sec	0.1	0.1	0.1
min headway	sec	**0.37**	**0.65**	**0.38**
min headway	m	10.26	17.93	10.48

Table 13a: Platoons without coordinated braking allowing 5mph collisions

		DRY	WET	UNIFORM
V_{lo}	mph	60	60	60
V_{fo}	mph	61.5	61.5	61.5
A_{lmax}	g	0.8	0.8	0.5
A_{fmax}	g	0.72	0.72	0.475
J_{lmax}	m/s^3	50	50	50
J_{fmax}	m/s^3	50	50	50
μ_{lmax}		1	0.5	1
μ_{fmax}		1	0.5	1
A_{fauto}	g	0	0	0
A_{fac}	g	0	0	0
J_{fc}	m/s^3	20	20	20
t_{fa}	sec	0.1	0.1	0.1
t_{fc}	sec	0.1	0.1	0.1
min headway	sec	**0.36**	**0.63**	**0.36**
min headway	m	9.90	17.22	9.94
max headway	sec	**0.076**	**0.186**	**0.277**
max headway	m	2.09	5.14	7.61

Table 14: Platoons of passenger vehicles without coordinated braking (tfc= 0.1 sec). Capacity Estimates with/without 5mph collisions.

A. Autonomous Platoons	**Dry road surface**	**Wet road surface**	**Uniform braking**
10 car platoons	6217/6090	4171/4059	6139/5955
20 car platoons	6399/6257	4280/4156	6349/6142
B. Free Agent Infrastructure Supported Platoons			
10 car platoons	6453/6317	4276/4158	6369/6172
20 car platoons	6522/6374	4335/4207	6470/6255
C. Free Agent Infrastructure Managed Platoons			
10 car platoons	6580/6438	4331/4211	6495/6289
20 car platoons	6586/6435	4363/4234	6534/6314

Table 15: Platoons with coordinated braking - no delay

		DRY	WET	UNIFORM
V_{lo}	mph	60	60	60
V_{fo}	mph	61.5	61.5	61.5
A_{lmax}	g	0.8	0.8	0.5
A_{fmax}	g	0.72	0.72	0.475
J_{lmax}	m/s^3	50	50	50
J_{fmax}	m/s^3	50	50	50
μ_{lmax}		1	0.5	1
μ_{fmax}		1	0.5	1
A_{fauto}	g	0	0	0
A_{fac}	g	0	0	0
J_{fc}	m/s^3	20	20	20
t_{fa}	sec	0	0	0
t_{fc}	sec	0	0	0
min headway	sec	**0.27**	**0.55**	**0.28**
min headway	m	7.51	15.18	7.73

Table 15a: Platoons with coordinated braking - no delay - allowing 5mph collisions

		DRY	WET	UNIFORM
V_{lo}	mph	60	60	60
V_{fo}	mph	61.5	61.5	61.5
A_{lmax}	g	0.8	0.8	0.5
A_{fmax}	g	0.72	0.72	0.475
J_{lmax}	m/s^3	50	50	50
J_{fmax}	m/s^3	50	50	50
μ_{lmax}		1	0.5	1
μ_{fmax}		1	0.5	1
A_{fauto}	g	0	0	0
A_{fac}	g	0	0	0
J_{fc}	m/s^3	20	20	20
t_{fa}	sec	0	0	0
t_{fc}	sec	0	0	0
min headway	sec	**0.26**	**0.52**	**0.26**
min headway	m	7.16	14.47	7.20
max headway	sec	**0.109**	**0.214**	**0.26**
max headway	m	3.00	5.89	7.20

Table 16: Platoons of passenger vehicles with coordinated braking (tfc= 0 sec). Capacity Estimates with/without 5mph collisions

A. Autonomous Platoons	**Dry road surface**	**Wet road surface**	**Uniform braking**
10 car platoons	7391/7217	4671/4531	7280/7028
20 car platoons	7733/7532	4841/4683	7660/7365
B. Free Agent Infrastructure Supported Platoons			
10 car platoons	7727/7537	4802/4654	7607/7331
20 car platoons	7913/7703	4911/4748	7836/7529
C. Free Agent Infrastructure Managed Platoons			
10 car platoons	7909/7710	4872/4720	7786/7498
20 car platoons	8007/7792	4947/4782	7930/7615

Table 17: Platoons with coordinated braking. (Delay of 0.1 sec from tail to head)

		DRY	WET	UNIFORM
V_{lo}	mph	60	60	60
V_{fo}	mph	61.5	61.5	61.5
A_{lmax}	g	0.8	0.8	0.5
A_{fmax}	g	0.72	0.72	0.475
J_{lmax}	m/s^3	50	50	50
J_{fmax}	m/s^3	50	50	50
μ_{lmax}		1	0.5	1
μ_{fmax}		1	0.5	1
A_{fauto}	g	0	0	0
A_{fac}	g	0	0	0
J_{fc}	m/s^3	20	20	20
t_{fa}	sec	0	0	0
t_{fc}	sec	-0.1	-0.1	-0.1
min headway	sec	**0.173**	**0.452**	**0.18**
min headway	m	4.76	12.431	4.98

Table 17a: Platoons with coordinated braking. (Delay of 0.1 sec from tail to head) - allowing 5mph collisions

		DRY	WET	UNIFORM
V_{lo}	mph	60	60	60
V_{fo}	mph	61.5	61.5	61.5
A_{lmax}	g	0.8	0.8	0.5
A_{fmax}	g	0.72	0.72	0.475
J_{lmax}	m/s^3	50	50	50
J_{fmax}	m/s^3	50	50	50
μ_{lmax}		1	0.5	1
μ_{fmax}		1	0.5	1
A_{fauto}	g	0	0	0
A_{fac}	g	0	0	0
J_{fc}	m/s^3	20	20	20
t_{fa}	sec	0	0	0
t_{fc}	sec	-0.1	-0.1	-0.1
min headway	sec	**0.160**	**0.426**	**0.164**
min headway	m	4.41	11.72	4.50
max headway	sec	**0.116**	**0.229**	**0.164**
max headway	m	3.19	6.30	4.50

Table 18: Platoons of passenger vehicles with coordinated braking (tfc= -0.1 sec). Capacity Estimates with/without 5mph collisions

A. Autonomous Platoons	Dry road surface	Wet road surface	Uniform braking
10 car platoons	7226/7060	4604/4468	7108/6889
20 car platoons	7637/7442	4802/4646	7551/7291
B. Free Agent Infrastructure Supported Platoons			
10 car platoons	7540/7359	4729/4586	7408/7171
20 car platoons	7808/7604	4870/4709	7716/7445
C. Free Agent Infrastructure Managed Platoons			
10 car platoons	7714/7525	4797/4649	7579/7330
20 car platoons	7901/7692	4905/4743	7808/7530

Table 19: Infrastructure Managed Slotting. Capacity Estimates

	Dry road surface	Wet road surface	Uniform braking
0% mixing	4047	2826	3773

Table 20: Capacity comparisons

Capacity without platooning	**0% mixing of vehicles**			**5% mixing of buses**			**5% mixing of trucks**		
	Dry	Wet	Uni-form	Dry	Wet	Uni-form	Dry	Wet	Uni-form
Autonomous Vehicles with class identification	4116	2860	3850	3746	2516	3525	3458	2278	3096
Autonomous Vehicles without class identification	4116	2860	3850	3631	2432	3416	3356	2207	3007
Free Agents - Infrastructure Supported with class identification	5400	3425	4942	4730	2923	4377	4276	2605	3730
Free Agents - Infrastructure Managed with class identification	6437	3823	5810	5472	3197	5018	4873	2820	4184
Infrastructure Managed Slotting	4047	2826	3773						
				2.5% buses + 2.5% trucks			**5% buses + 5% trucks**		
				Dry	Wet	Uni-form	Dry	Wet	Uni-form
Autonomous Vehicles with class identification				3596	2391	3297	3193	2054	2882
Autonomous Vehicles without class identification				3488	2314	3198	3026	1943	2735
Free Agents - Infrastructure Supported with class identification				4492	2755	4025	3845	2304	3400
Free Agents - Infrastructure Managed with class identification				5155	2997	4563	4299	2464	3756
Capacity with platooning	**10 car platoons**			**20 car platoons**					
	Dry	Wet	Uni-form	Dry	Wet	Uni-form			
Autonomous platoons without coordinated braking	6090	5652	5955	6257	5977	6142			
Infrastructure supported platoons without coordinated braking	6312	5843	6166	6372	6081	6252			
Infrastructure managed platoons without coordinated braking	6434	5947	6283	6433	6137	6311			
Autonomous platoons with coordinated braking	7217	4531	7028	7532	4683	7365			
Infrastructure supported platoons with coordinated braking	7531	4652	7323	7700	4747	7524			
Infrastructure managed platoons with coordinated braking	7704	4718	7489	7789	4780	7611			
Autonomous platoons with delayed braking	7060	4468	6889	7442	4646	7291			
Infrastructure supported platoons with delayed braking	7359	4586	7171	7604	4709	7445			
Infrastructure managed platoons with delayed braking	7525	4649	7330	7692	4743	7530			

Inter Vehicle Spacing

User's Manual

by
A. Kanaris
A. Grammagnat
P. Ioannou

Center for Advanced Transportation Technologies and California Path

Table of contents

I Introduction

The Inter Vehicle Spacing software tool (IVS) provides a user friendly interactive interface that allows you to perform the following:

- Calculate the minimum initial spacing between two vehicles with specified deceleration profiles, initial velocities, friction coefficient between the tires and the road and reaction times such that no collisions will occur and/or for collisions to occur with a relative speed less than a given upper bound.
- Calculate the possibility and severity of collision between two vehicles, given their initial intervehicle spacing and deceleration profiles, friction coefficients and reaction times.
- Visualize the motion of the two vehicles in the longitudinal direction during braking maneuvers for different deceleration profiles and initial intervehicle spacing.
- Calculate the highway capacity given the velocity, intervehicle spacing, interplatoon spacing, vehicle size and platoon size.

I.1- Installation and system requirements.

The Inter Vehicle Spacing software (IVS) can only run with Windows 3.1 and Windows 95. To install the program, run the file *setup.exe* found on the installation disk. A number of libraries will be installed in the Windows/System directory and the directory *Spacing* that contains the executable file will be installed in the root directory or to another directory of your choice.

If an older version of the software has been previously installed in the same directory, make sure it has been deleted before starting the installation process. When the installation process is done, you just have to click on the icon for "IVS" (the one that shows two cars) to run the program.

After the installation you will find the IVS icon under the Program Manager if you work with Windows 3.1x, or in the Program submenu under the Start icon (on the Taskbar) if you work with Windows 95.

I.2- The cursors

In addition to the primary cursor ("Arrow cursor"), IVS uses three different cursors to suggest different actions:

- The "Finger on key" cursor indicates you that you are pointing to a button on which you can click.
- The "Black Left Arrow" cursor appears whenever you are pointing to an item you can modify via the keyboard.
- The "Crosshair" cursor appears whenever you are positioned on the deceleration profile graph and indicates you that you can make changes to the profile.

II The controls and the input parameters

When you first start IVS, a window called "Inter Vehicle Spacing" appears in the middle of the screen. Initially in contains only a row of buttons, the "Button Bar". The IVS software uses pop-up windows that appear in response to your actions . For example, the Spacing window will appear when you press the "Minimum Spacing" button on the Button Bar.

II.1- The Button Bar

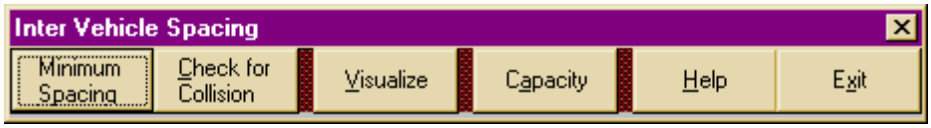

The Button Bar groups six commands, each command is represented by an individual button. You can activate Button Bar commands by clicking the appropriate button with the left mouse button or by pressing the corresponding letter on the keyboard. The buttons on the Button Bar perform the following functions:

Button	Description
Minimum Spacing	Clicking on this button extends the "Inter Vehicle Spacing" window to allow you to specify what type of computation you prefer: Either the minimum initial spacing for no collision or the minimum initial spacing both for no collision and for collision with a relative velocity less than an upper bound DeltaV that you can specify.
Check for Collision	Clicking on this button extends the Spacing window to specify an initial spacing between the two cars. You will then be able to evaluate if the initial spacing you gave is sufficient to avoid a collision or if you will have a collision with a certain relative velocity at the point of collision.
Visualize	Clicking on this button opens the "Plot Tool" window. This window is using the values of the input parameters from the Inputs window together with the initial spacing to offer a pictorial way to show the results. The graphical interface of the Plot window allows you to visualize the effect of the input parameters on vehicle following. A detailed description of the graphical interface is presented later in the manual (in section III).

Button	Description
Capacity	Clicking on this button opens the "Capacity" window. This window allows you to calculate the capacity (in number of vehicles per lane per hour) with reference to the following parameters: the number of vehicles in a platoon, the intra and inter platoon spacing, the length of the vehicle and the velocity. These parameters appear in the Capacity window and their values and units can be modified.
Help	Clicking on this button opens a window with the on-line help file.
Exit	This stops the execution of the software and closes the windows.

II.2 The input parameters

When you click on <Minimum Spacing>, <Check for Collision> or <Visualize>, the "Inputs window" appears in the upper left corner of the screen. This window is used to update the input parameters that describe the deceleration profiles of each vehicle, initial velocities, detection delay and friction coefficient.

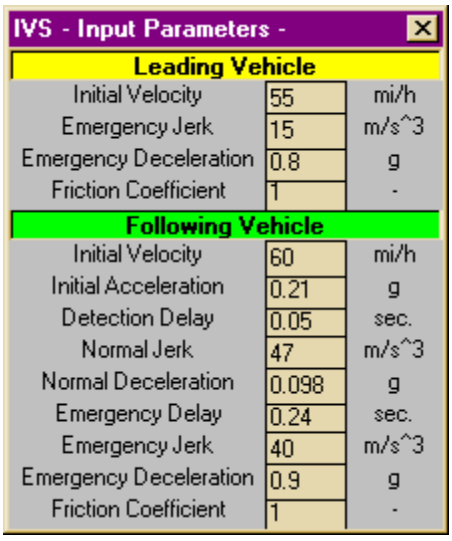

There are four input parameters associated with the leading vehicle:

- initial velocity,
- emergency jerk,
- emergency deceleration,
- friction coefficient.

There are nine input parameters associated with the following vehicle:

- initial velocity,
- initial acceleration,
- normal jerk,
- normal deceleration,
- emergency jerk,
- emergency deceleration,
- detection delay,
- emergency delay,
- friction coefficient.

The first time you open the "Inter Vehicle Spacing" window, the input parameters are initialized to an arbitrary (fixed) set of values. This particular choice of parameters results in a situation where there will be a collision between the two vehicles.

For convenience, all deceleration and jerk parameters are entered without a sign. In some cases i.e., the jerk, the actual sign is negative but you still have to input the value without a sign, otherwise a negative sign will be interpreted as a positive jerk. The initial acceleration must be entered with its real sign. For this one parameter, no sign signifies a positive value i.e., a vehicle speeding up.

There are some restrictions on the parameter values you can enter:

- velocities have to be positive,
- decelerations have to be positive,
- emergency decelerations cannot be equal to zero,
- friction coefficients have to be greater than zero and less or equal to one.

The last restriction is strict and if it is not observed the software will stop with an error.
The various input parameters for the leading and following vehicles are explained in section III.5.

II.3- The <Minimum Spacing> button

Located in the upper left hand corner of the Inter Vehicle Spacing window, the <Minimum Spacing> button allows you to compute the minimum initial spacing between vehicles. The minimum initial spacing is defined to be the initial spacing that will guarantee no collision under the given braking scenario or alternatively the initial spacing that will guarantee a relative velocity at the point of collision less than a given upper bound.

When you click on <Minimum Spacing> two options appear:

(a) Minimum initial spacing for no collision

(b) Minimum initial spacing for a collision with a relative velocity less than DeltaV.

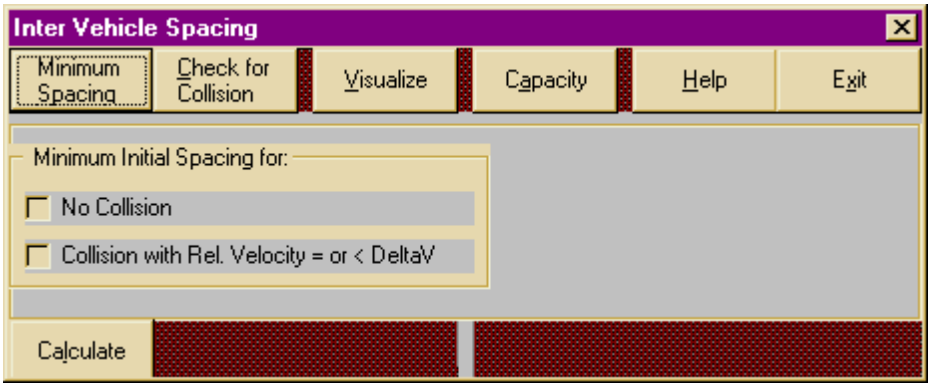

You can select an option by clicking on an item box. There are only two possible selections: either (a), or (a)+(b). If you select (b) (and then (a) also), you have to initialize the value of DeltaV and choose the units of DeltaV: mi/h (mph) or km/h. The choice of units has to be done carefully because it fixes the current units for the display. Thereafter, all the input parameters representing velocity and all the results will be given in the chosen units.

To start the computation, click the <Calculate> button. The computation depends on all the input parameters, (the initial velocities and the deceleration profiles of each car) as well as the value of DeltaV. After the computation is finished, one or two boxes containing the results will appear. The results specify the minimum initial spacing to avoid any and all collisions as well as the spacing that may lead to a collision with a relative velocity less or equal to the specified DeltaV. If a collision is indeed possible, the time, the positions and the velocities of the cars when the collision occurs are calculated and are reported.

II.3.1- The results

The results of the computation appear in one or two boxes located in the bottom left side of the Inter Vehicle Spacing window. They represent a summary answer corresponding to the chosen options. Different boxes can appear, depending on the input parameters and the chosen options:

- option (a):

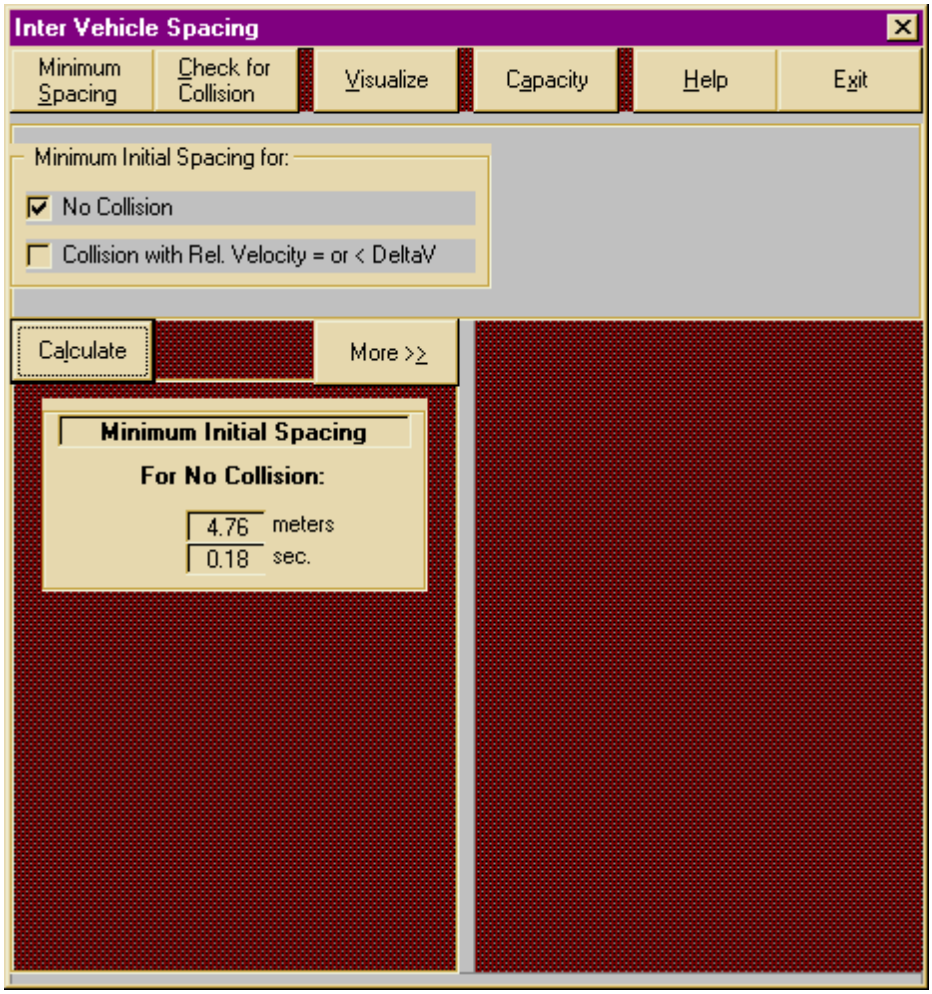
Inter Vehicle Spacing
Minimum Spacing
Check for Collision
Visualize
Capacity
Help
Exit
Minimum Initial Spacing for:
No Collision
Collision with Rel. Velocity = or < DeltaV
Calculate
More >>
Minimum Initial Spacing
For No Collision:
4.76 meters
0.18 sec.

- option (a)+(b):

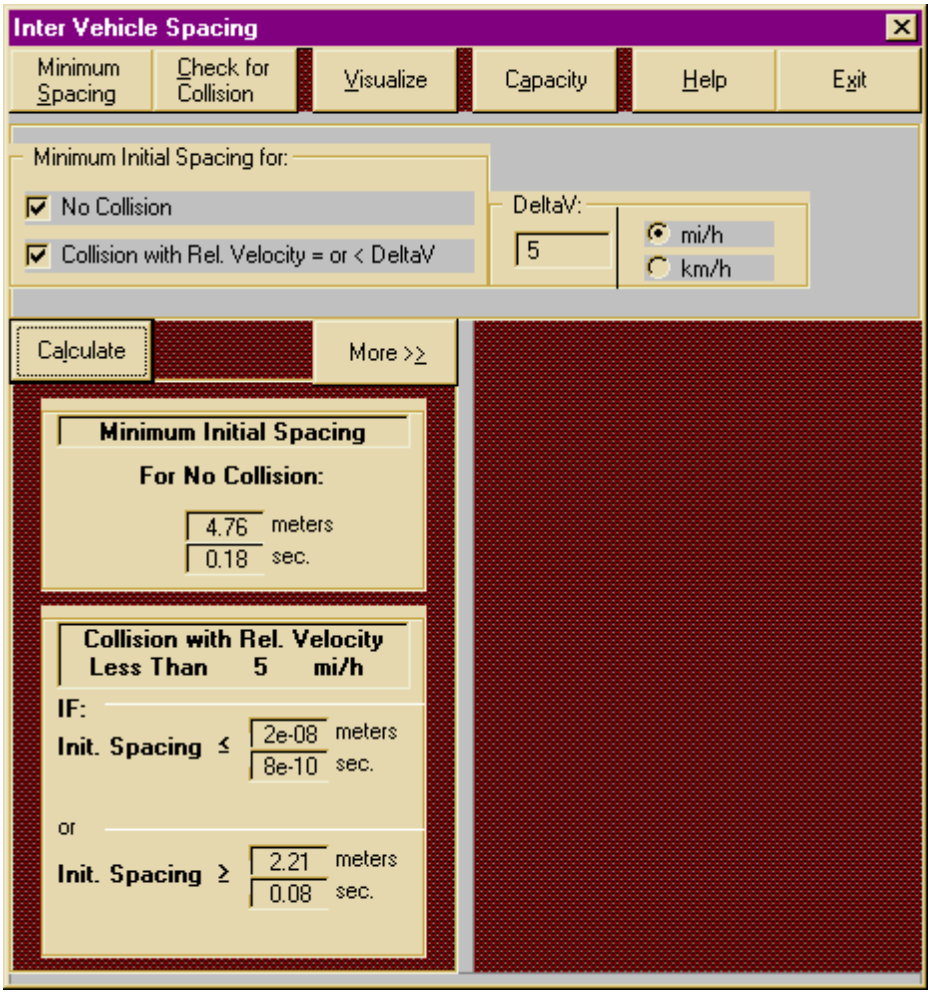

Under this option, additional results are available by clicking on the <More>>> button located at the top of the results area. These additional results are then displayed in the bottom right side of the Spacing window. They are presented in the following way:

- option (a)+(b):

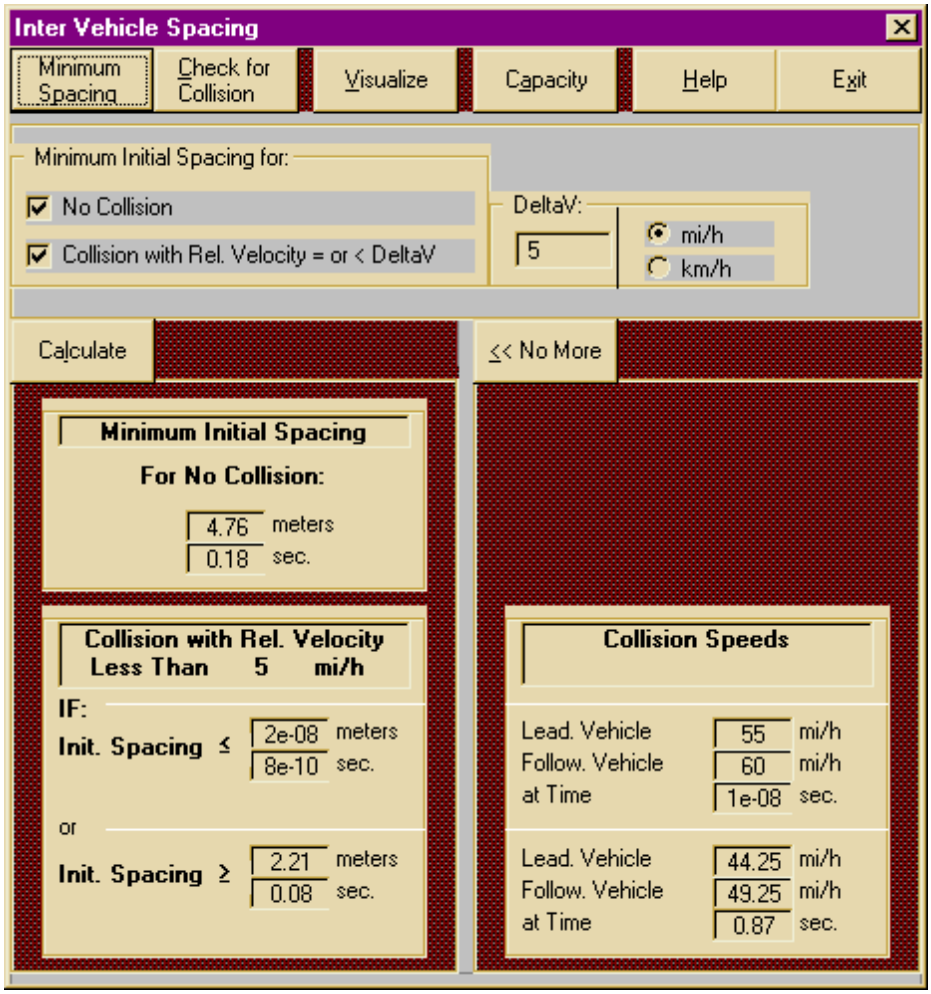

II.3.2- Interpretation of the results

The most fundamental result of the computation, the first that we need to look at is the "Minimum initial spacing" for no collision. This is quite unambiguous.

In addition to that we can compute the spacing that will result in a collision with a limited relative velocity. The initial conditions may allow for more than one point at which the relative velocity is equal to the given limit during the braking maneuver. If this is the case, the program will compute and determine all these points then it will produce the results representing the worst case. Depending on the initial conditions, the program will produce one or two results for the initial spacing. Each one is specified as a "greater than" or "less than" relation depending on the conditions. If the relative velocity that was specified occurs while the relative velocity between the vehicles is increasing, the spacing requirement is given as a "less than" limit because greater spacing will result in greater relative velocity. If the specified relative velocity occurs while the relative velocity between the vehicles is decreasing, the spacing requirement is given as a "greater than" limit because less spacing will result in greater relative velocity at the point of collision.

II.4- The <Check for Collision> button

Located in the upper left hand corner of the Inter Vehicle Spacing window next to the <Minimum Spacing> button, the <Check for Collision> button allows you to verify if a collision may occur given a value for the initial spacing between the vehicles. It will also compute the velocity of each vehicle and the relative velocity at the moment of the collision.

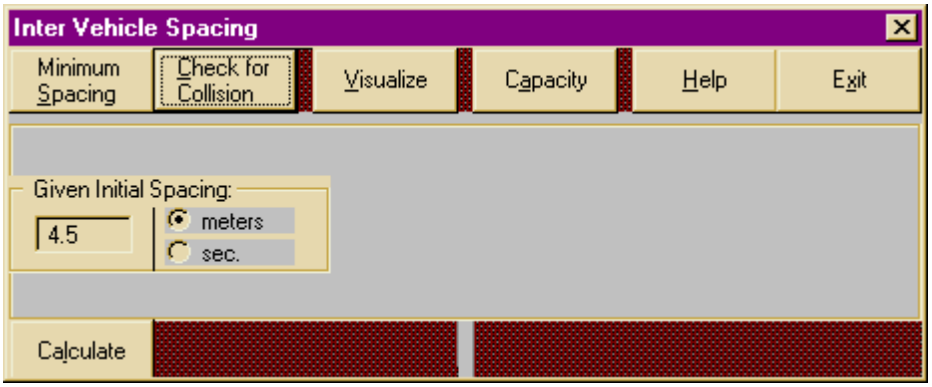

If you click <Check for Collision> then you have to specify the initial spacing between the two vehicles. The value has to be accompanied by the units, which can be meters or seconds. An initial spacing given in seconds is in reference to the velocity of the following vehicle (what is also known as "time headway").

To start the computation, click the <Calculate> button. The computation depends on all the input parameters, as well as the initial spacing between the vehicles. After the computation is finished, a box containing the results will appear. The results include the answer to whether a collision is possible, and if indeed a collision is possible, it will include the time of the collision and the relative velocity of the vehicles at the point of collision. The results will always include the minimum initial spacing no collision. The velocity of each car at the point of collision is calculated and reported.

II.4.1- The results

The results of the computation appear in one or two boxes located in the bottom left side of the Inter Vehicle Spacing window. They represent a summary answer corresponding to the chosen options. Different boxes may appear, depending on the input parameters and the chosen initial spacing:

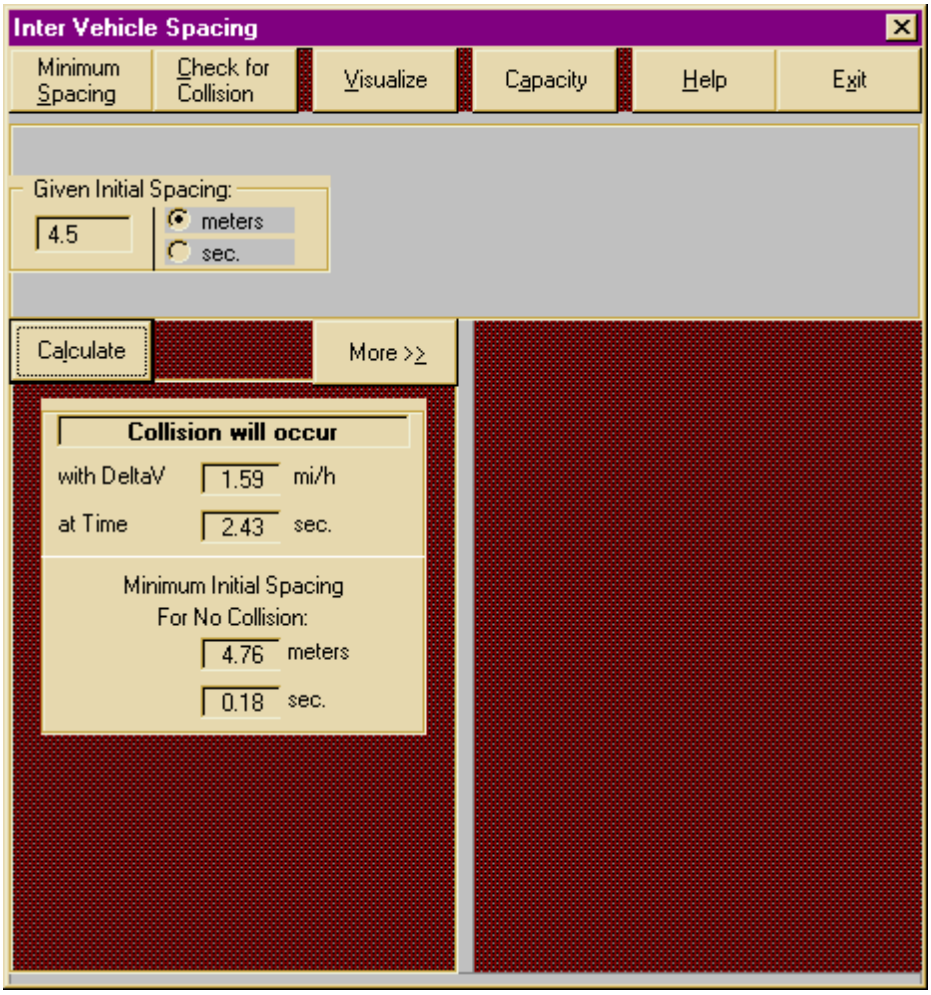

Additional results are available by clicking on the <More>>> button located at the top of the results area. These additional results are then displayed in the bottom right side of the Spacing window. They are presented in the following way:

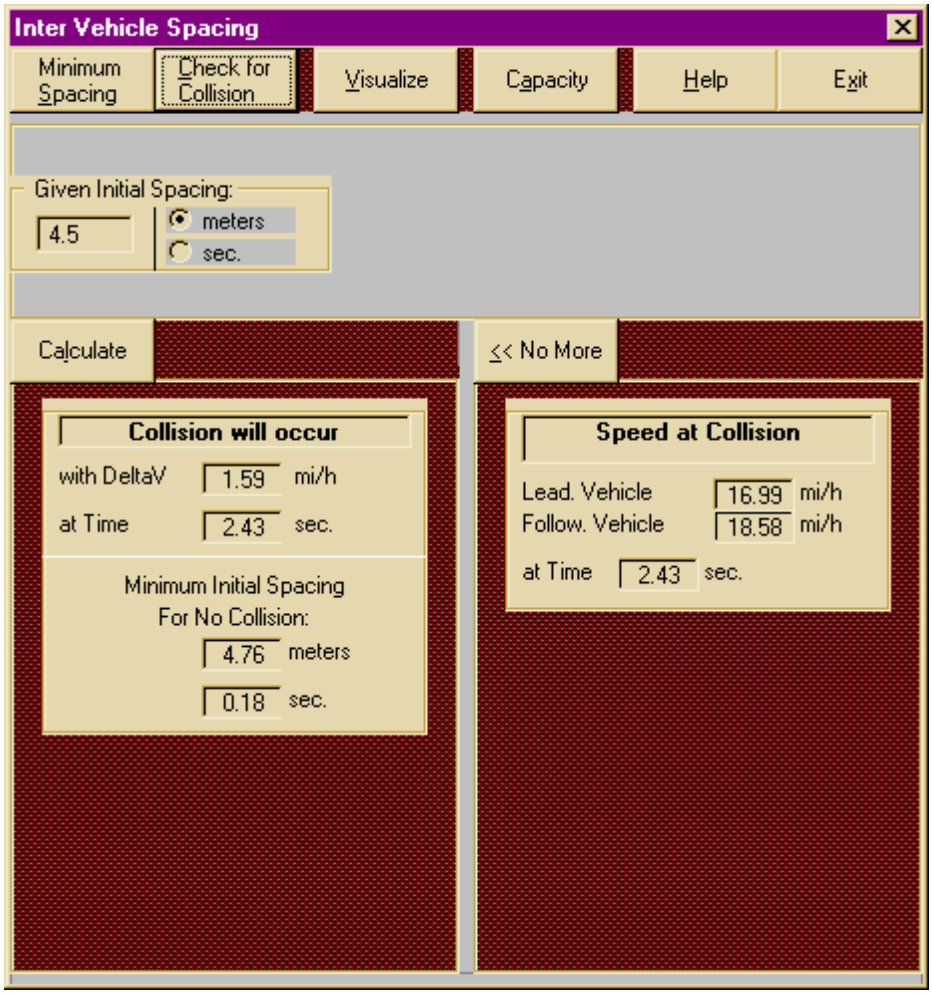

III Visualization and the Plot Tool window

The second component of the Inter Vehicle Spacing software tool is graphical and allows you to visualize the motion of the cars and to interact with the parameters involved in the car braking scenario. This is all done with the "Plot Tool" window, activated by the <Visualize> button on the button bar.

III.1- The <Visualize> button

The "Plot Tool" window opens when you click the <Visualize> button on the Button Bar. The Plot window consists of four parts: the Menu Bar at the top of the window, the Button Bar just bellow the Menu Bar, the animation area just bellow the Button Bar and finally the deceleration profiles of both vehicles. There are two points of interest in the Plot Tool window. First, you can directly modify each of the profiles using the mouse. The parameter values in the Input window are automatically updated. Second, you can visualize by computer animation the position and velocity trajectory of the vehicles, following the given deceleration profiles.

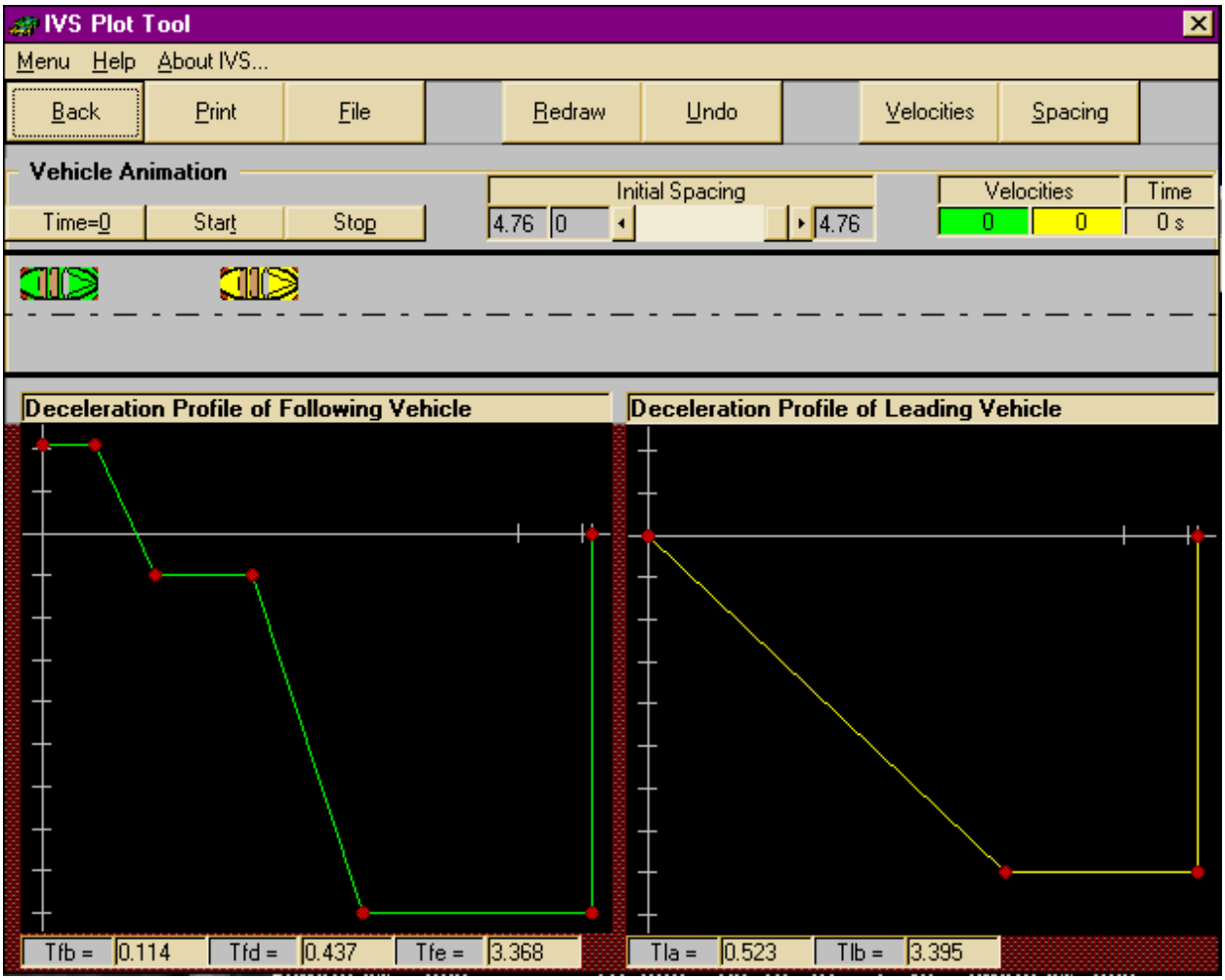

III.2- The Menu Bar

The Menu Bar includes three options 'Menu', 'Help' and 'About IVS …'. The 'About IVS …' option indicates the version number and the copyright of the software. The 'Menu' and 'Help' options call up a drop down menu of commands as described bellow.

Option	Description
Menu	The Menu option commands are 'Back', 'File', 'Print', 'Redraw', 'Undo', 'Velocities', 'Spacing' and 'Exit'. They will be described in section III.3. Selecting one of the manu commands by clicking the corresponding button. Selecting 'Exit' stops execution of the software without having to return back to the Spacing window.
Help	Four different help screens are available. One of them, 'IVS Tool…', is related to the Spacing window, whereas the three others are related to the Plot window i.e., the current window. We describe those accessible through the 'IVS Plot Tool…'. • The 'Interface Presentation' describes the commands represented by each button of the Button Bar (of Plot window) and give brief instructions on how to modify the profiles. This is done either by acting directly on the profile graph with the mouse or by entering new parameter values in the Input window. • The two other help screens, one referring to the leading vehicle and another one for the following vehicle, describe the general shape of the deceleration profile and show the relation between the parameters and the profiles. Moreover, the abbreviations used in the profile help are explained. For instance, the initial acceleration is denoted by I.A. This helps in drawing the profiles by referring to the names of the input parameters. You can also access the help screens by the short-keys F1, F2, F3 and F4. Help on the profiles is also available by positioning the cursor on a black part of the picture and clicking on the right mouse button.

III.3- The Plot Tool Button Bar

The Button Bar in the Plot Tool groups five buttons; As described previously, clicking one of these buttons has the same effect as selecting the corresponding command from the Menu Bar.

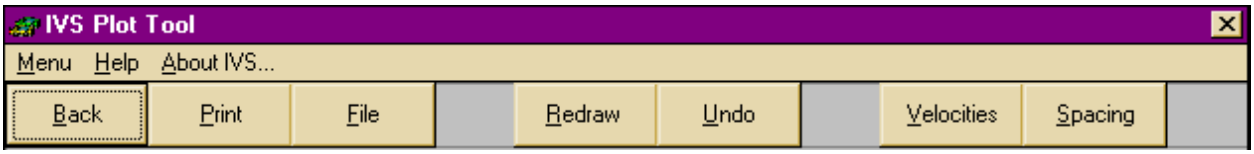

This section describes the effect of these buttons:

Button	Description
Back	Return to the first window, the Spacing window. Any modifications you have made on the profiles (in the Plot window) will be validated and reflected on the parameters in the Input window which are automatically updated. But, the updating of the input parameters is not done until the <Redraw> button (see below) is clicked. This button is symmetric to the <Visualize> button of the Spacing window.
Print	Open a dialog box to print either the leading vehicle profile, or the following vehicle profile, or both of them. Printing a profile also implies printing of the associated parameter values.
File	Open a dialog box to load a file containing the parameter values needed to build the two profiles, or to save the parameter values into a file. The box disappears when you click on the <Load> or <Save> button. Then a Windows dialog box opens to allow you to select (or, in the case of "Save", to create) the file from which the parameter values will be loaded or to which the parameters will be saved. Filenames for files that contain parameter values are of the form "*name*.ivs" where *name* represents the name of your file and *ivs* is the default extension. Therefore, the <File> button can be used to store and reload interesting scenarios. Note: Six Files (named: scheme1.ivs, ... , scheme6.ivs) are included in the setup directory of the software.

Button	Description
Redraw	Refresh the graph of the profiles after any modifications and repeat the computation according to the given parameters. The computation is the same as the <Calculate> button in the Spacing window. This button can also modify the values of the input parameters if some of them are not compatible. For instance, if the normal deceleration and emergency deceleration are different but the normal jerk is zero or null then the emergency deceleration value will be changed to the value of the normal deceleration. We will see in section III.5.2 when this button has to be used.
Undo	Restore the profiles obtained by the previous <Redraw> command. In other words, you can cancel the effect of the last <Redraw> command and all changes made between the previous and the last <Redraw>.
Velocities	Display a new window containing the velocity profile of each vehicle, versus time. These profiles are displayed with the implicit assumption that the vehicles are in different lanes, or as if the initial spacing is sufficient to not allow any collision between them. In other words, the velocity profiles are independent of each other and do not reflect the effect of collisions if any. You have the option to print the velocity profiles.
Spacing	Display a new window containing the inter-vehicle spacing versus time. The spacing profile takes into account the initial spacing that appears in the 'Initial Spacing' sliding bar. The spacing is displayed with the implicit assumption that the vehicles will not collide, as if they were in different lanes. Therefore, if the initial spacing between the vehicles is not sufficient to prevent a collision, the inter-vehicle spacing may become negative. This gives a sense of how much additional spacing would be needed to avoid a collision, which would occur at the moment that the spacing crosses the horizontal axis and becomes negative. You have the option to print the inter-vehicle spacing profile.

III.4- The animation area

The vehicle animation area is just below the Button Bar and consists of:

- three buttons controlling the animation,
- a sliding bar to define the initial spacing,
- three boxes indicating the current time in seconds and the current velocities of the vehicles as the animation advances. The units of velocity are either mi/h (mph) or km/h depending on the chosen unit of DeltaV in the Spacing window. By default, velocities are in mi/h (mph).
- the road and the two vehicles (yellow color for the leading vehicle, green for the following vehicle).

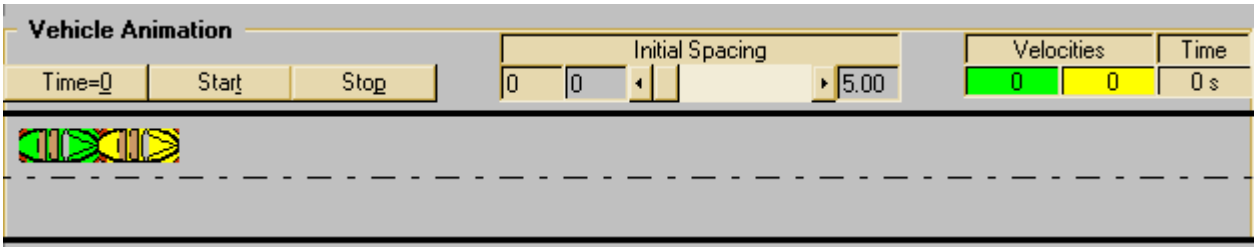

III.4.1- The Animation Control buttons

The three animation control buttons perform the following functions:

Button	Description
Time=0	Reset the vehicle animation. If the animation is not finished, clicking on this button stops the cars immediately, sets the time and the velocities to zero and moves the vehicles to their initial positions. These initial positions take into account the given (or computed) initial spacing.
Start	Start or restart the animation. Indeed, if you have clicked the <Stop> button to stop the animation, you can restart it from the current time. Warning: clicking twice the <Start> button, one after another, stops the animation.
Stop	Stop the animation. You can then either continue the animation by clicking the <Start> button or reset the animation by clicking the <Time=0> button.

III.4.2- Modify the initial spacing

An initial spacing is automatically computed after clicking the <Redraw> button, based on the minimum initial spacing for no collision. The numeric value of the initial spacing is printed in the white box located on the left of the sliding bar. The spacing is in meters.

You can modify the initial spacing in two different ways:

- by changing directly the value in the white box,
- by using the sliding bar:
  1. you can click on one of the scroll arrows,
  2. you can click on and drag the sliding box to any point along the bar.

The resulting initial spacing value, corresponding to the position of the sliding box, is displayed in the white box. It is always within the range of the minimum and the maximum values indicated on each side of the sliding bar.
If you want an initial spacing outside this range you have to modify the lower bound or the upper bound by clicking on it and entering a new bound. The initial spacing can never be negative.
If you modify directly the initial spacing in the white box (without using the sliding bar) and enter a value which is less than the minimum value of the sliding bar, then the lower bound will be changed automatically as soon you click <Start>.
You cannot modify the initial spacing while the animation is running. You have to stop and reset the animation (with <Time=0>) before modifying the initial spacing.

III.4.3- The animation display

The animation is obtained by moving the cars while the road is fixed. The scale is represented accurately with respect to road length, lane width, vehicle length and intervehicle distance. The length of the car is assumed to be three meters. The road length is fixed so we had to have a way to display the vehicles when the braking trajectory exceeds in length the available length of the road. For this purpose, the display "warps" around. As soon as the rear of a car reaches the end of the road on the right hand side of the screen, the car will instantly reappear on the left hand side. Therefore, this can generate a false display of a superposition of cars without a collision occurring. This will happen in the following cases:

- if the initial spacing is greater than the available "length" of the road
- if the velocity of the leader is much greater than that of the follower, then the cars can be in different "laps"
- if the follower has already stopped but the leader is still moving.

III.5- Deceleration profiles

The deceleration profiles of each car appear in the two black pictures located in the lower part of the Plot window. The left hand picture contains the deceleration profile of the following car and the right hand picture contains that of the leading car. The deceleration profile of the following vehicle is displayed in green and the leading vehicle in yellow. This matches the animation display where the following car is green and the leading car is yellow. When you move the cursor on one of these graphs it becomes a Crosshair cursor.

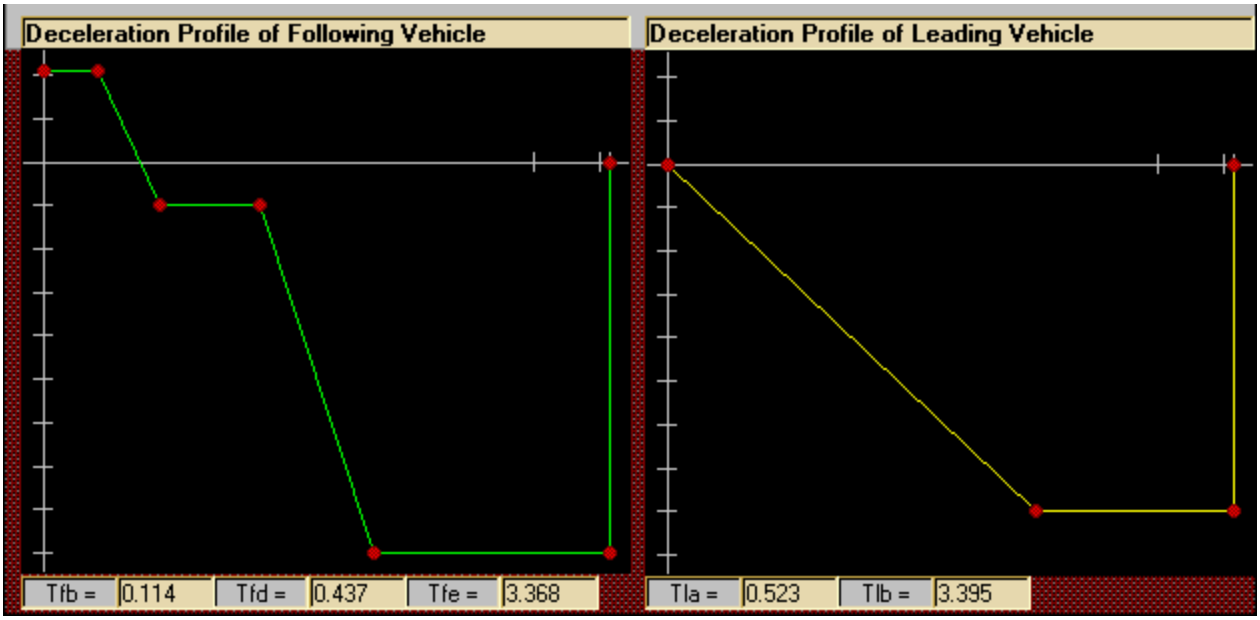

The relation of these profiles to the input parameters is the following: The leader starts to brake at time t = 0 with the given value of Emergency Jerk, which is shown as the initial slope on the yellow graph. When the Emergency Deceleration is reached (at time "Tla"), the deceleration becomes constant. This is shown on the horizontal part of the graph. The Emergency Deceleration is equal to the maximum deceleration that the leading vehicle is applying of. After a length of time "Tlb", a time which depends on the Initial Velocity and the rate of deceleration (i.e. Emergency Jerk and Emergency Deceleration), the leading vehicle comes to a full stop. This is shown on the graph as a vertical yellow line that goes all the way to zero.

The graph for the following vehicle is a little more complicated, to allow for the variety of possible braking scenarios that may occur under different Automated Highway Systems architectures.

The following vehicle deceleration profile starts with an Initial Acceleration phase which is shown as the first horizontal segment on the graph, which lasts as long as the given Detection Delay. At that point we enter the first sloped part of the graph which is representing the parameter Normal Jerk. This stage ends when either the Normal Deceleration level is reached (the second horizontal segment of the graph) or the Emergency Delay time is reached. In the first case, the time the

Normal Deceleration level is reached is denoted by "Tfb". In the second case the horizontal segment representing the Normal Deceleration does not exist. In this case, the Emergency Delay is automatically set equal to "Tfb". The Emergency Delay parameter represents the time the following vehicle to detect and respond to an emergency braking. This moment is shown with the beginning of the second sloped part of the graph, representing the Emergency Jerk. The Emergency Jerk stage lasts until the time "Tfd" at which the Emergency Deceleration level is reached. At this time the deceleration becomes constant and this is shown on the last horizontal part of the graph. The Emergency Deceleration is equal to the maximum deceleration that the following vehicle is applying for the braking scenario considered. After a length of time "Tfe", a time which depends on the Initial Velocity and the compound rate of deceleration, the vehicle comes to a full stop. This is shown on the graph as a vertical green line that goes all the way to zero.

The *y*-axis is scaled linearly with a step of 0.1*g* (0.981 meters per second square) whereas the *x*-axis has an exponential scale and is scaled with a step of 1 second.

When the animation begins (with the <Start> button, as described in section III.4.1), both the profiles are scanned progressively in red as time increases to indicate the actual point on the graph.

III.5.1- Modify the profiles

You can modify the profiles using the mouse, by selecting and moving the red dots on each graph. First place the Crosshair cursor on the point to be moved, click and hold the left mouse button then move the mouse to change the position of the red dot. If the cursor is close enough to a red dot when you click the mouse, a red circle will appear to indicate the selection. When you move the selected point the related parameters are automatically and instantaneously modified in the Inputs window.

III.5.2- Validate the profiles

After one or more input parameters have been modified (by editing on the "Input Parameters" windows or by manually modifying the profiles), you have to click the <Redraw> button in order to validate the new parameters and obtain new profiles. If necessary, the input parameters get automatically updated by the <Redraw> command.

IV.- The Capacity calculator

Clicking on the <Capacity> button, found on the "Inter Vehicle Spacing" window button bar, opens the "Capacity" window. This window allows you to calculate the capacity (in number of vehicles per lane per hour) with reference to the following parameters: the number of vehicles in a platoon, the intra and inter platoon spacing, the length of the vehicle and the velocity. The values of these parameters appear in the Capacity window and can be modified.

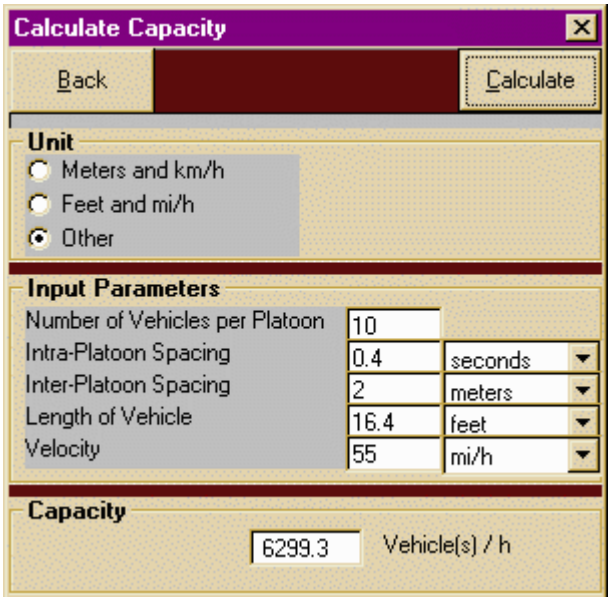

To modify a parameter value, position the cursor on the parameter value of interest (the Arrow cursor becomes then a Black Left Arrow cursor), delete the old value and enter the new one from the keyboard. The capacity is then calculated by clicking the <Calculate> button and its value is printed in the associated box, at the bottom of the Capacity window.

The default units are feet and miles per hour (mph), but you can choose between feet and mph and the international system of units, namely meters and kilometers per hour (meters and km/h). You may also choose 'Other' to use non-standard unit combinations. In this case, the unit options available can be seen by clicking the down arrow inside the unit box.

Remark: the choice of units is local in the Capacity window; in other words, it will not be taken into account and will not change the units used in any other windows.

The Capacity window can be closed by clicking on the <Back> button, which returns you to the initial Button Bar.

Strategies and Spacing Requirements for Lane Changing and Merging in Automated Highway Systems

Alexander Kanaris, Elias B. Kosmatopoulos, and Petros A. Ioannou

Department of Electrical Engineering — Systems
University of Southern California
Los Angeles, CA 90089
e-mail address: [kosmatop|ioannou]@bode.usc.edu

Abstract

In Automated Highway Systems (AHS) vehicles will be able to follow each other automatically by using their own sensing and control systems, effectively reducing the role of human driver in the operation of the vehicle. Such systems are therefore capable of reducing one source of error, human error, that diminishes the potential capacity of the highways and in the worst case becomes the cause of accidents. Amongst the riskiest maneuvers that the driver has to perform are that of merging into the traffic and that of lane changing. The degree of difficulty and the amount of risk involved in this maneuver depend on the driver performing the maneuver. With AHS, the vehicles in the neat vicinity sense or are notified of the intention of the vehicle to perform the merging or lane changing maneuver. When this intention has been identified, the vehicles that are affected have to increase their relative spacing, in effect to "make space" for the merging vehicle to occupy. How much spacing will be needed, and when and how should the affected vehicles provide that space by adjusting their position and speed is the subject of this study.

In this work, we analyze the problem of collision-free merging and lane changing. We examine various alternative scenaria for merging and lane changing and we present an algorithm for calculating the *Minimum Safety Spacing for Lane Changing (MSSLC)*, that is, we calculate the spacings that the vehicles should have during a merging or lane changing maneuver so that, in the case where one of the vehicles enters in an emergency braking situation, the rest of the vehicles will have enough time and space to stop without any collision taking place. The calculation of the MSSLC's for merging or lane changing maneuver is more complicated than the calculation of the Minimum Safety Spacing for longitudinal vehicle following, since, in the former case we have to take into account the particular lane changing policy of the merging vehicle as well as the effect of combined lateral/longitudinal motion during the lane changing maneuver. The braking profiles of the vehicles involved in an emergency scenario during lane changing maneuver depend on the particular AHS operational concept, i.e., on the degree of communication between the vehicles and between the vehicles and the infrastructure. We consider six different AHS operational concepts; we present the braking profiles of the vehicles for each operational concept and we investigate the effects of the particular operational concept to the MSSLC.

Contents

I. Introduction

Urban highways in many major cities are usually congested and this makes driving difficult and raises the possibility of accidents, especially during merging and lane changing maneuvers. Human drivers engage in information gathering and decision making about driving conditions to determine if and when the conditions are favorable for a lane change. When they decide that the lane change can be successfully completed, they use their signals to notify other vehicles of their intent. Errors might result because the driver failed to collect critical information, or failed to provide a signal, or the other drivers failed to notice and take corrective action, for example to provide additional spacing, when needed. One of the promises of Automated Highway Systems (AHS) is to increase the safety level of driving in highways, and especially the safety of maneuvers like merging and lane changing, by using advanced sensing and control systems to replace the inaccurate human actions. Therefore in AHS vehicles and/or infrastructure should have build in intelligence that allows them, to calculate the spacing requirements for safe merging and lane changing.

Vehicles need to maintain a certain "safety distance" between them, in order to be able to slow down or stop without collision when the leading vehicle performs slow down or stopping maneuver. When another vehicle wants to merge in-between, a spacing equal to the sum of the required safety distance between itself and the merging vehicle and the safety distance required between the merging vehicle and the leading vehicle plus the length of the merging vehicle has to be created. There are several approaches to estimate the required spacing. If the following vehicle has no information about the vehicle class and braking capabilities of the merging vehicle, it has to make worst case assumptions to allow for a large safety margin. Otherwise, extensive communications will be required between the vehicles involved, so that each one can be informed of the vehicle class and braking capabilities of the others. In the latter case, the requirement for a large allowance for a safety margin can be significantly reduced, in effect allowing just enough space for the merging vehicle, so that the spacing between them immediately after the merge is equal to the minimum safety distance calculated for longitudinal vehicle following [3].

The relative speed of the vehicle that intends to merge relative to the speed of the vehicles in the destination lane just prior to the merging is of great importance. The speed can be very different before the merging but it has to be matched after the merge. The speed before the merge is likely not to be the same because the merging vehicle might be accelerating from a ramp or it might be constrained by the speed of the traffic flow in the lane it occupies before merging into the new lane. This imposes additional constraints about the timing of the maneuver and mostly in the amount of additional safety distance that will be required.

In this work, we analyze the problem of collision-free merging and lane changing. We examine various alternative scenaria for merging and lane changing and we present an algorithm for calculating the *Minimum Safety Spacing for Lane Changing (MSSLC)*, that is, we calculate the spacings that the vehicles should have

during a merging or lane changing maneuver so that, in the case where one of the vehicles enters in an emergency braking situation, the rest of the vehicles will have enough time and space to stop without any collision taking place. The calculation of the MSSLC's for the merging or lane changing maneuver is more complicated from the calculation of the Minimum Safety Spacings of the pure longitudinal case, since, in the former case we have to take into account the particular lane changing policy of the merging vehicle as well as the effect of combined lateral/longitudinal motion during the lane changing maneuver. The braking profiles of the vehicles involved in an emergency scenario during lane changing maneuver depend on the particular AHS operational concept, i.e., on the degree of communication between the vehicles and between the vehicles and the infrastructure. We consider six different AHS operational concepts; we present the braking profiles of the vehicles for each operational concept and we investigate the effects of the particular operational concept to the MSSLC.

Due to the similarities between the lane changing and the merging problem, in this work we will consider and analyze only the lane changing problem. The results of this work can be easily extended/modified for the case of merging. Similar studies on the evaluation of safety spacing was performed in [1] for the case of no deceleration or emergencies. As a result the work in [1] leads to the calculation of safety spacing for lane changing under constant speed vehicle movement. In our case, we calculate the intervehicle spacing requirements under possible emergency stopping situations during lane changing.

II. The Lane-Changing Strategies

Consider the five vehicles shown in Figure 1 that will be directly affected when one of them is performing a lane change maneuver; the symbols ℓ_1, f_1, ℓ_2, m and f_2 stand for the leading vehicle in the destination lane, following vehicle in the destination lane, the leading vehicle in the originating lane, the vehicle which must perform the lane-changing (which will be called thereafter as the merging vehicle) and the following vehicle in the originating lane, respectively. Each vehicle has length L_i, $i = \ell_1, f_1, \ell_2, m, f_2$. By assuming a two-dimensional coordinate system as shown in Figure 1, the vehicle's motion can be completely described by the two-dimensional vectors $x^{(i)}, v^{(i)}$, and $a^{(i)}$, $i = \ell_1, f_1, \ell_2, m, f_2$ of position, velocity, and acceleration, respectively. The position of each vehicle is measured with respect to the center of the front end of the vehicle, while the velocity and acceleration are measured with respect to the center of gravity of the vehicle. The first entry of the vectors $x^{(i)}, v^{(i)}, a^{(i)}$ denotes the longitudinal position, velocity, and acceleration, respectively, while the second entry stands for the lateral position, velocity, and acceleration, respectively. Finally, $c^{(i)}$ denotes the distance in the longitudinal direction between the center of the front end and the center of gravity of of the i-th vehicle.

Let d_{ij} denote the intervehicle distance in the longitudinal direction between the vehicles i and j, i.e.,

$$d_{ij} := x_1^{(i)} - x_1^{(j)} - L_i$$

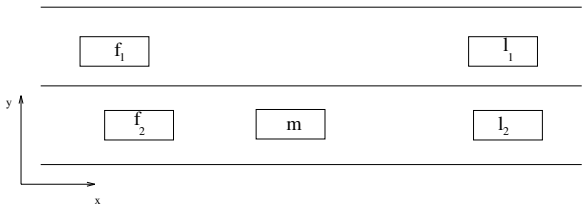

Figure 1: Vehicle about to make a lane change.

Obviously, during a lane changing operation, we are concerned about the longitudinal distances $d_{\ell_1 m}, d_{\ell_2 m}, d_{m f_1}$, $d_{m f_2}$. If one of the above distances measured in the same lane (which will be called thereafter intervehicle spacing) becomes nonpositive then a collision will occur. Moreover, following the work of [3] a lane-changing scenario must be such that it guarantees that no collision occurs if one of the vehicles enters in an emergency braking situation at any point in time before, during and after the end of the maneuver. In other words, during the lane-changing maneuver the intervehicle spacings $d_{\ell_1 m}, d_{\ell_2 m}, d_{m f_1}, d_{m f_2}$ must not only be positive but they must also be large enough so that, in the case where any of the five vehicles enters in an emergency braking situation, the other four vehicles will have sufficient time and spacing to stop without any collision taking place.

Suppose now that at the time-instant $t = 0$ the merging vehicle starts performing the lane change maneuver. There are many alternative lane changing policies for the merging vehicle and the best policy depends on many factors such as relative speed between the originating and destination lane, the spacing between the merging vehicle and the leading vehicle ℓ_2, etc. Despite the differences of the alternative lane changing policies they all can be described as follows: The merging vehicle starts adjusting its longitudinal velocity (by decelerating or accelerating) to make the spacing $d_{\ell_2 m}$ large enough; then it starts adjusting its longitudinal velocity (again by decelerating or accelerating) in order to make its longitudinal velocity equal to the velocity of the destination lane. Let us suppose that the time needed for the merging vehicle to adjust its longitudinal position and velocity is equal to t_{long}. Regarding now the lateral motion of the merging vehicle, at a certain time-instant $t_{lat} \geq 0$ the merging vehicle starts developing a lateral acceleration in order to enter the destination lane. The lateral adjustment of the merging vehicle's motion may start at the same time that the merging vehicle starts adjusting its longitudinal motion (in this case $t_{lat} = 0$), it may start when the merging vehicle has just completed the adjustment of its longitudinal motion (in this case $t_{lat} = t_{long}$), or, it may start any time after the merging vehicle have initiated adjustment of its longitudinal motion (in this case $0 < t_{lat} < t_{long}$). The time-instants t_{long}, t_{lat} as well as the profiles of the longitudinal and lateral accelerations specify the particular lane changing policy. In the next two subsections, we describe the possible profiles of the longitudinal and lateral accelerations of the merging vehicle.

A. The Longitudinal Acceleration Model for the Merging Vehicle

The profile of the longitudinal acceleration of the merging vehicle mainly depends on the relative velocity between the originating and the destination lane. When the destination lane moves faster than the originating one, then the merging vehicle must first decelerate in order to make its spacing with the leading vehicle ℓ_2 large enough for the lane changing maneuver, and then it must accelerate in order to adjust its velocity with the velocity of the destination lane. On the other hand, in the case where the destination lane moves slower than the originating one, then the merging vehicle must first decelerate in order to make its spacing with the leading vehicle ℓ_2 large enough for the lane changing maneuver, and then it may continue decelerating till its velocity becomes equal to the one of the destination lane.

Let V_d and V_o denote the velocity of the destination and originating lane, respectively, and let us examine the acceleration profiles of the merging vehicle in the case where $V_d > V_o$ (i.e., in the case where the destination lane moves faster than the originating one) and $V_d \leq V_o$ (i.e., in the case where the destination lane moves slower than the originating one).

- *The case where* $V_d > V_o$. In this case, the merging vehicle initially decelerates in order to create enough spacing in the originating lane for a safe and collision-free lane changing maneuver. As soon as a sufficient spacing has been created it starts accelerating in order to match its velocity with the velocity V_d of the destination lane. In this work, we will consider a simple model for the longitudinal acceleration profile of the merging vehicle. In particular, we will assume that the merging vehicle's acceleration initially decreases linearly with respect to time until it reaches a limit $-a_{comf}$, where a_{comf} is appropriately chosen to maintain safety and comfort of the passengers in the vehicle. Then, the acceleration remains constant and equal to $-a_{comf}$ until a sufficient spacing has been created in the originating lane and then it switches from decelerating to accelerating. In particular the acceleration starts increasing linearly until it reaches the positive acceleration limit a_{comf}. The acceleration remains constant and equal to a_{comf} for a certain time-interval and then it linearly decelerates to zero in such a way that the merging vehicle's velocity is equal to V_d at the time-instant t_{long}, i.e., at the time-instant that the merging vehicle's acceleration becomes zero.

  Using the above simple model for the longitudinal acceleration profile of the merging vehicle, we can see that the longitudinal acceleration profile, in the case where the destination lane moves faster than the originating one, is the one shown in Figure 2. The constant t_{ch} denotes the time-instant at which the merging vehicle switches from decelerating to accelerating (i.e., t_{ch} denotes the time-instant at which the longitudinal acceleration of the merging vehicle is zero and the vehicle starts accelerating) while the time-constant t_{long} is such that the longitudinal velocity of the merging vehicle equals to the velocity of the destination lane V_d.

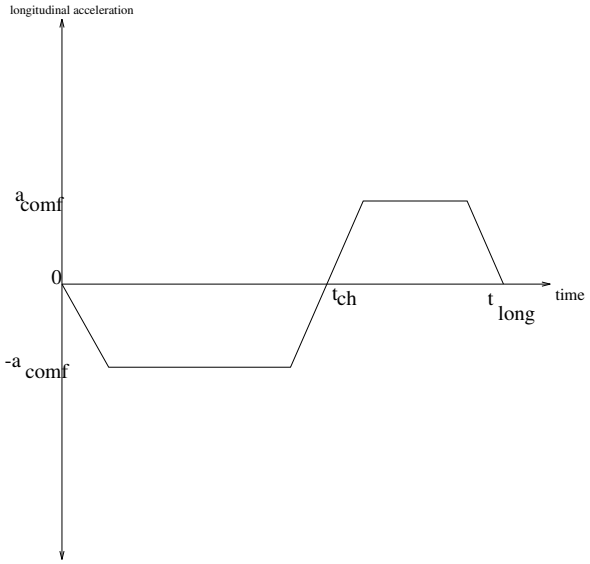

Figure 2: Longitudinal acceleration profile in the case where the destination lane moves faster than the originating one.

- *The case where* $V_d \leq V_o$. In this case, the merging vehicle decelerates in order to both create enough spacing in the originating lane for a safe and collision-free lane changing maneuver and match its velocity with the velocity of V_d of the destination lane. Similarly to the previous case, we will consider a very simple model for the longitudinal acceleration profile of the merging vehicle. In particular, we will consider that the merging vehicle's acceleration initially decreases linearly with respect to time until it reaches a limit $-a_{comf}$, where a_{comf} is appropriately chosen to maintain safety and comfort of the passengers in the vehicle. Then, the acceleration remains constant and equal to $-a_{comf}$ until both a sufficient spacing has been created in the originating lane and the merging vehicle's velocity is very close to V_d. When both the spacing in the originating lane guarantees safe and collision-free lane changing maneuver and the velocity of the merging vehicle is very close to V_d, the acceleration is linearly increased to zero, in such a way that the velocity of the merging vehicle at the time-instant t_{long} (i.e., at the time-instant at which the merging vehicle's acceleration becomes zero) is equal to V_d. The longitudinal acceleration profile, in the case where the destination lane moves slower than the originating one, is shown in Figure 3.

Note that the acceleration profile for the case where $V_d > V_o$ is a general one since we can get the acceleration profile for the case where $V_d \leq V_o$ by setting $t_{ch} = t_{long}$.

Several remarks are in order:

- In the above analysis we made the assumption that the velocities of the leading and following vehicles in the two lanes remain constant and, moreover, the following vehicles have the sampe velocity with that of the corresponding leading vehicle in the same lane. Such an assumption is made for simplicity and in many realistic situations does nto hold. Our results can be easily extended/modified to the case where

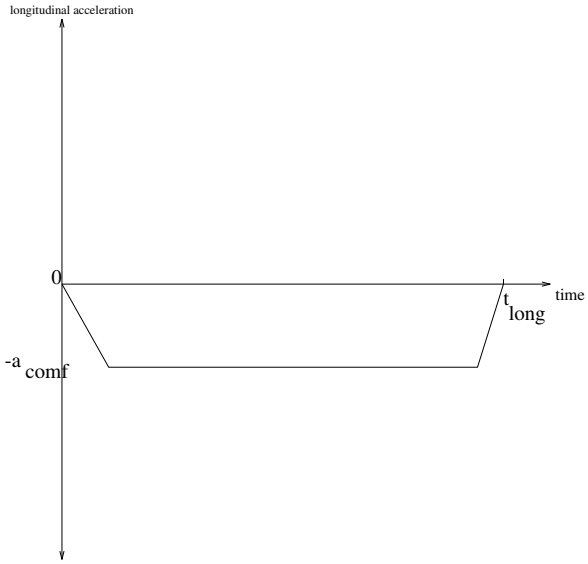

Figure 3: Longitudinal acceleration profile in the case where the destination lane moves slower than the originating one.

the vehicles' velocities do not remain constant, by appropriately modifying the algorithms presented in this paper. In fact, in the case where the velocities of the leading and following vehicles do not remain constant, the acceleration of the merging vehicle can still be assumed that is given by either figure 2 or figure 3, but the constants t_{ch} and t_{long} are chosen based on on-line information about the vehicles' velocities.

- In figures 2 and 3 the merging vehicle is shown to linearly accelerate or decelerate until it reaches a constant acceleration. The slope of such a linear acceleration/deceleration depends on the acceleration characteristics of the vehicle as well as on safety and comfort requirements.

- The results of this paper still hold if we assume a velocity profile for the merging vehicle instead of an acceleration profile. The simplest velocity profile could be the one at which the velocity of the merging vehicle linearly increases until the time-instant t_{ch} and then linearly increases until it becomes equal to V_d at the time-instant t_{long}.

- In the the above analysis we assumed that the following vehicles retain their velocity while the merging vehicle's velocity follows a time-varying trajectory in order to create enough spacing for merging and adjust its velocity. A similar trajectory like the one of the merging vehicle can be assumed for the following vehicles as well, in which case, the following vehicles adjust their velocities and spacings for the lane changing maneuver.

B. The Lateral Acceleration Model for the Merging Vehicle

For the purpose of our analysis, we will use a somewhat simplified model of the lane change maneuver trajectory which assumes a sinusoidal pattern of lateral acceleration. As a first order approximation, the

acceleration of a vehicle during normal lane change maneuvers can be modeled as a sine function of time [2, 5]. The variable parameters of this model are time and distance. The model is symmetric with respect to the direction of lane change, therefore the direction of the change is not a factor. Merging, exiting and weaving have all similar motions in terms of kinematic equations and the same model can be applied for all these cases. According to this model, the lateral acceleration is given by

$$a_{lat} = \begin{cases} \frac{2\pi d_I}{t_{LC}^2} \sin\left(\frac{2\pi}{t_{LC}}(t - t_{lat})\right) & \text{if } t \in [t_{lat}, t_{LC} + t_{lat}] \\ 0 & \text{otherwise} \end{cases} \tag{2.1}$$

where

- a_{lat} is the instantaneous lateral acceleration,
- t_{LC} is the total time to complete the lane change,
- t is the elapsed time,
- d_I is the lateral Intended Lane Change Distance.

Therefore, the lateral peak acceleration A is

$$A = \frac{2\pi d_I}{t_{LC}^2} \tag{2.2}$$

and the lane change frequency is

$$\omega = \frac{2\pi}{t_{LC}}$$

Given the lateral acceleration, the lateral velocity and the lateral distance traveled during a lane change can be derived by successive integration. The assumed sinusoidal acceleration pattern seems to be appropriate for automated lane changing in order to guarantee the comfort of the passengers of the vehicle. This is obvious from the fact that the corresponding jerk function (i.e., the time-derivative of the lateral acceleration) whose value affects passenger comfort does not have any pronounced peaks.

Empirical data collected by photographing several hundreds of lane changes on multi-lane highways [7] has been used to determine the distribution of lateral placement, lane change distance and total lane change time on the lateral acceleration model given by (2.1). The standard lane width on highways is 12 feet and this is the mean value of the d_I, which actually may vary from 9 feet to 15 feet. Total lane change times may vary widely. Lane changes of up to 16 seconds in duration are not outside the normal range, though most lane changes are significantly faster [2]. While the aerial photography method used in determining total lane change time involves a degree of underestimation due to the model used and the resolution limits available, a lower bound of about 2 seconds total lane change time has been determined [7]. The aggressiveness of the lane change depends primarily on the total time t_{LC} taken and also on the lane change distance.

The peak lateral acceleration A can be determined by substituting the d_I for the final distance and t_{LC} for the total time in the equation for A. Thus a range of lateral accelerations from 0.22 ft/sec^2 to 23.55

ft/sec^2 (or, equivalently, from 0.068 g to 0.73 g) has been found. If we assume that a nominal to slow lane change covers 12 feet in 5 seconds we have a peak acceleration of 3 ft/sec^2. The same distance covered in 4 seconds implies a peak acceleration of 4.7 ft/sec^2, while 3 seconds produce acceleration of 8.38 ft/sec^2 and 2.5 seconds produce acceleration of 12 ft/sec^2. It becomes obvious that very fast lane changes involve very large lateral acceleration, while slow lane changes involve negligible lateral acceleration.

C. Safe and Collision-Free Lane Changing Strategies

Using the above two models for the longitudinal and lateral acceleration profiles of the merging vehicle, one can obtain different merging strategies by appropriately chosing the parameters $t_{long}, t_{lat}, t_{ch}, a_{comf}$ and t_{LC}. In other words, a particular choice for these five parameters determines the merging strategy and, moreover, affects the safety of the lane changing maneuver.

We consider a lane changing to be safe and collision-free if there is sufficient spacing between the vehicles involved so that if any of the vehicles performs emergency braking at any time before, during, and after the lane changing all five vehicles could stop without colliding. In this scenario we did not consider the case where a possible collision could be avoided by using both braking and steering. The use of only braking is considered to be a worst case scenario and could lead to larger spacing requirements for collision-free lane change maneuvers. Moreover, this scenario is simpler since the use of both braking and steering for collision avoidance and the resulting spacing requirements for collision-free maneuvers are far more complex.

Since emergency braking can take place any time during a lane change maneuver, we could have a situation where the merging vehicle is decelerating for emergency stop while has both lateral and longitudinal motion. In this case its braking capabilities are limited due to the so-called friction-cycle. The explanation of the braking dynamics during lane change are presented in the following section.

III. Braking During Lane Changing

When a tire is operated under conditions of simultaneous longitudinal and lateral slip, the respective longitudinal and lateral forces depart markedly from those values derived under independent conditions (i.e., the values derived under only longitudinal or only lateral slip). The application of longitudinal slip generally tends to reduce the lateral force at a given slip angle[1] condition. Application of a slip angle reduces the longitudinal force developed under a given braking condition. This behavior can be seen in Figure 4 (taken from [4]).

The general effect on lateral force when braking is applied is illustrated in the traction field of Figure 5 (taken from [4]). The individual curves represent the lateral force at a given slip angle. As the brake force is applied, the lateral force gradually diminishes due to the additional slip induced in the contact area from

[1] *Slip Angle* is defined as the angle between the tire's direction of heading and its direction of travel.

Figure 4: Longitudinal and lateral forces (F_x, F_y) for different slip angles, as a function of longitudinal slip.

Figure 5: Lateral forces versus longitudinal force at constant lateral slip angles.

the braking demand. This type of diagram that displays the tire's traction field is the basis for the *friction circle* concept [4]. The "circle" in most cases is actually an ellipse. Recognizing that the friction limit for a tire, regardless of direction, will be determined by the coefficient of friction multiplied by the load, it is clear that the friction can be used for lateral force or brake (longitudinal) force or a combination of the two. The direction can be positive or negative and this make little difference. *But in no case can the vector total of the two exceed the friction limit.* The limit is therefore a circle (ellipse) in the plane of the lateral and longitudinal forces. The position of the circle in Figure 5 is the friction circle for the positive quadrant of the traction field. The limit is characterized as a friction circle for tires which have effectively the same limits for longitudinal and lateral forces. Certain specialized tires however, may be optimized for lateral traction or braking traction, in which case the limit is not a circle but an ellipse. By making the simplified assumption that the longitudinal and lateral forces F_x and F_y, respectively, during simultaneous longitudinal and lateral slip depend linearly on the longitudinal and lateral accelerations a_x and a_y, respectively, we have that, according to the above analysis regarding the "limited friction circle", the longitudinal and lateral accelerations must satisfy

$$a_x^2 + a_y^2 \leq F_c \tag{3.1}$$

where F_c is a positive constant. It is worth noticing, that in the case of pure longitudinal motion, the maximum longitudinal acceleration of the vehicle a_{max} is larger than $\sqrt{F_c}$. In other words, formula (3.1) applies only for the case of combined longitudinal/lateral braking and not for the case of pure longitudinal braking (in which case $a_y = 0$). The above inequality simply states that braking during combined longitudinal and lateral motion significantly degrades the braking capabilities of the vehicle, and, moreover, the stopping time of the vehicle depends on the time-history of the lateral accelerations; the larger is the lateral acceleration the more distance it takes for the vehicle to stop in the longitudinal direction.

IV. Emergency Braking during Lane Changing

In this section, we analyze the problem of emergency braking during lane changing. More precisely, we consider the problem of analyzing the behavior of the vehicles involved in a lane change maneuver in the case where one of these vehicles enters in an emergency braking situation. A braking scenario, which describes exactly how the vehicles brake, is usually specified by the deceleration profiles of the vehicles as a function of time. The deceleration profile depends, in general, not only on the road conditions and the braking abilities of the vehicle but also on the particular AHS operational concept and the sensors and communication devices that the vehicle is equipped with together with the associated capabilities [3, 6].

Contrary to the longitudinal case where only two vehicles are involved, in the lane changing case we have three different emergency braking scenaria:

1. The case where the vehicle ℓ_1 enters in an emergency braking situation.

2. The case where the vehicle ℓ_2 enters in an emergency braking situation.

3. The case where the merging vehicle m enters in an emergency braking situation.

Since the merging vehicle m is performing a lane changing when the emergency situation takes place, we may have the case where both the following vehicles f_1 and f_2 must enter in an emergency braking situation as well. This is because the merging vehicle is moving in both longitudinal and lateral directions, and therefore we might have the situation where the merging vehicle is in the originating lane when the emergency braking starts and ends up in the destination lane (or somewhere in-between) due to the lateral motion.

In order to simplify our analysis, we will describe only the case where the vehicle ℓ_1 enters in an emergency braking situation. The analysis for the other cases (vehicle ℓ_2 enters in an emergency braking situation, vehicle m enters in an emergency braking situation) are similar. Similarly, we will examine the deceleration profiles only for the case of the following vehicle f_1; the deceleration profiles for the following vehicle f_2 is similar.

Similar to the longitudinal case [3], the deceleration profiles for the vehicles involved in a lane changing maneuver depend on the particular AHS operational concept the vehicles operate under. However, the problem for the case of the lane change maneuver becomes more complicated because of many reasons such as the degraded braking capabilities of the merging vehicle as explained in the previous section. Let us examine the deceleration profiles for each AHS operational concept.

- *Autonomous Vehicles.* A possible AHS concept is the one where the vehicles operate independently, i.e., autonomously, using their own sensors, without any communication between the vehicles. Each vehicle senses its environment, including lane position, adjacent vehicles and obstacles. The infrastructure may provide basic traveler information services, i.e., road conditions and routing information.

  Since, for this particular AHS operational concept, each vehicle relies on its own sensors to determine the motion intentions of the vehicle ahead, we have to consider two different cases depending on whether the merging vehicle position prevents the sensors of the vehicle f_1 from sensing the position of the vehicle ℓ_1: in the first case, the vehicle f_1 can sense the position and relative velocity of the vehicle ℓ_1 since the merging vehicle is either still in the originating lane or, even if part of the vehicle m is already in the destination lane, its body is not in the operational range of the sensors of the vehicle f_1; in other words, in this case the vehicle ℓ_1 is "visible" by the vehicle f_1. The second case, is the case where the vehicle ℓ_1 is not "visible" by the f_1 one, because the merging vehicle prevents the sensors of the vehicle f_1 from sensing the motion of the vehicle ℓ_1. The situation where the vehicle ℓ_1 is "visible" and not "visible" by the vehicle f_1 is illustrated in Figures 6 and 7.

  Let us first analyze the case where the vehicle ℓ_1 is "visible" by the vehicle f_1. In this case, both the merging and the f_1 vehicles are assumed to behave similarly, in the sense that they both detect the

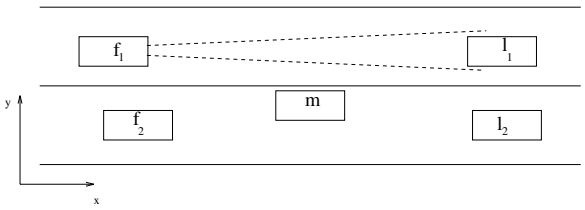

Figure 6: The case where the vehicle ℓ_1 is "visible" by the vehicle f_1.

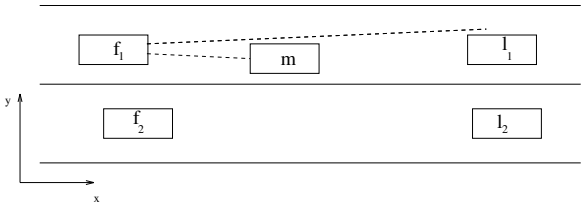

Figure 7: The case where the vehicle ℓ_1 is not "visible" by the vehicle f_1.

emergency braking at the same time. That is, after the vehicle ℓ_1 starts performing emergency braking, the merging and the vehicle f_1, which might have been accelerating initially, start decelerating after a detection and brake actuation delay in an effort to maintain the desired spacing. Since the two vehicles are not aware that the leader is performing emergency braking, they limit their jerks and decelerations in an effort to meet the vehicle control objective and at the same time maintain passenger comfort. The two vehicles detect and initiate emergency braking at possibly different time-instants (since the spacing between the merging vehicle and the vehicle ℓ_1 is less than the spacing between the vehicle f_1 and the vehicle ℓ_1, and thus it is natural to assume that the vehicle f_1 detects the emergency braking after the merging vehicle does). When emergency braking is detected, the passenger comfort is no longer an issue; the vehicles apply the maximum available deceleration in order to minimize the spacing needed for the vehicle to stop. The vehicles apply the maximum available deceleration at minimum time (maximum jerk). Due to the fact that the merging vehicle performs combined longitudinal/lateral braking it is expected (as explained in the previous section) that the maximum available deceleration are less than the ones when the vehicle performs pure longitudinal braking. In our analysis, we used a simplified model in order to incorporate the effect of combined longitudinal/lateral braking in the braking capabilities of the merging vehicle. More precisely, we assumed that if the merging vehicle detects and initiates emergency braking at the time-instant $t_{m_{emerg}}$ and its longitudinal and lateral accelerations at this time instant are $a_1^{(m)}(t_{m_{emerg}})$ and $a_2^{(m)}(t_{m_{emerg}})$, respectively, then both accelerations decrease linearly with respect to time, in such a way that at each time instant $t \geq t_{m_{emerg}}$ they satisfy constraint (3.1). In other words, we have assumed that the longitudinal and lateral accelerations after $t_{m_{emerg}}$ satisfy

$$a_1^{(m)}(t) = \begin{cases} a_1^{(m)}(t_{m_{emerg}}) - J_1[t - t_{m_{emerg}}] & \text{if } |a_1^{(m)}(t)|^2 < F_c \\ \sqrt{F_c} & \text{otherwise} \end{cases} \tag{4.1}$$

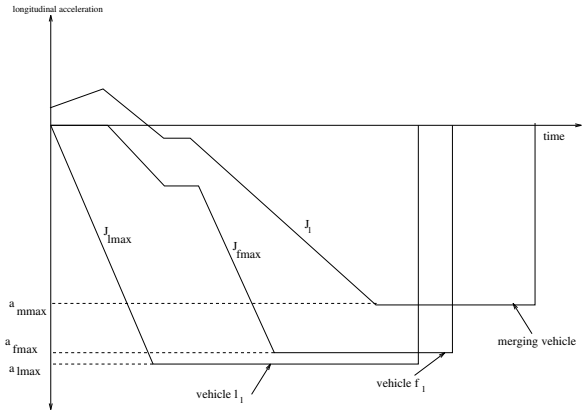

Figure 8: Autonomous Vehicles: The case where the leader is "visible" by the follower.

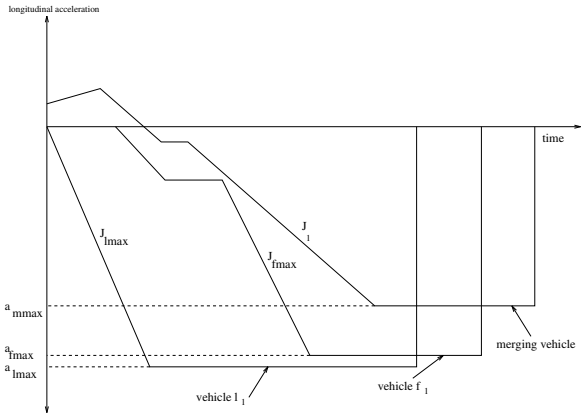

Figure 9: Autonomous Vehicles: The case where the leader is not "visible" by the follower.

$$a_2^{(m)}(t) = \begin{cases} a_2^{(m)}(t_{m_{emerg}}) - J_2[t - t_{m_{emerg}}] & \text{if } v_2^{(m)}(t) > 0 \\ 0 & \text{otherwise} \end{cases} \tag{4.2}$$

where J_1 and J_2 are such that the longitudinal and lateral accelerations $a_1^{(m)}(t)$ and $a_2^{(m)}(t)$ satisfy constraint (3.1) at each $t > t_{m_{emerg}}$. Figure 8 shows the deceleration profiles for the case where the vehicle ℓ_1 is "visible" by the vehicle f_1, where $a_{mmax} = \sqrt{F_c}$.

Let us now analyze the case where the vehicle ℓ_1 is not "visible" by the vehicle f_1. In this case, the deceleration profile for the vehicle f_1 becomes more complicated, while the deceleration profiles of other two vehicles remain the same. The fact, that the sensors of the vehicle f_1 sense only the merging vehicle has the effect the follower to detect the emergency braking situation t_d seconds after the merging vehicle has detected it. The deceleration profiles for the case where the vehicle ℓ_1 is not "visible" by the follower are shown in Figure 9.

- *Free Agents - Infrastructure Supported.* A vehicle is considered a "free agent" if it has the capability to operate autonomously but it is also able to receive communications from other vehicles and from the infrastructure. This implies that the infrastructure may get involved in a supporting role, by issuing warnings and recommendations for desired speed and headways but the infrastructure will not have the

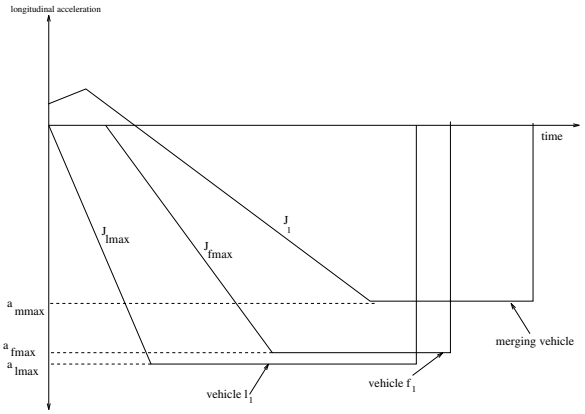

Figure 10: Infrastructure supported free agent vehicles.

authority to issue direct control commands.

Since there exists vehicle to vehicle communication, the leader communicates with the merging vehicle and the merging vehicle, in turn, communicates with the follower, and, therefore, in the case where the leader enters in an emergency braking situation, the merging vehicle and the follower are informed about the emergency braking situation and verify using their own sensors. When the merging and the vehicle f_1 detect that the vehicle ℓ_1 is braking and at the same time receive the information that this is an emergency braking, they bypass the limited jerk/limited braking stage of the autonomous vehicles case. However, as it is shown in Figure 10, there will be a time-delay before the merging vehicle and the follower apply emergency braking. Such a delay is due to the communication delays between the three vehicles and the time needed for the sensors to verify the emergency braking situation. It must expected that the time-delay for the follower to detect and verify emergency braking is larger than the one for the merging vehicle since, similar to the autonomous vehicles case, the vehicle ℓ_1 may be "invisible" from the follower, the follower and the merging vehicle are not at the same lateral position, etc. Finally, the braking capabilities of the merging vehicle will be degraded due to the combined longitudinal/lateral braking. Figure 10 shows the deceleration profiles for the case of infrastructure supported-free agent vehicles. Similar to the autonomous case, the braking capabilities of the merging vehicle will be degraded (see equations (4.1) (4.2)).

- *Free Agents - Infrastructure Managed.* The concept of Free Agents with Infrastructure Management is based on the assumption that the traffic is composed of vehicles acting as free agents while the infrastructure assumes a more active and more complex role in the coordination of the traffic flow and control of vehicles. Each vehicle is able to operate autonomously and uses its sensors to sense its position and environment, including lane position, adjacent vehicles and obstacles. The difference in this centrally managed architecture is that the infrastructure has the ability to send commands to individual vehicles. This is envisioned to be a "request-response" type architecture, in which individual vehicles

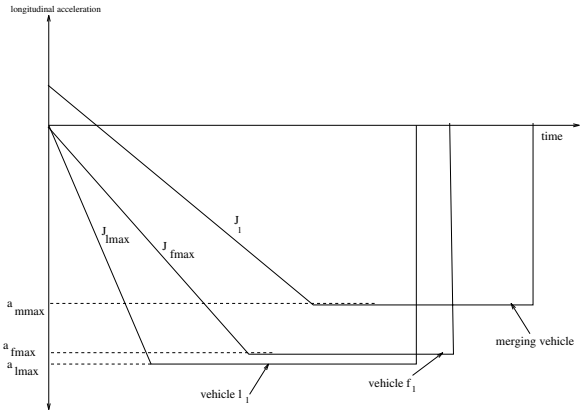

Figure 11: Infrastructure managed free agent vehicles.

ask permission from the infrastructure to perform certain activities and the infrastructure responds by sending commands back to the requesting vehicle and to other vehicles in the neighborhood.

It is expected and assumed that the infrastructure is able to detect emergency situations and whenever it detects such an emergency, the infrastructure will have the responsibility to send an emergency braking command to all the vehicles affected. This concept minimizes the delay in performing emergency braking. The infrastructure may simply issue the command "begin emergency braking now" and all vehicles receiving this will have to apply maximum braking without further delay. This, not only simplifies the task of determining when the vehicle ℓ_1 is performing emergency braking but also minimizes the relative delay in propagating the onset of emergency braking from each vehicle to the vehicle behind, effectively down to zero. In Figure 11, we have plotted the deceleration profiles for the case of free agents with infrastructure management. Notice that the deceleration profiles for the three vehicles will be similar (and moreover the vehicles ℓ_1 and f_1 will stop at the same time-instant in the case where the two vehicles have the same braking capabilities, i.e., in the case where $J_{\ell max} = J_{f max}$ and $a_{\ell max} = a_{f max}$). Similar to the autonomous case, the braking capabilities of the merging vehicle will be degraded (see equations (4.1) (4.2)).

- *Vehicles Platoons without Coordinated Braking.* This concept represents the possibility that the safest and possibly most cost-effective way of achieving maximum capacity is by making platoons of vehicles the basic controlling unit. Platoons are clusters of vehicles with short spacing between individual vehicles in each group and longer spacings between platoons. The characterizing differentiation is the the platoon is to be treated by the infrastructure as an "entity" thereby minimizing some of the need for communicating with and coordinating individual vehicles. The infrastructure does not attempt to control any individual vehicle under normal circumstances, keeping the cost and necessary bandwidth low. The infrastructure is expected to be an intelligent agent which monitors and coordinates the operation of the platoons. Tight coordination is required within the platoon in order to maintain a close

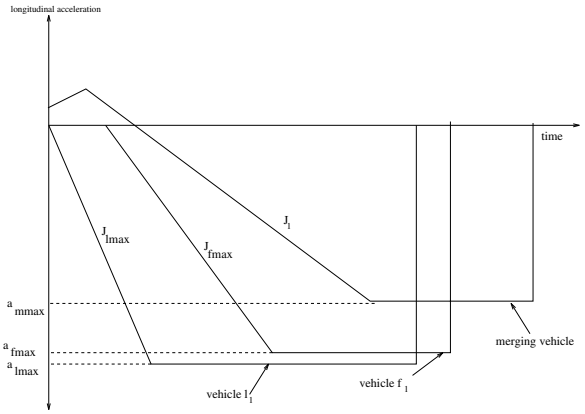

Figure 12: Platoons without coordinated braking.

spacing and this requires that the vehicles must be communicating with each other constantly. The significantly longer inter-platoon spacing is required to guarantee no inter-platoon collisions.

Each vehicle is expected to be equipped with sensors and intelligence to maintain its lane position, sense its immediate surroundings, and perform the functions of merging into and splitting off a platoon. It is not expected to accomplish lane changes, or merging and splitting without the infrastructure's or the platoons entity's help. The main mode of operation of the infrastructure would be of a request-response type. Each platoon's and/or vehicle's request is processed and appropriate commands are sent to the appropriate vehicles/platoons to respond that request. The infrastructure takes a more pro-active role in monitoring traffic flow, broadcasting traffic flow messages, advising lane changes to individual vehicles and platoons in addition to the usual information provider functions.

Once a vehicle has merged into a platoon, the headway maintenance controller must take into account the braking capabilities of the vehicle ahead in order to set an appropriate separation distance that minimizes the possibility of collision. The platoon leader may also provide corrections to the individual intra-platoon headways in order to reduce the possibility of a rear-end collision between two vehicles propagating to the other members of the platoon.

In this concept we assume that no coordination of the braking sequence takes place within a platoon in order to distinguish it from the next one where coordinated braking is employed. Despite the fact that there is no coordinated braking, each vehicle notifies the vehicle behind about its braking capabilities and the magnitude and timing of the braking force used. When the platoon leader detects an emergency, it immediately notifies the vehicle that follows. There will be a delay while the message propagates from each vehicle to the vehicle behind, as well as an actuation delay. The deceleration profiles for the case of platoons without coordinated braking is shown in Figure 12. Notice that the merging vehicle's profile is slightly different than the one of the vehicle f_1, due to the degraded braking capabilities of the merging vehicle.

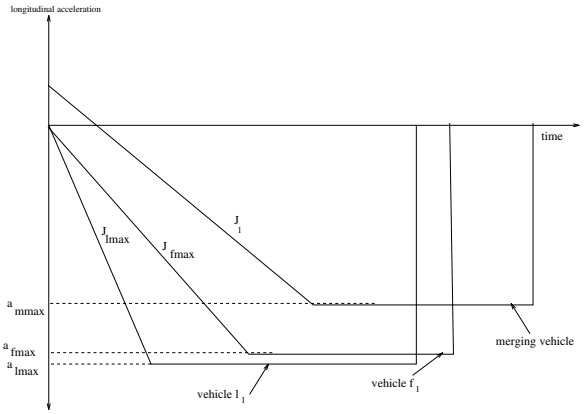

Figure 13: Platoons with coordinated braking and no delay.

- *Vehicles Platoons with Coordinated Braking.* The platooning concept with coordinated braking is based on the concept of maximizing capacity by carefully coordinating the timing and degree of braking among the vehicles participating in a platoon entity. This allows the minimization of spacing between vehicles without compromising safety. During a braking maneuver the platoon leader may dictate a braking sequence to be followed by each vehicle so that the maneuver is performed without any intra-platoon collision. Such a sequence may require the last vehicle to brake first followed by the second last vehicle, etc.

  In platooning with coordinating braking we assume that the platoon leader assumes the primary responsibility of detecting emergencies and notifying each and every vehicle in the platoon. This notification takes place through a network style vehicle to vehicle communication system that minimizes the communication delays. The platoon leader notifies all the vehicles in the platoon about the magnitude of the braking force that is to be applied and also the exact time this is to be applied. This architecture, not only eliminates the need for each vehicle to detect the magnitude of the braking and if the braking should be limited or emergency braking, but also can adjust the onset of emergency braking for an effective 0 seconds relative delay, or even to an artificial negative relative delay. The brake actuation delay can be completely compensated for and it is not affecting the scenario as long as it is approximately the same for each vehicle. Figure 13 shows the deceleration profiles for the case of platooning with coordinated braking and no delays.

V. Safe Spacing for Lane Changing

Consider again the five vehicles involved in a lane changing maneuver as shown in Figure 1. For simplicity, we will assume that during the lane change maneuver the leading and following vehicles ℓ_1, ℓ_2, f_1, f_2 travel with constant velocities unless an emergency braking happens. Suppose that the j-th vehicle (where $j \in \{\ell_1, \ell_2, m\}$) enters in emergency braking situation at the time-instant t_s. Then, we have that the longitudinal and lateral

accelerations of the five vehicles are as follows

$$a_1^{(i)}(t;t_s) = \begin{cases} 0 & \text{if } t < t_s \\ \bar{a}_1^{(i)}(t;j) & \text{otherwise} \end{cases} \qquad i \in \{\ell_1, \ell_2, f_1, f_2\} \tag{5.1}$$

$$a_2^{(i)}(t) = 0, \ \forall t, \qquad i \in \{\ell_1, \ell_2, f_1, f_2\} \tag{5.2}$$

$$a_1^{(m)}(t;t_s) = \begin{cases} \tilde{a}_1^{(m)}(t) & \text{if } t < t_s \\ \bar{a}_1^{(m)}(t;j) & \text{otherwise} \end{cases} \tag{5.3}$$

$$a_2^{(m)}(t;t_s) = \begin{cases} \tilde{a}_2^{(m)}(t) & \text{if } t < t_{m_{emerg}} \\ \bar{a}_2^{(m)}(t;j) & \text{otherwise} \end{cases} \tag{5.4}$$

where $\bar{a}_1^{(i)}(t;j), i \in \{\ell_1, \ell_2, f_1, f_2\}$ is the deceleration profile of the i-th vehicle in the case where the j-th vehicle performs an emergency braking as described in the previous section, $\tilde{a}_1^{(m)}(t)$, $\tilde{a}_2^{(m)}(t)$ denote the longitudinal and lateral, respectively, acceleration models for the merging vehicle when it performs the lane changing maneuver, and $\tilde{a}_1^{(m)}(t;j)$, $\tilde{a}_2^{(m)}(t;j)$ denote the longitudinal and lateral, respectively, deceleration profiles of the merging vehicle in the case where the j-th vehicle performs an emergency braking as described in the previous section. More precisely, the longitudinal acceleration $\tilde{a}_1^{(m)}(t)$ is given in Figures 2 and 3, depending on whether the destination lane moves faster than the originating one, the lateral acceleration $\tilde{a}_2^{(m)}(t)$ is the sinusoidal function given in equation (2.1) and finally the longitudinal and lateral decelerations $\tilde{a}_1^{(m)}(t;j)$, $\tilde{a}_2^{(m)}(t;j)$ are given in equations (4.1) and (4.2), respectively. Finally note that $t_{m_{emerg}}$ is equal to $t_s + t_d$, where t_d denotes the time needed for the merging vehicle to detect and initiate emergency braking.

Based on the above equations, we can calculate the position and velocity of the vehicle i, $i \in \{\ell_1, \ell_2, m, f_1, f_2\}$ as follows

$$x^{(i)}(t) = x^{(i)}(0) + \int_0^t v^{(i)}(\tau) d\tau \tag{5.5}$$

$$v^{(i)}(t) = v^{(i)}(0) + \int_0^t a^{(i)}(\tau) d\tau \tag{5.6}$$

where $x^{(i)}(0), v^{(i)}(0)$ denote the initial position and velocity of the vehicle, respectively.

If the initial intervehicle spacings are large enough, then there would be no collision in the case of emergency braking during the lane change maneuver. For a given lane changing policy and a given AHS operational concept, we would like to calculate the minimum value of the initial intervehicle spacing for which there will be no collision. We refer to this value as the *Minimum Safety Spacing during Lane Changing - (MSSLC)* between those two vehicles. Note that we are interested in the following intervehicle distances $d_{\ell_1 f_1}, d_{\ell_1 m}, d_{\ell_2 f_2}, d_{\ell_2, m}, d_{m f_1}$ and $d_{m f_2}$.

Our approach in calculating the MSSLC is as follows: let us consider the intervehicle spacing d_{kh} where d_{kh} is one of the spacings of interest $d_{\ell_1 f_1}, d_{\ell_1 m}, d_{\ell_2 f_2}, d_{\ell_2, m}, d_{m f_1}$ and $d_{m f_2}$. Suppose now that each of the five vehicles travels in the freeway alone, i.e., assume that the rest four vehicles are absent. Let $T_s^{(h)}(t_s;j)$ be the *stopping time* of the h-th vehicle in the case where the j-th vehicle $j \in \{\ell_1, \ell_2, m\}$ starts an emergency braking

at $t = t_s$, i.e., $T_s^{(h)}(t_s; j)$ is the time at which the h-th vehicle velocity is zero. Note now that a collision occurs if the following holds: there exists a time instant $t_c \in [0, {}_s^{(h)}(t_s; j)]$ such that $d_{kh}(t_c)$ is negative and moreover the lateral positions of the vehicles k and h satisfy $|x_2^{(k)}(t_c) - x_2^{(h)}(t_c)| < L_{lat}^{kh}$; here L_{lat}^{kh} is defined as follows: suppose that the two vehicles k and h are in two adjacent lanes and their longitudinal positions are the same. Then L_{lat}^{kh} denotes the minimum lateral distance of the vehicles k and h such that if the lateral distance between these two vehicles is larger than L_{lat}^{kh} then the two vehicle do not collide. The definition of the constant L_{lat}^{kh} is necessary because we may have the case where the spacing d_{hk} is negative at a given time-instant but a collision does not occur because the two vehicles are in two different lanes (or their lateral distance is large enough) at this time-instant. In order to incorporate the case where the two vehicles have large enough lateral distance we define the variable $\mathcal{I}_{hk}$ as follows: $\mathcal{I}_{hk} = 1$ if $|x_2^{(k)} - x_2^{(h)}| < L_{lat}^{kh}$ and $\mathcal{I}_{hk} = 0$, otherwise. Then, the MSSLC for the spacing d_{kh} is defined as follows

$$D_{min}^{kh} = - \min_{t_s \in [0, t_{LC}], j \in \{\ell_1, \ell_2, m\}} \left\{ \min_{t \in [0, T_s^{(h)}(t_s, j)]} \{ I_{hk}(t) \cdot d_{kh}(t), 0 \} \right\} \tag{5.7}$$

In other words, D_{min}^{kh} is equal to the maximum distance by which the vehicle h would overtake vehicle k, for all possible different emergency braking situations, in the case where the two vehicles travel alone. $D_{min}^{kh} < 0$ implies that a collision occurs, while $D_{min}^{kh} = 0$ implies that the initial spacing between the vehicles k and h is such that there will be no collision in the case where any of the vehicles ℓ_1, ℓ_2, m at any time-instant during the lane change maneuver enters in an emergency braking situation.

We employ a exhaustive search technique in order to calculate the MSSLCs D_{min}^{kh}, i.e., we calculate the intervehicle spacings for all the possible cases of emergency braking situation as it is demonstrated in the following algorithm

Algorithm for the Calculation of MSSLCs

1. **Choose** the sampling time interval Δt.

2. **Specify** the velocities in originating lane V_o and in destination lane V_d, the initial positions of the vehicles, and the intended lane change distance d_I. For each vehicle $j \in \{\ell_1, \ell_2, m, f_1, f_2\}$, specify the maximum available acceleration a_{jmax} and jerk J_{jmax}; specify the friction limit constant F_c for the merging vehicle. Finally, specify the deceleration profiles of the five vehicles based on the analysis of section IV, the constants L_{lat}^{kh} and the time constant t_d such that $t_{m_{emerg}} = t_s + t_d$.

3. **Specify the Merging Strategy**: Choose the parameters $t_{long}, t_{lat}, t_{ch}, t_{LC}$ and a_{comf} that determine the merging strategy.

4. **FOR** all $D_{min}^{kh} \in \{D_{min}^{\ell_1,f_1}, D_{min}^{\ell_1,m}, D_{min}^{\ell_2,f_2}, D_{min}^{\ell_2,m}, D_{min}^{m,f_1}, D_{min}^{m,f_2}\}$ **DO**

   (a) Set $D_{min}^{kh} = 0$.

   (b) **FOR** all $j \in \{\ell_1, \ell_2, m\}$ **DO**

      i. **FOR** all $t_s \in \{0, \Delta t, 2\Delta t, \ldots, t_{LC}\}$ **DO**

         A. Set $t = 0$.

         B. Calculate $a^k(t)$ and $a^h(t)$, based on equations (5.1)-(5.4).

         C. Update $v^{(k)}, v^{(h)}, x^{(k)}, x^{(h)}$ based on equations (5.5), (5.6), i.e., set

$$v^{(i)}(t+\Delta t) = v^{(i)}(t) + \int_t^{t+\Delta t} a^{(i)}(\tau)d\tau,\ i = k, h$$

$$x^{(i)}(t+\Delta t) = x^{(i)}(t) + \int_t^{t+\Delta t} v^{(i)}(\tau)d\tau,\ i = k, h$$

         D. **IF** $D_{min}^{kh} > -I_{hk}(t+\Delta t) \cdot d_{kh}(t+\Delta t)$ **THEN** set

$$D_{min}^{kh} = -I_{hk}(t+\Delta t) \cdot d_{kh}(t+\Delta t)$$

         E. **IF** $v^{(h)}(t+\Delta t) > 0$ **THEN** set $t = t + \Delta t$ and **GOTO STEP B**
         OTHERWISE set $T_s^{(h)}(t_s, j) = t + \Delta t$ and **ENDFOR**

   (c) **ENDFOR**

5. **ENDFOR**

VI. Simulations

We used the algorithm presented in the previous section in order to calculate the Minimum Safety Distances for different conditions during a lane changing maneuver. Only the case of autonomous vehicles was considered; for simplicity all the five vehicles was assumed to have the same characteristics and performance. More precisely, we considered five vehicles with length 5 meters, and maximum deceleration (during braking) and jerk equal to $0.5g$ and 50 m/sec^3, respectively. The constant F_c for the merging vehicle was set equal to 0.25. In the case where one of the leading vehicles enters in an emergency braking situation, we assumed that the merging vehicle needs a time of 0.3 seconds to start decelerating and a time of 1 second to confirm the emergency braking and 0.3 seconds to start performing emergency braking. For the two following vehicles, we assumed the same time-delays in the case where the emergency-braking leading vehicle is "visible" and in the case where it is not visible we assumed that the following vehicle needs 2 seconds to start decelerating, 1 second to confirm the emergency braking and and 0.3 seconds to start performing emergency braking. The constants L_{lat}^{kh} were all set equal to 2 meters.

Regarding now the particular lane changing policy of the merging vehicle we choose the various parameters as follows: In order to simplify the problem we assumed that the time (delay) needed for the merging vehicle to switch from a_{comf} deceleration/acceleration to 0 or a_{comf} acceleration/deceleration was negligible (i.e. this time was set equal to zero in the simulations). Moreover, we set $t_{lat} = t_{ch} = 0$ and tried different values for the a_{comf} in order to cover many possible cases of different lane changing maneuver strategies.

We run three different simulations. In all three simulations we calculated the MSSLC functions for the case where the speed in the destination and originating lane covers the range between 10 and 30 m/sec. In the first simulation we set $a_{comf} = 0.1g$ and the time t_{LC} needed for the lane changing maneuver to be completed was set equal to 5 seconds. In the second simulation, we increased a_{comf} to $0.3g$ and we kept $t_{LC} = 5$ seconds. In the third simulation we set a_{comf} equal to $0.1g$ and we increased t_{LC} to 10 seconds.

Figures 14-17 plot the MSSLC values versus relative speed between the originating and the destination lanes for the three different simulations while Figures 18-21 plot the worst case emergency braking time for the various intervehicle spacings versus the the relative speed $V_d - V_o$ between the two lanes for the three different simulations. By "worst case emergency braking time" for a particular intervehicle spacing between two vehicles and given velocities in the two lanes, we define the time-instant which is such that, if an emergency braking starts at this instant, then the required safety spacing for the particular two vehicles is the maximum. Note that at each figure more than one points (i.e., more than one MSSLC) correspond to each relative speed point; those MSSLC points correspond to different absolute speed values. For example, when the relative speed is -5 the various MSSLC points that correspond to this relative speed are for the cases where $(V_o = 30, V_d = 25)$, $(V_o = 28, V_d = 23)$, $(V_o = 26, V_d = 21)$, etc. The points that correspond to

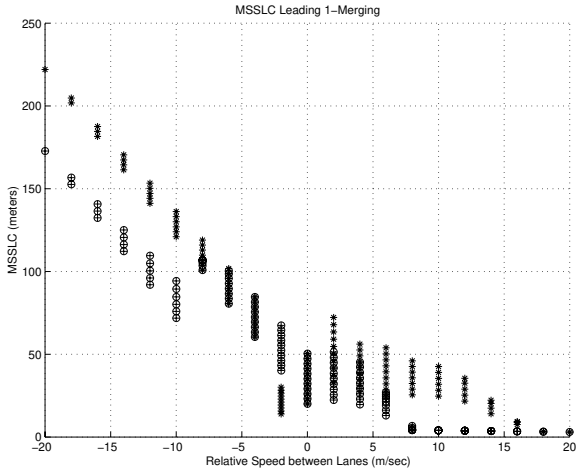

Figure 14: MSSLC for the spacing between the Vehicle ℓ_1 and the Merging Vehicle versus Relative Speed between Lanes ($\circ$: $a_{comf} = 0.1g$ and $t_{LC} = 5$ seconds; $\star$: $a_{comf} = 0.3g$ and $t_{LC} = 5$ seconds; $+$: $a_{comf} = 0.1g$ and $t_{LC} = 10$ seconds).

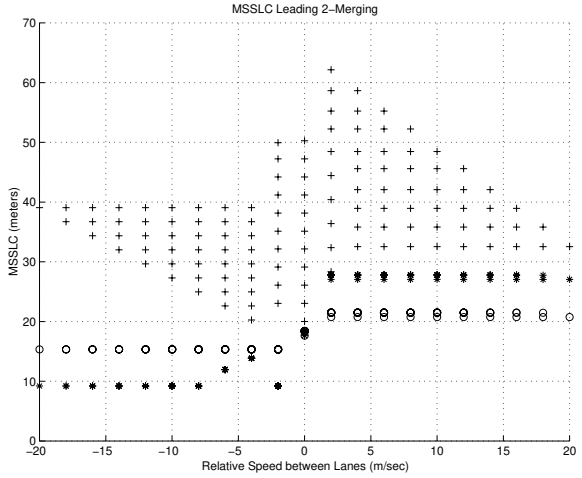

Figure 15: MSSLC for the spacing between the Vehicle ℓ_2 and the Merging Vehicle versus Relative Speed between Lanes ($\circ$: $a_{comf} = 0.1g$ and $t_{LC} = 5$ seconds; $\star$: $a_{comf} = 0.3g$ and $t_{LC} = 5$ seconds; $+$: $a_{comf} = 0.1g$ and $t_{LC} = 10$ seconds).

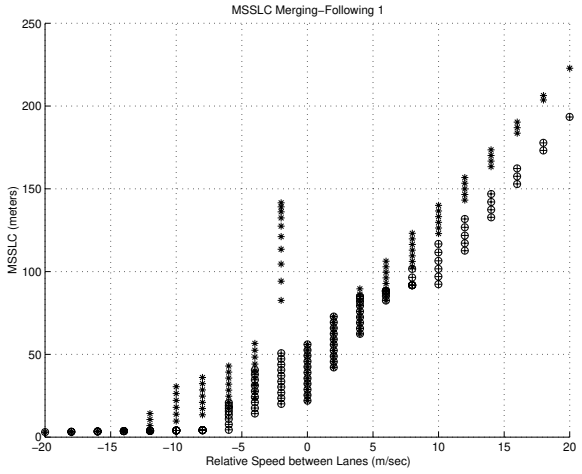

Figure 16: MSSLC for the spacing between the Merging Vehicle and the Vehicle f_1 versus Relative Speed between Lanes ($\circ$: $a_{comf} = 0.1g$ and $t_{LC} = 5$ seconds; $\star$: $a_{comf} = 0.3g$ and $t_{LC} = 5$ seconds; $+$: $a_{comf} = 0.1g$ and $t_{LC} = 10$ seconds).

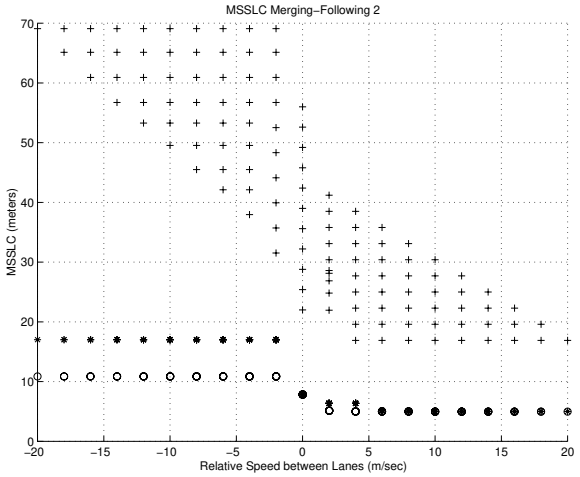

Figure 17: MSSLC for the spacing between the Merging Vehicle and the Vehicle f_2 versus Relative Speed between Lanes ($\circ$: $a_{comf} = 0.1g$ and $t_{LC} = 5$ seconds; $\star$: $a_{comf} = 0.3g$ and $t_{LC} = 5$ seconds; $+$: $a_{comf} = 0.1g$ and $t_{LC} = 10$ seconds).

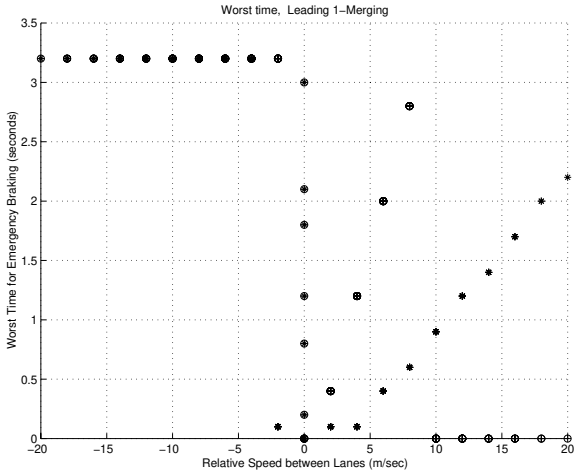

Figure 18: Worst case emergency braking time for the spacing between the Vehicle ℓ_1 and the Merging Vehicle versus Relative Speed between Lanes ($\circ$: $a_{comf} = 0.1g$ and $t_{LC} = 5$ seconds; $\star$: $a_{comf} = 0.3g$ and $t_{LC} = 5$ seconds; $+$: $a_{comf} = 0.1g$ and $t_{LC} = 10$ seconds).

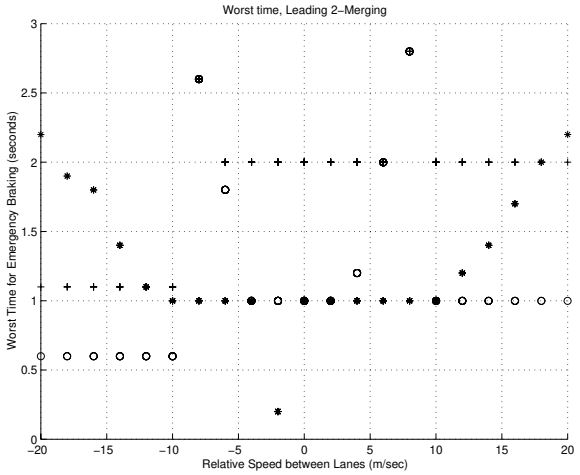

Figure 19: Worst case emergency braking time for the spacing between the Vehicle ℓ_2 and the Merging Vehicle versus Relative Speed between Lanes ($\circ$: $a_{comf} = 0.1g$ and $t_{LC} = 5$ seconds; $\star$: $a_{comf} = 0.3g$ and $t_{LC} = 5$ seconds; $+$: $a_{comf} = 0.1g$ and $t_{LC} = 10$ seconds).

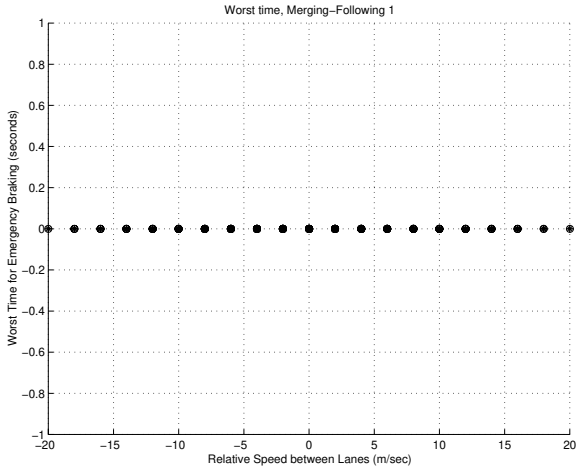

Figure 20: Worst case emergency braking time for the spacing between the Merging Vehicle and the Vehicle f_1 versus Relative Speed between Lanes ($\circ$: $a_{comf} = 0.1g$ and $t_{LC} = 5$ seconds; $\star$: $a_{comf} = 0.3g$ and $t_{LC} = 5$ seconds; $+$: $a_{comf} = 0.1g$ and $t_{LC} = 10$ seconds).

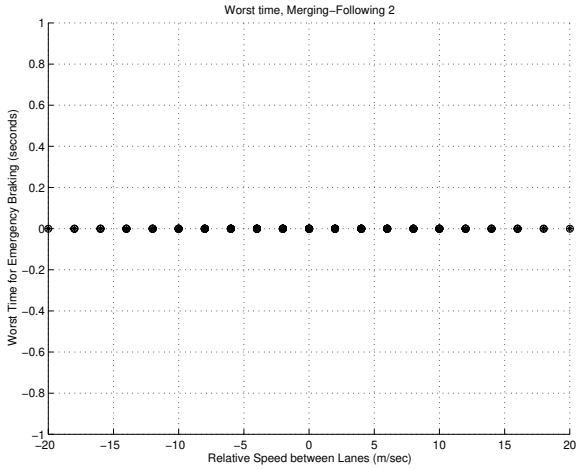

Figure 21: Worst case emergency braking time for the spacing between the Merging Vehicle and the Vehicle f_2 versus Relative Speed between Lanes ($\circ$: $a_{comf} = 0.1g$ and $t_{LC} = 5$ seconds; $\star$: $a_{comf} = 0.3g$ and $t_{LC} = 5$ seconds; $+$: $a_{comf} = 0.1g$ and $t_{LC} = 10$ seconds).

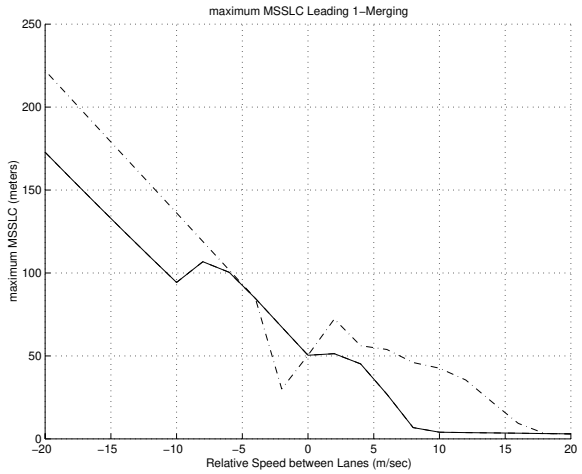

Figure 22: Maximum MSSLC for the spacing between the Vehicle ℓ_1 and the Merging Vehicle versus Relative Speed between Lanes (solid curve: $a_{comf} = 0.1g$ and $t_{LC} = 5$ seconds; dash-dotted curve: $a_{comf} = 0.3g$ and $t_{LC} = 5$ seconds; dashed curve: $a_{comf} = 0.1g$ and $t_{LC} = 10$ seconds).

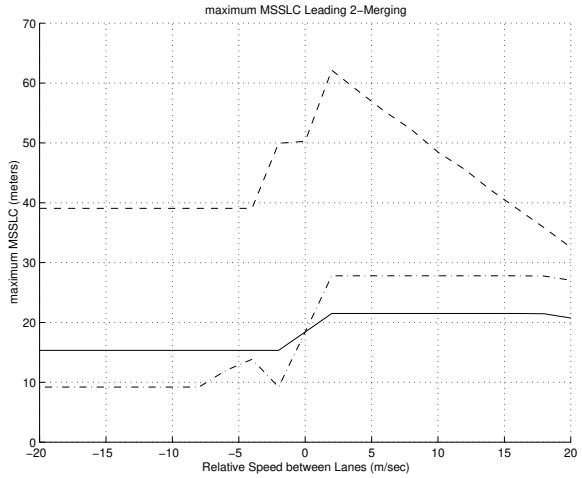

Figure 23: Maximum MSSLC for the spacing between the Vehicle ℓ_2 and the Merging Vehicle versus Relative Speed between Lanes (solid curve: $a_{comf} = 0.1g$ and $t_{LC} = 5$ seconds; dash-dotted curve: $a_{comf} = 0.3g$ and $t_{LC} = 5$ seconds; dashed curve: $a_{comf} = 0.1g$ and $t_{LC} = 10$ seconds).

the highest MSSLCs are the points that correspond to the highest absolute speed values. In Figures 22-25, we plot the Maximum MSSLC's versus relative speed between the two lanes, where by Maximum MSSLC we mean the maximum MSSLC that corresponds to a given relative speed point.

By observing the Figures 14-25, we can see that

- The MSSLC for the spacing between the leading vehicle in the destination lane and the merging vehicle increases very fast as the relative speed between the originating and the destination lane increases. On the other hand, the MSSLC for the spacing between the merging vehicle and the following vehicle in the destination lane increases very fast as the relative speed between the originating and the destination lane decreases, while the spacings between the merging vehicle and the leading and following vehicle in the originating lane remain small. Moreover, for $a_{comf} = 0.1$, the spacings between the merging vehicle and the leading and following vehicle in the originating lane remain almost constant as soon as the sign

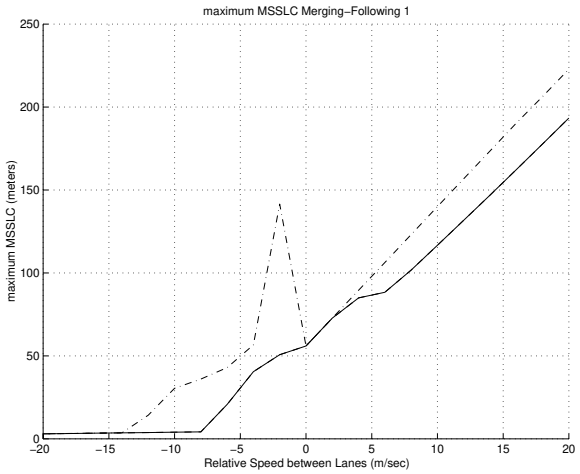

Figure 24: Maximum MSSLC for the spacing between the Merging Vehicle and the Vehicle f_1 versus Relative Speed between Lanes (solid curve: $a_{comf} = 0.1g$ and $t_{LC} = 5$ seconds; dash-dotted curve: $a_{comf} = 0.3g$ and $t_{LC} = 5$ seconds; dashed curve: $a_{comf} = 0.1g$ and $t_{LC} = 10$ seconds).

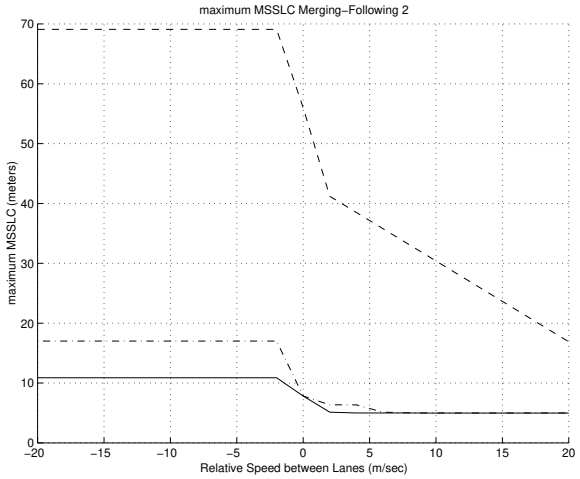

Figure 25: Maximum MSSLC for the spacing between the Merging Vehicle and the Vehicle f_2 versus Relative Speed between Lanes (solid curve: $a_{comf} = 0.1g$ and $t_{LC} = 5$ seconds; dash-dotted curve: $a_{comf} = 0.3g$ and $t_{LC} = 5$ seconds; dashed curve: $a_{comf} = 0.1g$ and $t_{LC} = 10$ seconds).

of the relative speed between the two lanes remains constant.

- The magnitude of the "control variable" a_{comf} affects significantly the MSSLC. In general, as can be seen in figures 14-17, the more aggressive is the adjustment in the longitudinal direction (i.e., the larger is a_{comf}), the larger are the safety spacings required.

- The "aggressiveness" of the lane change maneuver specified by the magnitude of the variable t_{LC} does not affect the MSSLC for the spacings between the merging vehicle and the vehicles in the originating lane, but affects considerably the MSSLC for the spacings between the merging vehicle and the vehicles in the originating lane. For instance, the MSSLC's for the spacings between the merging vehicle and the vehicles in the originating lane are in the range $4m - 30m$ in the case where $t_{LC} = 5$ seconds and they increase considerably (in the range $16m - 70m$) in the case where $t_{LC} = 10$ seconds.

- The main factor that affects the MSSLC is the relative speed between the two lanes. In general, the smaller is the relative speed between the two lanes the less is the required safety spacing.

- The sensitivity of the MSSLC with respect to the absolute speed of the two lanes is large. As it can be seen in the figures 14-17, for a given relative speed between the two lanes the MSSLC obtained for high absolute speeds is sometimes up to 50 meters larger than the MSSLC obtained for the same relative speed but for low absolute speeds. On the contrary, the worst case emergency braking time is not affected by the absolute speed, as it can be seen in Figures 18-21.

- The worst time for an emergency braking heavily depends on the relative speed between the two lanes as well. Moreover, the worst case emergency braking time for a particular spacing between two vehicles as a function of the relative speed between the two lanes, differs a lot with the worst case emergency braking time of the spacing between two other vehicles. Therefore, we cannot specify (given the lane changing policy and the relative speed between the two lanes) a particular time-instant of the lane-changing maneuver as the most "dangerous" for en emergency braking situation, i.e., as the time-instant at which an emergency braking will produce the worst results.

VII. Conclusions

In this work, we analyzed the problem of collision-free merging and lane changing. We examined various alternative scenaria for merging and lane changing and we presented an algorithm for calculating the *Minimum Safety Spacings for Lane Changing (MSSLC)*. The calculation of the MSSLC's for the merging or lane changing maneuver is more complicated from the calculation of the minimum safety spacings of the pure longitudinal case, since, in the former case we have to take into account the particular lane changing policy of the merging vehicle as well as the effect of combined lateral/longitudinal motion during the lane changing

maneuver. The braking profiles of the vehicles involved in a lane changing maneuver depend on the particular AHS operational concept, i.e., on the degree of communication between the vehicles and between the vehicles and the infrastructure. We considered six different AHS operational concepts; we presented the braking profiles of the vehicles for each operational concept and we investigated the effects of the particular operational concept to the MSSLC.

References

[1] J. L. Bascunana, "Analysis of lane change crash avoidance," *Systems and Issues in ITS*, (SP-1106), 1997.

[2] K. Enke, "Possibilities for improving safety within the driver vehicle environment control loop," *7th International Technical Conference on Experimental Safety Vehicles*, Washington, DC, National Highway Traffic Safety Administration, 1979.

[3] P. A. Ioannou, A. Kanaris, and F.-S. Ho, "Spacing and capacity evaluations for different AHS concepts," *Technical Report*, University of Southern California, 1995.

[4] T.D. Gillespie, *Fundamentals of Vehicle Dynamics*. Published by the SAE, 1992.

[5] S.E. Shladover, C.A. Desoer, J.K. Hedrick, M. Tomizuka, J. Walrand, W.B. Zhang, D.McMahon, and S. Sheikholeslam, "Automatic vehicle control development in the PATH program," *IEEE Transactions on Vehicular Technology*, vol. 40, pp. 114-130, 1991.

[6] Y. Sun and P.A. Ioannou, "A handbook for inter-vehicle spacing in vehicle following," *California PATH Research Report*, UCB-ITS-PRR-95-1, University of Southern California, 1995.

[7] R.D. Worall and A.G.R. Bullen, "An empirical analysis of lane changing on multilane highways," *Highway Research Board*, vol. 303, pp. 30-43, 1970.

Macroscopic Modeling and Analysis of Traffic Flow of Automated Vehicles*

H. Raza and P. Ioannou
Dept. of Electrical Engineering-Systems
University of Southern California
Los Angeles, CA 90089-2562

Abstract

With the development of near term automatic vehicle following concepts such as intelligent cruise control (ICC) and cooperative driving, vehicles will be able to follow each other automatically in the longitudinal direction. The modeling of traffic flow consisting of such vehicles is important for analyzing the effects of vehicle automation on the characteristics of traffic flow and for suggesting macroscopic control strategies to improve efficiency. Such analysis may also suggest ways for modifying the microscopic vehicle controllers in order to improve the macroscopic behavior of traffic.
In this paper a macroscopic traffic flow model of automated vehicles is developed by using the microscopic control laws that govern the longitudinal motion of individual vehicles together with the dynamics of the interconnection with other vehicles. The model is a very general one and is applicable to a wide range of concepts associated with automated highway systems (AHS). The developed model is used to analyze the steady state behavior of traffic flow for different operating conditions. The analysis indicates that some of the proposed modes of AHS which operate without a traffic flow controller may not be effective in avoiding traffic congestion problems resulting from traffic flow disturbances. The model also predicts the existence of shock waves in extreme cases for the same modes of AHS. The results of this analysis can be used as guidelines for designing macroscopic as well as microscopic control laws.

Keywords: Modeling, Macroscopic Modeling, Automated Highway Systems, Interconnected Systems, Hybrid Systems

*This work is supported by the California Department of Transportation through PATH of the University of California. The contents of this paper reflect the views of the authors who are responsible for the facts and accuracy of the data presented herein. The contents do not necessarily reflect the official views or policies of the State of California or the Federal Highway Administration. This paper does not constitute a standard, specification or regulation.

1 Introduction

In order to increase the capacity and safety of the existing highway system, a variety of concepts have been introduced that allow vehicles to follow each other automatically with varying degree of authority between human drivers and automatic control laws. Some of these concepts which have the potential to appear in the near future without extensive infrastructure modifications are the intelligent cruise control (ICC) and cooperative driving systems. Vehicles equipped with ICC can follow autonomously other automated or manually driven vehicles, hence can provide partial or even full automation in the longitudinal direction. On the other hand, cooperative driving systems require some exchange of information between neighboring vehicles and/or infrastructure to coordinate maneuvers, hence may require a dedicated lane where only automated vehicles are allowed to operate. As the number of vehicles with automatic vehicle following features increases, the behavior of traffic flow will be changed in a way that needs to be understood.

Judging from the way airbags and anti-lock brake systems (ABS) have penetrated the vehicle market, it is reasonable to expect that sometime in the future almost all of the vehicles will be equipped with ICC and therefore will have the automatic vehicle following capability. Even though the motivating force for the consumer for having an ICC system on his/her vehicle is safety and driving comfort, the impact of such vehicles on the characteristics of traffic flow is also important to the consumer and traffic engineers.

The purpose of this paper is to use the microscopic dynamics of vehicles that follow each other automatically to develop a macroscopic model that describes the flow of traffic. Historically, the macroscopic behavior of highway traffic has been modeled by approximating the control actions of a human driver while driving within a group of vehicles [1]. These simple models based on human car following behavior [2] were progressively improved to account for certain observed phenomena on highways [4, 5]. In many occasions these traditional models describing the behavior of human drivers were used to approximate the traffic flow of automated vehicles [5, 6]. These models, however, have limited scope only, as the randomness of human driver functions introduces certain uncertainties in the model that vary from one place to another due to different driving patterns. For example a traffic flow model that is validated using traffic data from a certain city may not accurately describe the behavior of traffic in another city. On the other hand the automatic vehicle following control laws behave in a predictable manner. Hence an accurate macroscopic model of the traffic flow can be obtained by using the deterministic microscopic vehicle dynamics.

We define the macroscopic variables of interest in terms of the well defined relationships for the speed and relative distance for a group of vehicles under automatic control. This enables us to study the effects of changing the individual control strategies on the macroscopic behavior of the traffic flow. Given one set of operating conditions, these automatic vehicle following controllers behave in a predictable fashion, unlike human drivers who tend

to produce random control actions for the same situation. Hence a representation of the system in terms of these deterministic functions can be used to analyze the traffic flow of automated vehicles.

The modeling of the traffic flow is subdivided into two parts: The first part deals with the conceptual abstraction of the system as a continuous fluid, so that the dynamics of the system can be obtained by applying the hydrodynamic theory of traffic flow. In this part, we have assumed one dimensional streamline flow, i.e., no lane changes and no on-ramps or off-ramps. The second part, which deals with the global connectivity of the system, assumes the responsibility of providing the necessary information so that a given highway with multiple lanes and on-ramps and off-ramps can be viewed as a collection of single lanes with lateral traffic flow defined across these lanes.

In order to complete the first part of the modeling task, we start with the microscopic model which describes the relationships of motion of vehicles within each platoon. By using this microscopic model, we develop a local macroscopic model which describes the instantaneous speed and density of traffic flow in a section of highway by treating each section, containing an arbitrary collection of platoons of vehicles, separately. In the second part, we connect different sections to form a single lane by using appropriate boundary conditions. A model of traffic flow in a multi-lane highway system is then obtained from these single lane models by defining lateral flow across adjacent lanes. This modeling structure is quite flexible as different automated vehicle following concepts can be represented by the same model by changing the global connectivity conditions which are implementation dependent.

The resulting system representation is a useful tool for analysis and design of automated traffic flow. In particular, we have used the model to study the steady state behavior of such traffic flow. The analysis reveals the existence of some of the undesirable phenomena observed on current highways, such as shock waves, for traffic flow on automated highways. The analysis indicates that some of the proposed modes of operation of automatic vehicle following, which operate without a roadway (link layer) controller, have a limited region of operation within which the desired traffic throughput can be guaranteed. The results of this analysis can be used as guidelines to design macroscopic control laws which could avoid or attenuate these undesirable phenomena.

The paper is organized as follows: The dynamics of vehicles within a platoon under automatic vehicle following control are discussed in section 2. The local macroscopic model is developed in section 3. In section 4, the local macroscopic model is extended to represent traffic flow on a single highway lane. A multi-lane macroscopic model is described in section 5. An analysis of the equilibrium states of the automated traffic flow, using the model developed in this paper, is presented in section 6. The simulation results of the model are discussed in section 7. The paper ends with the main results summarized in the conclusion section.

2 Microscopic Model

In this study we are modeling the macroscopic behavior of automated traffic flow in terms of the kinematics of individual vehicles. These vehicles are assumed to be grouped together in platoons of different sizes[1]. The first step in the proposed modeling process is to model the dynamics of the vehicles following each other, according to a given inter-vehicle spacing policy, in a platoon. A platoon of such vehicles is shown in Figure 1. The variables used in the microscopic model which are also shown in Figure 1 are:

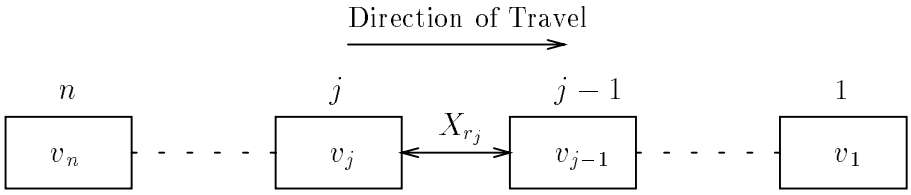

Figure 1: A platoon of vehicles.

j : vehicle number within a platoon, $j \in \{1, \ldots, n\}$, where n is the number of vehicles, referred to as the size of the platoon,

X_{r_j} : relative distance between the vehicle j and $(j-1)$,

v_{r_j} : relative speed between the vehicle j and $(j-1)$,

δ_j : deviation from the desired spacing between the vehicle j and $j-1$,

v_j : speed of the vehicle j,

V : external speed command (provided locally or globally),

h : desired headway (time headway when measured in seconds or constant spacing when measured in length units),

V_{d_j} : desired speed for the vehicle j,

V_l : speed of the vehicle in front of platoon leader.

Remark

- In the discussion to follow, s will be used to represent both the differential operator $\frac{d}{dt}(.)$ and the Laplace operator.

[1] A vehicle traveling alone, referred to as free agent in literature, is considered as a platoon of size $n = 1$

The general expression for the speed and relative distance for the jth vehicle in a platoon is given as:

$$\begin{aligned} v_j(t) &= W_{1_j}(s) V_{d_j}(t), \\ X_{r_j}(t) &= W_{2_j}(s) V_{d_j}(t), \qquad j = 1, \ldots, n \end{aligned} \tag{1}$$

where V_{d_j} is the desired speed for the jth vehicle and $W_{1_j}(s)$, $W_{2_j}(s)$ are stable proper transfer functions. The exact form of these transfer functions depends on the type of longitudinal controller used, but they have certain characteristics which are common, irrespective of the type of controller. These characteristics are defined by the control objectives, each of these controllers have to achieve for a stable vehicle following in a platoon formation. These objectives are:

C–I $\delta_j,\ v_{r_j} \to 0$ exponentially or at least asymptotically[2].

C–II $\|\delta_j\|_\infty \leq \|\delta_{j-1}\|_\infty$ and $\|v_{r_j}\|_\infty \leq \|v_{r_{j-1}}\|_\infty$.

The objective **C–II** guarantees that there is no slinky type effect in the platoon. For the vehicles to follow each other in a platoon it is required that:

$$\begin{aligned} V_{d_1}(t) &= \min(V(t), V_l(t)) \\ V_{d_j}(t) &= v_{j-1}(t) \qquad\qquad j = 2, \ldots, n \end{aligned} \tag{2}$$

where $V(t)$ is the speed command which can be selected by the driver or is provided by the roadway when such an architecture is present and $V_l(t)$ is the speed of the vehicle in front of the platoon leader. It should be noted that under normal operating conditions $V_{d_1} = V$, however, during congestion or incidents the leader of the platoon has to track the speed of the vehicle in front which may be well below the commanded speed due to abnormal operating conditions. In order to simplify the notation, we will use V to represent V_{d_1} in (2), i.e., assume ideal operating conditions unless there is a need to differentiate between these two variables.

By substituting the value of V_{d_j} from (2) to (1), we get:

$$\begin{aligned} v_j(t) &= \left[\prod_{\alpha=1}^{j} W_{1_\alpha}(s) \right] V(t) \\ X_{r_j}(t) &= W_{2_j}(s) \left[\prod_{\alpha=1}^{j-1} W_{1_\alpha}(s) \right] V(t) \qquad\qquad j = 1, \ldots, n \end{aligned} \tag{3}$$

Since the longitudinal controllers are designed to satisfy **C–I**, the properties of W_{1_α} and W_{2_α} guarantee that for constant V [8, 9]:

$$\begin{aligned} \lim_{t \to \infty} v_j(t) &= V \\ \lim_{t \to \infty} Xr_j(t) &= X_{r_d}, \end{aligned}$$

[2]With the assumption that there is no disturbance.

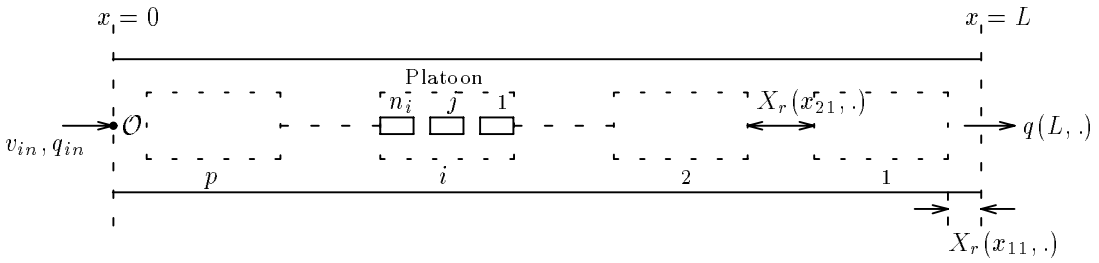

Figure 2: A section of a lane.

where X_{r_d} is the desired spacing which for time headway policy is hV and for fixed distance headway policy h. Now we have the expressions for the speed and relative distance for each vehicle in a platoon. These expressions will be used to derive the model of traffic flow within a section of a single highway lane.

3 Local Macroscopic Model

In this section we develop the macroscopic model of traffic flow in a section of a single highway lane shown in Figure 2. Equation (3) describing the motion of vehicle in a platoon will be used to obtain the traffic flow model of vehicles in a section of highway lane. This model is referred to as the local macroscopic model since it is localized to a section of a lane. The local macroscopic models of the sections of the lane will be linked to form the model of traffic flow in a single lane, referred to as the global macroscopic model.

In addition to the variables defined in the microscopic model, the variables used in the local macroscopic model are:

i : platoon number within a section, $i \in \{1, \ldots, p\}$, where p is the total number of platoons,

$\mathcal{O}$: Origin for local distance measurements, located at the section boundary at the center of the lane,

j : vehicle number within a platoon, $j \in \{1, \ldots, n_i\}$, where n_i is the size of platoon i,

x : distance measured with respect to origin $\mathcal{O}$,

$v(x,t)$: instantaneous speed distribution function,

$k(x,t)$: instantaneous density distribution function,

$q(x,t)$: instantaneous longitudinal traffic flow rate,

x_{ij} : position of the front of the vehicle j in platoon i,

$v(x_{ij},t)$: speed of the vehicle j in platoon i,

$V(x_{i1},t)$: desired speed for platoon i, where x_{i1} denotes the position of the leader of platoon i,

l : length of the vehicle, assumed to be the same for all vehicles,

L : length of the section of a lane,

Remarks

- The local origin $\mathcal{O}$ is used only for the longitudinal distance, x, measured from the center of the lane. The lateral deviations within the lane are ignored.
- According to our notation, both $v(x_{ij},t)$ and $v_{ij}(t)$ represent the same variable, i.e. the speed of vehicle j in platoon i. These two variations will be used throughout this paper.

The model of the traffic flow in a section of a lane will be described by the equations that generate the speed and density at each time t and distance x. In order to simplify these equations, so they become manageable for analysis, we make the following realistic assumption:

Assumption:

A–I The vehicles have similar closed loop characteristics, i.e.,

$$\sup_{\alpha,\beta} \|W_{1_\alpha} - W_{1_\beta}\|_\infty \leq \epsilon$$
$$\sup_{\alpha,\beta} \|W_{2_\alpha} - W_{2_\beta}\|_\infty \leq \epsilon \qquad \alpha,\beta \in \{1,\ldots,p\} \times \{1,\ldots,n_p\}$$

where ϵ is some small number.

The justification for this assumption becomes clear once we consider one of the objectives of automatic vehicle following, which is to make these vehicles behave similarly with respect to their vehicle following characteristics.

In addition to **A–I**, we assume the general case, where the desired speed for each platoon denoted as $V(x_{i1},t)$[3] is different. Another reasonable assumption is that the desired headway h, that appears in the transfer functions $W_1(s)$ and $W_2(s)$ [7, 9], is constant, changes in h could be modeled as disturbances [7].

[3] In previous section we were considering only a single platoon hence the speed command was represented as V.

From assumption **A–I**, we can make the following approximation:

$$\begin{aligned} W_{1_\lambda}(s) &= W_1(s) \\ W_{2_\lambda}(s) &= W_2(s) \qquad \lambda \in \{1,\ldots,p\} \times \{1,\ldots,n_p\} \end{aligned} \tag{4}$$

Using assumption **A–I**, we extend the relationships developed for the speed and relative distance for vehicles within a single platoon, given in (3), to that for each vehicle in the given section as follows:

$$v(x_{ij},t) = [W_1(s)]^j V(x_{i1},t) \tag{5}$$

$$X_r(x_{ij},t) = W_2(s)[W_1(s)]^{j-1} V(x_{i1},t) \quad j = 1,\ldots,n_i,\ i = 1,\ldots,p. \tag{6}$$

In (5) and (6) the value of x_{ij} is calculated as:

$$\begin{aligned} x_{ij} \;\; &= \;\; L - \left[\sum_{\alpha=1}^{i-1} \sum_{\beta=1}^{n_\alpha} (X_r(x_{\alpha\beta},t) + l) + \sum_{\beta=1}^{j} X_r(x_{i\beta},t) + \sum_{\beta=1}^{j-1} l \right], \\ & \quad j = 1,\ldots,n_i,\ i = 1,\ldots,p \end{aligned} \tag{7}$$

where L is the length of the section and l is the length of the vehicle, assumed to be the same for all vehicles. The density at position x_{ij} and time t may also be calculated as:

$$k(x_{ij},t) \triangleq \frac{1}{X_r(x_{ij},t) + l} \tag{8}$$

Equations (5)-(7) generate:
(i) The speed $v(x_{ij},t)$ of the vehicle j in platoon i.
(ii) The relative distance $X_r(x_{ij},t)$ between the vehicle j in platoon i and the vehicle in front. When $j = 1$, the vehicle in front is the last vehicle of the platoon $i-1$ and therefore $X_r(x_{i1},t)$ denotes the inter-platoon spacing between platoon i and $i-1$.
(iii) The position x_{ij} of the front of the vehicle j in the platoon i from the origin $\mathcal{O}$, which is the beginning of the section.

The distribution of the speed and density at each instant in time and space may be obtained by interpolating between the speed and density at the discrete locations x_{ij}. Using linear interpolation and (5)-(8), we can obtain the following equations for the speed, $v(x,t)$, and density, $k(x,t)$, distribution functions:

$$v(x,t) \triangleq v(x_{ij},t) + \Big[v(x_{i(j-1)},t) - v(x_{ij},t)\Big] \left[\frac{x - x_{ij}}{X_r(x_{ij},t) + l}\right] \tag{9}$$

$$k(x,t) \triangleq k(x_{ij},t) + \Big[k(x_{i(j-1)},t) - k(x_{ij},t)\Big] \left[\frac{x - x_{ij}}{X_r(x_{ij},t) + l}\right] \tag{10}$$

$$x_{ij} \le x \le x_{i(j-1)};\ j = 1,\ldots,n_i,\ i = 1,\ldots,p$$

The equations (9) and (10) describe the speed and density distributions along the section of the lane for x in the range, $x_{pn_p} \leq x \leq x_{11}$, where x_{pn_p}, x_{11} are the location of the vehicles closest and farthest from the origin $\mathcal{O}$ respectively. However, their definitions can be extended to all values of $x \in [0, L]$ by considering the boundary conditions and extrapolating accordingly. The boundary conditions are:

$$\begin{aligned} v(0,t) &= v_{in}(t) \\ q(0,t) &= q_{in}(t) \end{aligned} \tag{11}$$

where v_{in}, q_{in} are the speed and flow rate respectively of the traffic entering the section shown in Figure 2 and are external inputs. We use the following extrapolation:

$$\begin{aligned} 0 \leq x < x_{pn_p} &\Rightarrow x_{ij} = x_{(p+1)1} = 0 \ , x_{i(j-1)} = x_{pn_p} \\ x_{11} < x \leq L &\Rightarrow x_{ij} = x_{11} \ , x_{i(j-1)} = x_{01} = L \end{aligned}$$

Hence to use the definitions (9) and (10) outside the region $x_{pn_p} \leq x \leq x_{11}$, we have introduced fictitious vehicles at $x = 0$ and $x = L$, denoted as $x_{(p+1)1}$, x_{01} respectively. The speed at $x = 0$ is given by the boundary condition in (11), however, that at $x = L$ can be assumed to be the speed of the closest vehicle, i.e.,

$$\begin{aligned} v(x_{(p+1)1}, t) &= v(0,t) = v_{in}(t) \\ v(x_{01}, t) &= v(L,t) = v(x_{11}, t). \end{aligned} \tag{12}$$

The linear interpolation given in (9)-(10) is a good approximation for representation of the speed and density as continuous functions as long as the traffic density is not negligibly small. Hence an inherent assumption in the definition of the speed and density distribution function is that the traffic flow rates are above a certain threshold.

Having developed a continuous approximation for the states of the automated traffic flow, $[v, k]^\top$, we can develop update laws for these states by using the hydrodynamic traffic flow theory. According to this, the acceleration of an observer moving with the traffic stream is given as:

$$\dot{v}(x,t) = \frac{\partial}{\partial t} v(x,t) + v(x,t) \frac{\partial}{\partial x} v(x,t). \tag{13}$$

It should be noted that the well defined expressions for $\frac{\partial}{\partial t} v(x,t)$ and $\frac{\partial}{\partial x} v(x,t)$ can be obtained by using (9) and are given below:

$$\begin{aligned} \frac{\partial}{\partial t} v(x,t) &= \dot{v}(x_{ij}, t) + \Big\{ \dot{k}(x_{ij}, t) \left[v(x_{i(j-1)}, t) - v(x_{ij}, t) \right] + \\ &\quad k(x_{ij}, t) \left[\dot{v}(x_{i(j-1)}, t) - \dot{v}(x_{ij}, t) \right] \Big\} (x - x_{ij}) - \\ &\quad k(x_{ij}, t) v(x_{ij,t}) \left[v(x_{i(j-1)}, t) - v(x_{ij}, t) \right], \end{aligned} \tag{14}$$

$$\frac{\partial}{\partial x} v(x,t) = k(x_{ij}, t)[v(x_{i(j-1)}, t) - v(x_{ij}, t)]. \tag{15}$$

Hence the acceleration at any point along the highway can be represented as a deterministic function of the known transfer functions $W_1(s)$ and $W_2(s)$ by substituting the expressions for $v(x_{ij},t)$, $k(x_{ij},t)$, $\dot{v}(x_{ij},t)$, $\dot{k}(x_{ij},t)$ from (5), (8) and (6) into the equations (14) and (15).

Using law of conservation of vehicles and assuming no lane changing or on-ramp/off-ramp traffic, we obtain:

$$\frac{\partial}{\partial t}k(x,t) + \frac{\partial}{\partial x}q(x,t) = 0 \tag{16}$$

where $q(x,t) = k(x,t)v(x,t)$ is the instantaneous longitudinal traffic flow rate. By substituting $q = kv$ in (16) we get:

$$\begin{aligned} &\frac{\partial}{\partial t}k(x,t) + v(x,t)\frac{\partial}{\partial x}k(x,t) + k(x,t)\frac{\partial}{\partial x}v(x,t) = 0 \\ &\dot{k}(x,t) = -k(x,t)\frac{\partial}{\partial x}v(x,t), \end{aligned} \tag{17}$$

where $\dot{k}(x,t) = \frac{\partial}{\partial t}k(x,t) + v(x,t)\frac{\partial}{\partial x}k(x,t)$. To solve equations (13) and (17) uniquely, the required initial conditions are:

$$\begin{aligned} v(x,t_0) &= g(x) \\ k(x,t_0) &= f(x) \end{aligned} \tag{18}$$

where $f(.)$, $g(.)$ are assumed to be known at $t = t_0$. By substituting the expressions for $\frac{\partial}{\partial t}v(x,t)$ and $\frac{\partial}{\partial x}v(x,t)$ from (14) and (15) into (13) and (17), we get:

$$\dot{v}(x,t) = [1 - k(x_{ij},t)(x - x_{ij})]\,\dot{v}(x_{ij},t) + k(x_{ij},t)(x - x_{ij})\dot{v}(x_{i(j-1)},t) \tag{19}$$

$$\begin{aligned} &\dot{k}(x,t) = \Big[k(x_{ij},t)^3(x - x_{ij}) - k(x_{i(j-1)},t)k(x_{ij},t)^2(x - x_{ij}) - k(x_{ij},t)^2\Big] \\ &\Big[v(x_{i(j-1)},t) - v(x_{ij},t)\Big] \end{aligned} \tag{20}$$

The expressions for $\dot{v}(x,t)$ and $\dot{k}(x,t)$ in terms of the microscopic dynamics can be obtained by substituting the values of $\dot{v}(x_{ij},t)$, $v(x_{ij},t)$ and $k(x_{ij},t)$ from (5), (8) and (6) into the equations (19) and (20) and are given below:

$$\begin{aligned} \dot{v}(x,t) = &\left[1 - \frac{(x - x_{ij})}{W_2(s)[W_1(s)]^{j-1}V(x_{i1},t) + l}\right] s[W_1(s)]^j V(x_{i1},t) + \\ &\left[\frac{(x - x_{ij})}{W_2(s)[W_1(s)]^{j-1}V(x_{i1},t) + l}\right] s[W_1(s)](j-1)V(x_{i1},t) \end{aligned} \tag{21}$$

$$\begin{aligned} \dot{k}(x,t) = &\left[\frac{-(x - x_{ij})}{[W_2(s)[W_1(s)]^{j-2}V(x_{i1},t) + l][W_2(s)[W_1(s)]^{j-1}V(x_{i1},t) + l]^2} + \right. \\ &\left. \frac{(x - x_{ij})}{[W_2(s)[W_1(s)]^{j-1}V(x_{i1},t) + l]^3} - \frac{1}{[W_2(s)[W_1(s)]^{j-1}V(x_{i1},t) + l]^2}\right] \\ &\Big[[W_1(s)]^{j-1}V(x_{i1},t) - [W_1(s)]^j V(x_{i1},t)\Big] \end{aligned} \tag{22}$$

The terms in equation (19) can be compared with similar terms in the macroscopic model derived for manually driven vehicles [3, 5]. These terms are:

The anticipation term, $k(x_{ij},t)(x-x_{ij})\dot{v}(x_{i(j-1)},t)$,

shows that the automated vehicle anticipates changes in the acceleration of the vehicle in front. In contrast to the similar term in the model for manually driven vehicles this term does not depend on the downstream density.

The relaxation term, $[1-k(x_{ij},t)(x-x_{ij})]\,\dot{v}(x_{ij},t)$,

reduces to zero at equilibrium when, $\dot{v}(x_{ij},t)=0$.

It should be noted that even though the vehicle speed at any point is affected by the speed of the downstream vehicles, no term in the model (19) can be compared with the convection term, which appears in the models described for human car following [3, 5].

For easy reference, we will summarize the model here: The update laws for continuous states $[v,k]^\top$ in (19), (20) along with a representation of individual vehicle states $[v_{ij},k_{ij}]^\top$ in (5)-(8) form a complete subsystem model. This model is referred to as the local macroscopic model and is summarized in (23):

$$\dot{v}(x,t)=[1-k(x_{ij},t)(x-x_{ij})]\,\dot{v}(x_{ij},t)+k(x_{ij},t)(x-x_{ij})\dot{v}(x_{i(j-1)},t) \tag{23}$$

$$\dot{k}(x,t)=\Big[k(x_{ij},t)^3(x-x_{ij})-k(x_{i(j-1)},t)k(x_{ij},t)^2(x-x_{ij})-k(x_{ij},t)^2\Big]\Big[v(x_{i(j-1)},t)-v(x_{ij},t)\Big]$$

$$q(x,t)=k(x,t)v(x,t)$$
$$v(x,t_0)=g(x),\ k(x,t_0)=f(x)$$
$$x_{ij}\le x\le x_{i(j-1)};\ j=1,\dots,n_i,\ i=1,\dots,p$$
$$v(0,t)=v_{in}(t),\ q(0,t)=q_{in}(t)$$

$$x_{ij}=L-\left[\sum_{\alpha=1}^{i-1}\sum_{\beta=1}^{n_\alpha}(X_r(x_{\alpha\beta},t)+l)+\sum_{\beta=1}^{j}X_r(x_{i\beta},t)+\sum_{\beta=1}^{j-1}l\right]$$
$$k(x_{ij},t)=\frac{1}{X_r(x_{ij},t)+l}$$
$$v(x_{ij},t)=[W_1(s)]^jV(x_{i1},t)$$
$$X_r(x_{ij},t)=W_2(s)[W_1(s)]^{j-1}V(x_{i1},t)$$

The model in (23) describes the dynamical behavior of traffic flow in a section of single

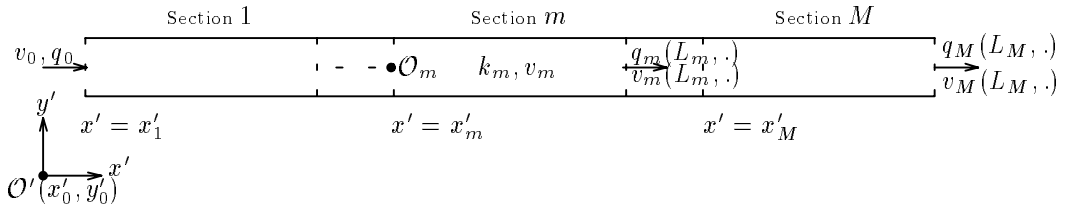

Figure 3: A single highway lane.

highway lane. The external inputs to the model are the desired speed, $V(x,t)$, and the boundary conditions, $v_{in}(t)$, $q_{in}(t)$. As pointed out earlier, the global macroscopic model is an interconnection of the local macroscopic models developed in this section and will be considered next in order to derive the traffic flow model in a single highway lane.

4 Global Macroscopic Model: Single Lane

While developing the local macroscopic model, we have considered only a single section of a lane in the given highway system. To model traffic flow in a single highway lane shown in Figure 3, as an interconnected system, we need a set of global inputs which include boundary and initial conditions. In the following we will describe the required conditions to connect the contiguous sections to form a single lane of highway.

The notation specific to the single lane macroscopic model is:

m : section number within a lane, $m \in \{1, \ldots, M\}$, where M is the total number of sections,

$\mathcal{O}'$: Origin for global distance measurements, located at a fixed point (x'_0, y'_0),

x' : distance measured with respect to origin $\mathcal{O}'$ along the direction of flow,

$\mathcal{O}_m$: Origin for local distance measurements, located at $x' = x'_m$ with respect to $\mathcal{O}'$,

L_m : length of the section m

x : distance measured with respect to origin $\mathcal{O}_m$,

$v_m(x,t)$: instantaneous speed distribution function of the section m,

$k_m(x,t)$: instantaneous density distribution function of the section m,

$q_m(x,t)$: instantaneous longitudinal traffic flow rate of the section m,

We have formulated the problem of modeling the traffic flow in a single highway lane, shown in Figure 3, as an interconnection of the local macroscopic models. The local macroscopic model in (23) gives a representation of the states, $[v_m, k_m]^\top$ and output q_m of a particular element m of the single lane. The interconnection of these local macroscopic models can be achieved through appropriate boundary conditions. As shown in Figure 3, the vehicles enter the section 1 of the given lane with the boundary conditions:

$$\begin{aligned} v_1(0,t) &= v_0(t), \\ q_1(0,t) &= q_0(t), \end{aligned} \tag{24}$$

where $v_0(t)$ and $q_0(t)$ are the external inputs and represent the instantaneous speed and flow rate of the vehicles entering the given lane. The rest of the sections require similar boundary conditions, which are:

$$\begin{aligned} v_m(0,t) &= v_{(m-1)}(L_{(m-1)},t), \\ q_m(0,t) &= q_{(m-1)}(L_{(m-1)},t),\ m = 2,\ldots,M. \end{aligned} \tag{25}$$

It should be noted that the boundary conditions in (25) are generated locally, in contrast to $v_0(t)$ and $q_0(t)$ which are supplied externally. The instantaneous speed and flow rate of the vehicles exiting the given lane, represented as $v_M(L_M,t)$ and $q_M(L_M,t)$ can be used for further interconnection.

To solve the system states uniquely, the required initial conditions are:

$$\begin{aligned} v_m(x,t_0) &= g_m(x), \\ k_m(x,t_0) &= f_m(x),\ m = 1,\ldots,M, \end{aligned} \tag{26}$$

where t_0 is the initial time and $f_m(.)$, $g_m(.)$ are known functions.

Hence, the local macroscopic model in (23) together with the initial and boundary conditions given in (26), (24)-(25) respectively represent the model of traffic flow in a single highway lane shown in Figure 3 and is summarized below for reference.

$$\dot{v}_m(x,t) = \left[1 - k_m(x_{ij},t)(x - x_{ij})\right]\dot{v}_m(x_{ij},t) + k_m(x_{ij},t)(x - x_{ij})\dot{v}_m(x_{i(j-1)},t) \tag{27}$$

$$\begin{aligned} \dot{k}_m(x,t) = &\Big[k_m(x_{ij},t)^3(x - x_{ij}) - k_m(x_{i(j-1)},t)k_m(x_{ij},t)^2(x - x_{ij}) - \\ &k_m(x_{ij},t)^2\Big]\Big[v_m(x_{i(j-1)},t) - v_m(x_{ij},t)\Big], m = 1,\ldots,M \end{aligned}$$

$$\begin{aligned} &q_m(x,t) = k_m(x,t)v_m(x,t) \\ &v_m(x,t_0) = g_m(x),\ k_m(x,t_0) = f_m(x) \\ &x_{ij} \le x \le x_{i(j-1)};\ j = 1,\ldots,n_i,\ i = 1,\ldots,p \\ &v_1(0,t) = v_0(t),\ q_1(0,t) = q_0(t) \end{aligned}$$

$$v_m(0,t) = v_{(m-1)}(L_{(m-1)},t),\ q_m(0,t) = q_{(m-1)}(L_{(m-1)},t),\ m = 2,\ldots,M$$

$$x_{ij} = L_m - \left[\sum_{\alpha=1}^{i-1}\sum_{\beta=1}^{n_\alpha}(X_{r_m}(x_{\alpha\beta},t)+l) + \sum_{\beta=1}^{j} X_{r_m}(x_{i\beta},t) + \sum_{\beta=1}^{j-1} l\right]$$

$$k_m(x_{ij},t) = \frac{1}{X_{r_m}(x_{ij},t)+l}$$

$$v_m(x_{ij},t) = [W_1(s)]^j V_m(x_{i1},t)$$

$$X_{r_m}(x_{ij},t) = W_2(s)[W_1(s)]^{j-1} V_m(x_{i1},t)$$

The model in (27) describes the dynamical behavior of traffic flow in a single highway lane. The external inputs to the model are the desired speed, $V_m(x,t)$, and boundary conditions, $v_0(t)$, $q_0(t)$. Having developed the conditions to connect the contiguous sections to form a single lane, in the next section we will consider the effect of lane changes and on-ramp and off-ramp flow, to model traffic flow in a multi-lane automated highway system.

5 Global Macroscopic Model: Multi Lane

In this section we will model traffic flow in a multi-lane automated highway system, as shown in Figure 4, by superimposing the effect of lateral flow on the model of single highway lane. The model of traffic flow in a single highway lane is derived, in the previous section, by considering longitudinal flow only. We will extend this model so that the effect of lane changes and on-ramp/off-ramp flow can be incorporated into the model. This technique allows us to model traffic flow in a multi-lane highway by connecting the single lane models through the relations developed for lateral flow in this section.

As shown in Figure 4, by convention, we will consider the on-ramps and off-ramps to be always on the right most lane. In this study the on-ramp and off-ramp flow will be abstractly considered as a set of lane changes, even though some other operations may be required before the vehicles can enter into or exit the automated lanes. These additional processes, ensuring the safety of the system, can be ignored from the macroscopic point of view. In Figure 4, a transition lane is shown to identify the presence of incoming and outgoing traffic through the network, even though no physical lane may be present. In the following we will discuss the notation specific to the multi-lane macroscopic model.

y : lane number, $y \in \{1,\ldots,Y\}$, where Y is the total number of lanes,

y' : distance measured with respect to origin $\mathcal{O}'$ perpendicular to the direction of flow,

$\mathcal{O}_{ym}$: Origin for local distance measurements, located at (x'_m, y'_y) with respect to $\mathcal{O}'$,

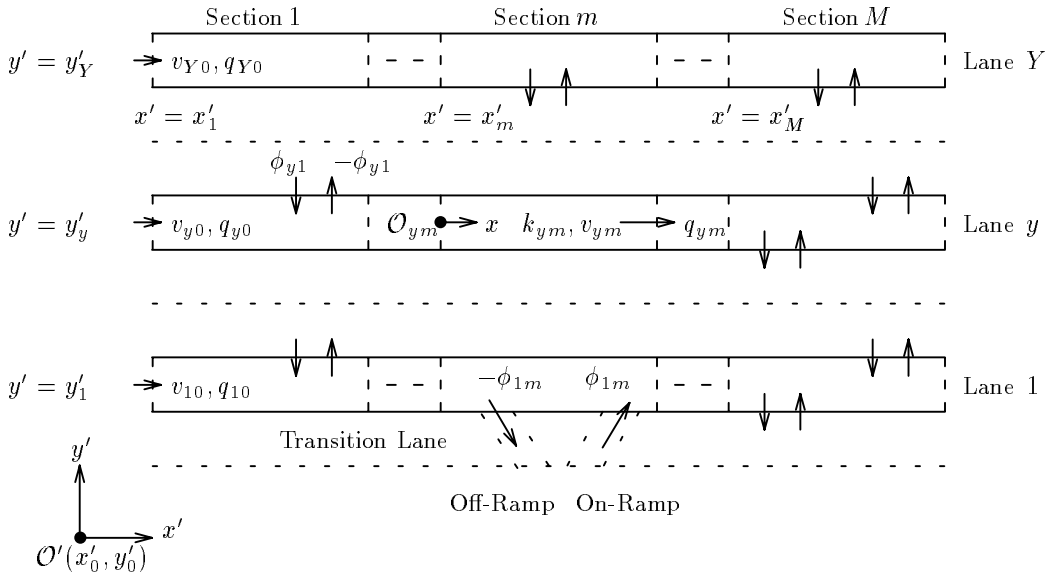

Figure 4: A multi-lane automated highway system.

L_{ym} : length of the section m in lane y,

x : distance measured with respect to origin $\mathcal{O}_{ym}$,

$v_{ym}(x,t)$: instantaneous speed distribution function of the section m in lane y,

$k_{ym}(x,t)$: instantaneous density distribution function of the section m in lane y,

$q_{ym}(x,t)$: instantaneous longitudinal traffic flow rate of the section m in lane y,

In this study we assume that the lane changes are executed after coordination, either at the local or at the infrastructure level. In the simplest case this coordination can be through the turn signal issued by the vehicle requesting the lane change or may require a detailed exchange of information, in the case of infrastructure involvement. This information, about the operating conditions near the regions affected by the lane changes, can be analyzed to select a strategy, if any, to execute these requests. These strategies depend on the upstream density of the two affected sections, their speed differentials etc. The complete discussion of selecting an optimal strategy which has the minimum impact on the capacity and safety of the system can be found in [10] and will not be covered here.

To describe the dynamic effects of lane changes on the longitudinal flow within a single highway lane, we will start by outlining a mechanism of lane change operations. This discussion will help to clarify the necessary conditions for a safe lane change operation in the

case of automated traffic flow. Without loss of generality, in the following, we will describe one lane change operation originating from the section m in lane y to the section m in lane $(y+1)$.

Till now we have assumed the desired headway h to be a constant, however, in the case of lane changes, the desired headway is no longer constant around the region affected by these operations and can be represented as $h(x,t)$. In addition, depending on the operating conditions, a change in the desired speed may also be required. If we assume that the requesting vehicle is located at a local position $x_{i_o j_o}$ in the originating section and after the lane change operation the vehicle has to occupy the location $x_{i_t j_t} < x < x_{i_t (j_t - 1)}$ in the target section. In this case, the desired speed and headway in the originating and the target section can be represented as:

Originating section:

$$\begin{aligned} V_{ym}(x,t) &= V_{ym}(x,t') + \Delta V_o(x,t) \text{ for } x < x_{i_o j_o} \\ h_{ym}(x,t) &= h_{ym}(x,t') + \Delta h_o(x,t) \text{ for } x_{i_o (j_o+1)} < x < x_{i_o (j_o-1)} \end{aligned} \tag{28}$$

Target section:

$$\begin{aligned} V_{(y+1)m}(x,t) &= V_{(y+1)m}(x,t') + \Delta V_t(x,t) \text{ for } x < x_{i_t j_t} \\ h_{(y+1)m}(x,t) &= h_{(y+1)m}(x,t') + \Delta h_t(x,t) \text{ for } x_{i_t (j_t+1)} < x < x_{i_t (j_t-1)} \end{aligned} \tag{29}$$

where $t \geq t'$, t' is the time at which the lane change operation is requested, ΔV_o, Δh_o and ΔV_t, Δh_t represent changes in the desired speed and headway in the originating and the target sections respectively. These values are calculated to guarantee that the safe inter-vehicle spacing is not violated during and after the execution of the lane change operation with a minimum impact on the capacity of the system.

These changes in the desired speed and/or headway, given above, required to make the operating conditions suitable for a lane change operation, are necessary for the safety of the system, and should be guaranteed by the microscopic controllers at all levels of automation. The impact of these changes on the efficiency or capacity of the system depends on the level of coordination available and will not be discussed here.

Hence to extend the model developed for a single highway lane to that for a multiple lane highway, we consider the desired headway $h_{ym}(x,t)$ to be an external input to the model. In this case we allow the desired headway to be non-uniform and time varying. As discussed in [7], the variations in the desired headway can be modeled as the asymptotically decaying disturbances in the microscopic dynamics and hence the states of the system around the affected regions. The attenuation characteristics of these disturbances, caused by the changes in headway, depend on the particular concept of automatic vehicle following being used. For modeling purposes, the impact of these necessary conditions for safe lane

changes can be represented by rewriting (5) and (6) as:

$$v_{ym}(x_{ij},t) = [W_1(s,h_{ym})]^j V_{ym}(x_{i1},t), j = 1,\ldots,n_i,\ i = 1,\ldots,p, \tag{30}$$

$$X_{r_{ym}}(x_{ij},t) = W_2(s,h_{ym})[W_1(s,h_{ym})]^{j-1} V_{ym}(x_{i1},t), \tag{31}$$

$$m = 1,\ldots,M,\ y = 1,\ldots,Y,$$

where the dependence of transfer functions W_1 and W_2 on the desired headway input $h_{ym}(x,t)$ is shown explicitly. Hence, any changes in the desired speed and/or headway required to initiate a lane change operation will show up in the model as a change in the states of the system around the region affected by these operations.

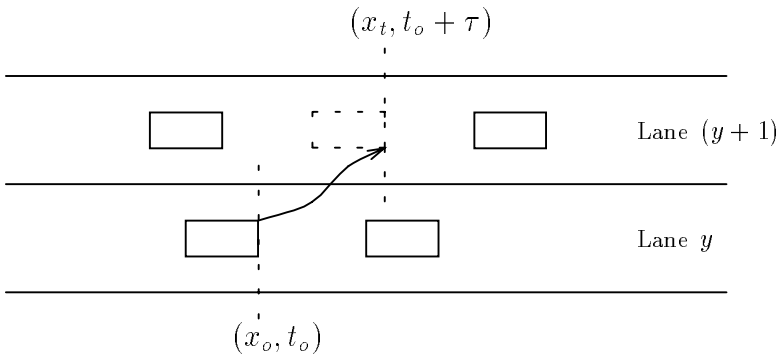

Figure 5: A typical lane change operation.

Having modeled the effects of the necessary conditions for a safe lane change operation, we will model the dynamics of lane change operations. As shown in Figure 5, a lane change operation is initiated at time t_o from the location x_o in the originating section. Here $t_o \geq t'$ and $x_o \geq x_{i_o j_o}$, t', $x_{i_o j_o}$ are as defined in (28). After the completion of this lane change operation, the vehicle location is x_t in the target section at time $t_t = t_o + \tau$, where τ is the time to complete the lane change operation. This lateral flow across the lanes will change the density and speed distributions around the affected region. The law of conservation of vehicles, which was used to calculate density in (17) can be modified to account for the effect of lateral flow as:

$$\dot{k}_{ym}(x_o,t_o) = -k_{ym}(x_o,t_o)\frac{\partial}{\partial x} v_{ym}(x_o,t_o) - \phi_{ym}(x_o,t_o) \tag{32}$$

where $\phi_{ym}(x_o,t_o) = k_{ym}(x_o,t_o)v_{ym}(x_o,t_o)$ is the instantaneous longitudinal flow rate at the time the lane change process started in the originating section. A similar expression for the change in density in the target section can be written as:

$$\dot{k}_{(y+1)m}(x_t,t_t) = -k_{(y+1)m}(x_t,t_t)\frac{\partial}{\partial x} v_{(y+1)m}(x_t,t_t) + \phi_{(y+1)m}(x_t,t_t) \tag{33}$$

where $\phi_{(y+1)m}(x_t, t_t) = k_{(y+1)m}(x_t, t_t) v_{(y+1)m}(x_t, t_t)$ is the instantaneous longitudinal flow rate at the completion of the lane change in the target section. As described earlier, $t_t = t_o + \tau$, where t_o is the time at which the lane change process started and τ is the time to complete this process. It should be noted that, in general, ϕ_{ym} can be different than $\phi_{(y+1)m}$ and accounts for any difference in the operating conditions in the two lanes/sections. In addition to the changes in the density, the speed distribution will also change during this lane change operation. This change is captured by the variations in acceleration around the affected region, i.e.,

$$\dot{v}_{ym}(x,t) = \frac{\partial}{\partial t} v_{ym}(x,t) + v_{ym}(x,t) \frac{\partial}{\partial x} v_{ym}(x,t). \tag{34}$$

Hence there may be a change in the acceleration and the speed of the vehicles upstream the location x_o in the originating section, due to a possible change in $\frac{\partial}{\partial x} v_{ym}(x,t)$, for $x \leq x_o$, $t \geq t_o$. A similar change will be reflected in the target section.

After the completion of the lane change operation, the desired speed and/or headway may have to be changed to resume normal operation. These post-lane-change effects will show up in the model through (30) and (31) as described earlier.

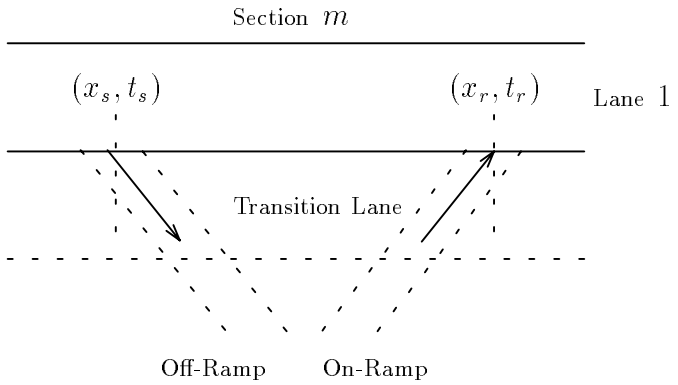

Figure 6: A generalized configuration of on-ramp and off-ramp traffic flow.

Finally, we will model on-ramp and off-ramp flow through a procedure similar to that adopted for the lane changes. As described earlier, the on-ramp and off-ramp flow can be abstractly considered as a set of lane change operations. The entry and exit can take place either at the designated locations or can be completely arbitrary, in the case where a transition lane is provided. As shown in Figure 4, the presence of incoming and outgoing traffic is shown through a transition lane which may or may not be present. Without loss of generality, as shown in Figure 6, the on-ramp or incoming traffic is assumed to be entering section m in lane 1 at a location x_r (with respect to local origin) and the off-ramp or outgoing traffic is exiting from the same section at a location x_s. Then by using the law of

conservation of vehicles, we have:

$$\dot{k}_{1m}(x,t) = \begin{cases} -k_{1m}(x_r,t_r)\frac{\partial}{\partial x}v_{1m}(x_r,t_r) + \phi_{1m}(x_r,t_r) & \text{for } x = x_r,\ t = t_r \\ -k_{1m}(x_s,t_s)\frac{\partial}{\partial x}v_{1m}(x_s,t_s) - \phi_{1m}(x_s,t_s) & \text{for } x = x_s,\ t = t_s \\ -k_{1m}(x,t)\frac{\partial}{\partial x}v_{1m}(x,t) & \text{else} \end{cases} \tag{35}$$

where $\phi_{1m}(x_r,t_r)$, $\phi_{1m}(x_s,t_s)$ are the instantaneous longitudinal flow rates at the time the vehicle enters or exits the given section, t_r, t_s are the times at which these changes take place. Similarly, a change in the speed distribution is captured through the acceleration around the affected regions as given in (34). It should be noted that since the on-ramp and off-ramp flow requires a set of lane changes, the necessary conditions for a safe lane change operation have to be satisfied. These conditions are very similar to those described earlier during lane change operations and will not be repeated.

In addition to the dynamic effects of lane changes, the steady state effect will show up in the form of a change in the size of two interacting platoons. The number and size of platoons in each section, which are required to calculate the speed and density distribution functions, are assumed to be known at all times. Hence after a successful lane change operation these values have to be updated to reflect a change in the respective distribution functions.

To summarize, the lateral flow, in the case of multi-lane highway, introduces change in the states of the system calculated by considering the longitudinal flow only. These changes can be modeled by modifying the macroscopic state update laws and microscopic dynamics around the regions affected by this lateral flow. These changes are summarized below for reference:

$$\dot{v}_{ym}(x,t) = \frac{\partial}{\partial t}v_{ym}(x,t) + v_{ym}(x,t)\frac{\partial}{\partial x}v_{ym}(x,t) \tag{36}$$

$$\dot{k}_{ym}(x,t) = \begin{cases} -k_{ym}(x_t,t_t)\frac{\partial}{\partial x}v_{ym}(x_t,t_t) + \phi_{ym}(x_t,t_t) & \text{for } x = x_t,\ t = t_t \\ -k_{ym}(x_o,t_o)\frac{\partial}{\partial x}v_{ym}(x_o,t_o) - \phi_{ym}(x_o,t_o) & \text{for } x = x_o,\ t = t_o \\ -k_{ym}(x,t)\frac{\partial}{\partial x}v_{ym}(x,t) & \text{else} \end{cases}$$

$$\phi_{ym}(x_t,t_t) = k_{ym}(x_t,t_t)v_{ym}(x_t,t_t),\ \phi_{ym}(x_o,t_o) = k_{ym}(x_o,t_o)v_{ym}(x_o,t_o)$$

$$v_{ym}(x_{ij},t) = [W_1(s,h_{ym})]^j V_{ym}(x_{i1},t), j = 1,\ldots,n_i,\ i = 1,\ldots,p,$$

$$X_{r_{ym}}(x_{ij},t) = W_2(s,h_{ym})[W_1(s,h_{ym})]^{j-1}V_{ym}(x_{i1},t),$$

$$m = 1,\ldots,M,\ y = 1,\ldots,Y.$$

It should be noted that the expression for density in (36) is a generalization of those given separately for lane changes and on-ramp/off-ramp flow in (32), (33) and (35). For completeness sake, we will rewrite the model given in (27) to reflect the changes made for multi-lane highway configuration, and is given below in (37) for reference.

$$\dot{v}_{ym}(x,t) = [1 - k_{ym}(x_{ij},t)(x - x_{ij})]\,\dot{v}_{ym}(x_{ij},t) + k_{ym}(x_{ij},t)(x - x_{ij})$$

$$\dot{v}_{ym}(x_{i(j-1)},t),\ y=1,\ldots,Y,\ m=1,\ldots,M \tag{37}$$

$$\dot{k}_{ym}(x,t)=\begin{cases} -k_{ym}(x_t,t_t)\frac{\partial}{\partial x}v_{ym}(x_t,t_t)+\phi_{ym}(x_t,t_t) & \text{for } x=x_t,\ t=t_t \\ -k_{ym}(x_o,t_o)\frac{\partial}{\partial x}v_{ym}(x_o,t_o)-\phi_{ym}(x_o,t_o) & \text{for } x=x_o,\ t=t_o \\ -k_{ym}(x,t)\frac{\partial}{\partial x}v_{ym}(x,t) & \text{else} \end{cases}$$

$$-k_{ym}(x,t)\frac{\partial}{\partial x}v_{ym}(x,t)=\Big[-k_{ym}(x_{ij},t)^2+k_{ym}(x_{ij},t)^3(x-x_{ij})-$$
$$k_{ym}(x_{i(j-1)},t)k_{ym}(x_{ij},t)^2(x-x_{ij})\Big]\Big[v_{ym}(x_{i(j-1)},t)-v_{ym}(x_{ij},t)\Big]$$
$$\phi_{ym}(x_t,t_t)=k_{ym}(x_t,t_t)v_{ym}(x_t,t_t),\ \phi_{ym}(x_o,t_o)=k_{ym}(x_o,t_o)v_{ym}(x_o,t_o)$$

$$q_{ym}(x,t)=k_{ym}(x,t)v_{ym}(x,t)$$
$$v_{ym}(x,t_0)=g_{ym}(x),\ k_{ym}(x,t_0)=f_{ym}(x)$$
$$x_{ij}\le x\le x_{i(j-1)},\ j=1,\ldots,n_i,\ i=1,\ldots,p$$
$$v_{y1}(0,t)=v_{y0}(t),\ q_{y1}(0,t)=q_{y0}(t)$$
$$v_{ym}(0,t)=v_{y(m-1)}(L_{y(m-1)},t),\ q_{ym}(0,t)=q_{y(m-1)}(L_{y(m-1)},t),$$
$$y=1,\ldots,Y,\ m=2,\ldots,M$$

$$x_{ij}=L_{ym}-\left[\sum_{\alpha=1}^{i-1}\sum_{\beta=1}^{n_\alpha}(X_{r_{ym}}(x_{\alpha\beta},t)+l)+\sum_{\beta=1}^{j}X_{r_{ym}}(x_{i\beta},t)+\sum_{\beta=1}^{j-1}l\right]$$
$$k_{ym}(x_{ij},t)=\frac{1}{X_{r_{ym}}(x_{ij},t)+l}$$
$$v_{ym}(x_{ij},t)=[W_1(s,h_{ym})]^jV_{ym}(x_{i1},t)$$
$$X_{r_{ym}}(x_{ij},t)=W_2(s,h_{ym})[W_1(s,h_{ym})]^{j-1}V_{ym}(x_{i1},t)$$

The model in (37) describes the dynamical behavior of traffic flow in a multi-lane automated highway system. The external inputs to the model are the desired speed, $V_{ym}(x,t)$, the desired headway, $h_{ym}(x,t)$ and the boundary conditions, $v_{y0}(t)$, $q_{y0}(t)$. In the next section, we will use the model given in (37) to analyze the properties of traffic flow for different automatic vehicle following concepts. In particular, we will find the steady state speed and density distributions in a section of highway for different operating scenarios. This analysis will identify the region of attraction of equilibrium states in each case. This information can be used to design macroscopic control laws with the property that the states of the system will remain within the specified region.

6 Analysis of Automated Traffic Flow

In this section we will analyze the model developed in section 5 to study the properties of automated traffic flow, with emphasis on their equilibrium states. Since the model devel-

oped in this study is independent of the implementation details of a particular system, it can be used to compare the properties of different automatic vehicle following concepts. In this way the macroscopic behavior of these systems can be studied by choosing the appropriate microscopic dynamics governing these concepts. As an example we will compare controller designs based on time headway and fixed distance headway policies, in terms of the convergence properties of their desired equilibrium sets. Similarly different control designs within the same category can be compared by selecting appropriate dynamics in terms of transfer functions $W_1(s)$ and $W_2(s)$ in (37).

For simplicity, we will consider only a single highway lane with no lateral traffic flow, referred to as the pipeline flow in transportation literature. The main objective of this analysis is to show that there are operating conditions under which the system will end up in undesirable steady state leading to congestion or interrupted flow. In extreme cases these disturbances may lead to shock waves, a phenomenon observed on existing highways. We will formulate the main results of this analysis in the form of following propositions; the proof is given by the analysis to follow.

Proposition 6.1 *The automatic vehicle following controllers designed with the constraints* **C–I** *and* **C–II** *are not sufficient to make the desired equilibrium point globally attractive.*

Proposition 6.2 *Under time headway policy, if the system is in undesirable equilibrium state, convergence to the desired state requires cooperative control laws*[4]*. However, for fixed distance headway policy, the system will return to its desired equilibrium state if the disturbance is removed and this convergence can occur without any external control laws.*

Proposition 6.3 *There are operating conditions under which shock waves are produced in automated traffic flow.*

These propositions outline one of the major difference in the macroscopic properties of control laws designed with the two different headway policies, time headway and fixed distance headway in this case. To prove these claims, we will derive the steady state solution of the system represented in (27) for different operating conditions. We will consider the stationary and non-stationary flow as two special cases of interest. We will show that the system formulation in (27) restricts the steady state speed distribution to be identically constant in both cases. However, it permits non-stationary density distribution in steady state, which captures a rich class of operating conditions. These cases are discussed below in detail.

6.1 Stationary Flow

Since we are considering traffic flow in a single highway lane with no lateral flow, we will use the model (27) for this analysis. For stationary flow conditions to exist it is required

[4]By cooperative control laws we mean that vehicles have some way of accommodating the requests issued by the surrounding vehicles.

that at any fixed point there are no variations in traffic flow rate, i.e., traffic flow appears as stationary to any static observer. The stationary flow conditions are satisfied if:

$$\frac{\partial}{\partial x} q_m(x,t) = 0 \ \forall t \quad \Rightarrow \quad \frac{\partial}{\partial t} k_m(x,t) = 0 \ \forall x. \tag{38}$$

Now we can solve the system in (27), which is derived from (13) and (17), for steady state:

$$\dot{k}_m(x,t) = -k_m(x,t)\frac{\partial}{\partial x} v_m(x,t) = 0 \quad \Rightarrow \quad \frac{\partial}{\partial x} v_m(x,t) = 0 \tag{39}$$

with the assumption that $k_m(x,t) > 0$. Also combining (39) with the requirement that $\dot{v}_m(x,t) = 0$ at steady state and with the assumption that $v_m(x,t) > 0$, we get:

$$\frac{\partial}{\partial t} v_m(x,t) = 0. \tag{40}$$

From (39) and (40), we have that at steady state:

$$v_m(x,t) = \bar{V}_m \tag{41}$$

where $\bar{V}_m > 0$ is any constant. Since at steady state:

$$\dot{k}_m(x,t) = \frac{\partial}{\partial t} k_m(x,t) + v_m(x,t)\frac{\partial}{\partial x} k_m(x,t) = 0 \tag{42}$$

and we are considering stationary flow, i.e., $\frac{\partial}{\partial t} k_m = 0 \Rightarrow \frac{\partial}{\partial x} k_m = 0$, hence:

$$k_m(x,t) = \bar{K}_m \tag{43}$$

where $\bar{K}_m > 0$ is any constant. First, we will consider time headway policy, in this case, under stationary flow conditions, $\bar{K}_m$ is not arbitrary but is related to $\bar{V}_m$ in (41) as:

$$\bar{K}_m = \frac{1}{h\bar{V}_m + l} \tag{44}$$

where h is the constant time headway. As expected for stationary flow conditions, the model produces static speed and density distributions as steady state solutions. Furthermore, the set of equilibrium points, $\mathcal{E} = \{\bar{V}_m, \bar{K}_m\}$, is not unique. Next we will isolate the set of equilibrium points into desirable and undesirable ones and will identify the region of attraction of the desirable set. This analysis will help us to identify the operating conditions under which the system may end up in the undesirable region as pointed out by proposition 6.1.

6.1.1 Structure of Equilibrium States

If we assume that under steady conditions the desired speed $V_m(x,t) = V_m$, where $V_m > 0$ is any constant, then for time headway policy, the desired equilibrium point is unique and is given as:

$$\mathcal{E}_d = \{V_m, K_m\},\ K_m = \frac{1}{hV_m + l} \tag{45}$$

We will show that the desired equilibrium point $\mathcal{E}_d \in \mathcal{E}$ and derive the relationship between $\mathcal{E}_d$ and $\mathcal{E}$ which is dictated by the properties of transfer functions $W_1(s)$ and $W_2(s)$. This relationship is given by the following lemma.

Lemma 6.1 *If the automatic vehicle following controllers satisfy the constraints* **C–I** *and* **C–II** *then:*

$$\|v_m(x,.)\|_\infty \leq \|V_m(x,.)\|_\infty \ \ \forall\ x$$

and at steady state $v_m(x,t) \leq V_m(x,t)$.

Proof: If we assume normal operating conditions within a platoon, then we have, $\delta_m(x_{ij},t) = G_\delta(s)v_m(x_{i(j-1)},t)$, where $G_\delta(s)$ is a stable, proper, minimum phase transfer function. The transfer function relating $\delta_m(x_{ij},t)$ and $\delta_m(x_{i(j-1)},t)$ can be found as:

$$\begin{aligned}\frac{\delta_m(x_{ij},t)}{\delta_m(x_{i(j-1)},t)} &= \frac{\delta_m(x_{ij},t)}{v_m(x_{i(j-1)},t)}W_1(s)\frac{v_m(x_{i(j-2)},t)}{\delta_m(x_{i(j-1)},t)},\\ &= W_1(s),\end{aligned} \tag{46}$$

where $v_m(x_{ij},t) = W_1(s)v_m(x_{i(j-1)},t)$. Similarly, we can show that $\frac{v_{r_m}(x_{ij},t)}{v_{r_m}(x_{i(j-1)},t)} = W_1(s)$. From constraint **C–II**, that guarantees platoon stability, it is required that:

$$\|w_1(t)\|_1 \leq 1, \tag{47}$$

where $w_1(t) = \mathcal{L}^{-1}\{W_1(s)\}$. Now from (5) and (9), by using the condition (47), we have:

$$\begin{aligned}&\|v_m(x_{ij},.)\|_\infty \leq \|V_m(x_{i1},.)\|_\infty;\ j = 1,\ldots,n_i,\ i = 1,\ldots,p\\ \Rightarrow\quad &\|v_m(x,.)\|_\infty \leq \|V_m(x,.)\|_\infty\ \forall x.\end{aligned} \tag{48}$$

Now to prove the second part of the lemma, we will differentiate between the desired speed V and the actual speed followed by the platoon leader V_{d_1} given in (2). The constraint **C–I** on $W_1(s)$ and $W_2(s)$ guarantees that $\lim_{t\to\infty} v_m(x_{ij},t) = V_{d_m}(x_{i1},t)$, where $V_{d_m}(x_{i1},t)$ is the actual speed followed by the leader of platoon i in section m. Now since:

$$V_{d_m}(x_{i1},t) = \min(V_m(x_{i1},t), V_l(t)) \tag{49}$$

where $V_l(t)$ is the speed of the vehicle in front of platoon leader. Hence, it follows that in steady state $v_m(x,t) \leq V_m(x,t)$.

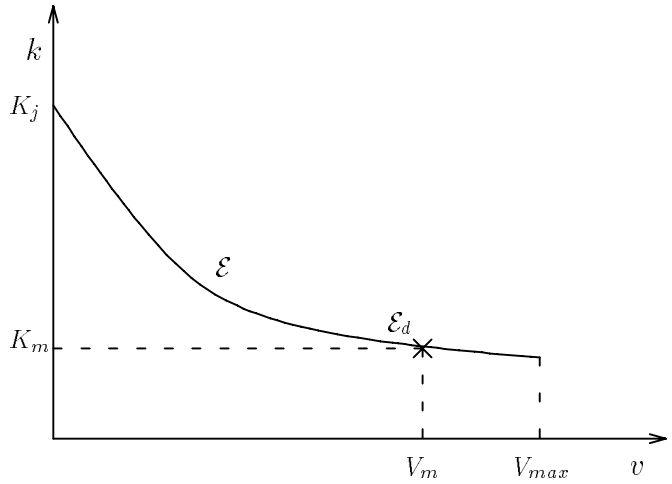

Figure 7: Equilibrium states for stationary flow, under time headway policy.

□

For time headway policy, Lemma 6.1 implies that in steady state:

$$\bar{V}_m \leq V_m \Rightarrow \bar{K}_m \geq K_m. \tag{50}$$

Since we are assuming positive velocities only, the plot of the equilibrium states $\mathcal{E} \in \mathcal{R}^2$ is shown in Figure 7, here K_j is the density at traffic jam conditions, when $\bar{V}_m = 0$. To show that the desired equilibrium point $\mathcal{E}_d$ is contained in the set $\mathcal{E}$, we will use the expressions of $\frac{\partial}{\partial t} v_m(x,t)$ and $\frac{\partial}{\partial x} v_m(x,t)$ as given in (14) and (15):

$$\begin{aligned} \frac{\partial}{\partial t} v_m(x,t) &= \dot{v}_m(x_{ij},t) + \Big\{ \dot{k}_m(x_{ij},t) \left[v_m(x_{i(j-1)},t) - v_m(x_{ij},t) \right] + \\ &\quad k_m(x_{ij},t) \left[\dot{v}_m(x_{i(j-1)},t) - \dot{v}_m(x_{ij},t) \right] \Big\} (x - x_{ij}) - \\ &\quad k(x_{ij},t) v(x_{ij},t) \left[v(x_{i(j-1)},t) - v(x_{ij},t) \right] \qquad (51) \\ \frac{\partial}{\partial x} v_m(x,t) &= k_m(x_{ij},t)[v_m(x_{i(j-1)},t) - v_m(x_{ij},t)] \qquad (52) \end{aligned}$$

From (51) and (52) we see that the conditions given in (39) and (40) are satisfied if and only if:

$$\begin{aligned} & \dot{v}_m(x_{ij},t) = 0 \\ \text{and} \quad & v_m(x_{ij},t) = v_m(x_{i(j-1)},t),\ j = 1,\ldots,n_i,\ i = 1,\ldots,p. \end{aligned} \tag{53}$$

Since we want to find the region of attraction of the desired equilibrium point, we will again differentiate between V, the desired speed, and V_{d_1}, the speed followed by the platoon leader,

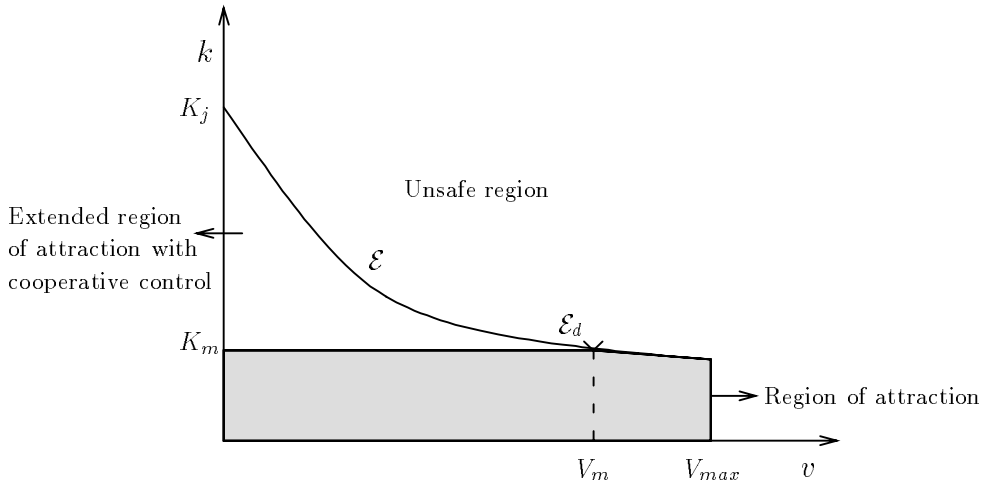

Figure 8: Region of attraction for stationary flow under time headway policy.

given in (2). Now from (5) we have that the conditions given in (53) are satisfied if and only if the desired speed, $V_{d_m}(x_{i1}, t)$, is constant for all i. The desired speed $V_{d_m}(x_{i1}, t) = V_m$ if $k_m(x, t) \leq K_m$ for all x. Hence the region of attraction of $\mathcal{E}_d$ is:

$$k_m(x, t) \leq K_m. \tag{54}$$

This region is mapped in Figure 8 and proves proposition 6.1 for time headway policy. Now we will show the same result for fixed distance headway policy. In this case the desired equilibrium states are:

$$\mathcal{E}_d = \{V_m, K_m\},\ K_m = \frac{1}{X_{r_d} + l}, \tag{55}$$

where X_{r_d} is the desired spacing, which is fixed and independent of the operating speed. Since Lemma 6.1 is independent of a particular control design, it also applies to the controllers designed with the fixed distance headway policy satisfying the constraints **C–I** and **C–II**. In this case we have that:

$$\bar{V}_m \leq V_m \text{ and } \bar{K}_m = K_m. \tag{56}$$

The plot of the equilibrium states for fixed distance headway policy is shown in Figure 9. The equilibrium state density is fixed, which is a property of this headway policy, however, the equilibrium speed can be lower than the desired one, if $v_m(x, t) < V_m$ for some x. This proves proposition 6.1 for fixed distance headway policy.

To prove proposition 6.2, we will start by identifying different regions shown in Figures 8. The constraint **C–I** imposed on the vehicle following controllers guarantees that the set

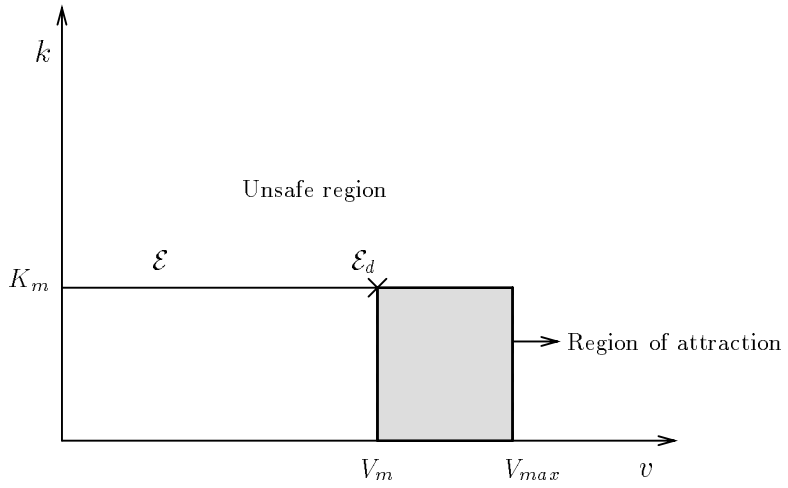

Figure 9: Region of attraction for stationary flow under fixed distance headway policy.

$\mathcal{E}$ is asymptotically attractive for all trajectories within the domain, $V_m \leq V_{max}$. The region above the equilibrium set $\mathcal{E}$, given as:

$$k_m > \frac{1}{h\bar{V}_m + l} \tag{57}$$

is unsafe, as the minimum safety distance policy is violated. Since the vehicle following control laws are designed to guarantee local safety, these trajectories are rejected at the microscopic level. Any transient in this region will eventually be terminated on the set $\mathcal{E}$. From (54) it is obvious that the desired equilibrium point is only locally attractive. In case of a disturbance, the system will end up in undesirable state with $\bar{K}_m > K_m$. Now to recover from this state it is required that:

$$\dot{k}_m(x,t) < 0 \text{ when } \bar{K}_m > K_m. \tag{58}$$

Since $\dot{k}_m = -k_m \frac{\partial v_m}{\partial x}$, to satisfy (58) it is required that there is a strictly positive spatial gradient in the speed distribution which cannot be guaranteed without some kind of cooperation between the vehicles.

On the other hand, for fixed distance headway policy, Figure 9, the equilibrium set $\mathcal{E}$ is asymptotically attractive for all of trajectories above or below this set. Furthermore, since the density remains equal to the desired one, the recovery to the desired set will occur if the disturbing condition is removed, without any need for external cooperation. Since

$$\begin{aligned} &\bar{K}_m = K_m \text{ (always)} \\ \text{and} \quad &\bar{V}_m < V_m \text{ when } v_m(x,t) < V_m \text{ for some } x, \end{aligned}$$

when the disturbance is removed, $v_m(x,t) \to V_m$, i.e., the system returns to its desired equilibrium state. This proves proposition 6.2.

We will make few comments here regarding implications of propositions 6.1 and 6.2. In the case of time headway policy, after the system is disturbed, the recovery to the desired equilibrium state requires a certain degree of cooperation between vehicles as suggested by (58). Hence in cooperative driving environment some improvement in the congestion reduction can be achieved. However, the control laws that can significantly enhance the convergence properties of the desired equilibrium state can be implemented at the infrastructure level, which has knowledge about the system states sufficiently upstream and downstream the affected area. Hence in the presence of roadway controller, the region of attraction (54), which is guaranteed by the microscopic controllers, can be extended to include the complete region below the set $\mathcal{E}$ in Figure 8. A corollary to proposition 6.2 is that: *Active involvement of infrastructure enhances the region of attraction of the desired equilibrium state.*

In the next section we will extend some of these results to the case of non-stationary flow.

6.2 Non-Stationary Flow

In this section we assume non-stationary flow conditions, i.e., $\frac{\partial}{\partial x}q_m(x,t) \neq 0$ or $\frac{\partial}{\partial t}k_m(x,t) \neq 0$ for some $x \in [0, L_m]$. Again for steady state we require that $\frac{\partial}{\partial x}v_m(x,t) = 0$ and $\frac{\partial}{\partial t}v_m(x,t) = 0 \Rightarrow v_m(x,t) = \bar{V}_m$. Since at steady state:

$$\dot{k}_m(x,t) = \frac{\partial}{\partial t}k_m(x,t) + v_m\frac{\partial}{\partial x}k_m(x,t) = 0.$$

By substituting $v_m = \bar{V}_m$ in the equation above we get:

$$\frac{\partial k_m}{\partial t} + \bar{V}_m\frac{\partial k_m}{\partial x} = 0. \tag{59}$$

Since in this case $\frac{\partial}{\partial t}k_m \neq 0$, the solutions of (59) have the form:

$$k_m(x,t) = f_m(x - \bar{V}_m t) \tag{60}$$

where $k_m(x,0) = f_m(x)$ is the initial condition and $x - \bar{V}_m t = \xi$ is the characteristic line, along which $k_m(x,t)$ has a constant value $f_m(\xi)$. Hence we have a wave traveling to the right with a constant velocity $\bar{V}_m$ that carries the non-constant density distribution $f_m(x)$, since at time $t = 0$ if we have $k_m(x_0, 0) = f_m(x_0)$ then at time $t_1 > 0$ for $x_1 = x_0 + \bar{V}_m t_1$ we have $k_m(x_1, t_1) = f_m((x_0 + \bar{V}_m t_1) - \bar{V}_m t_1) = f_m(x_0) = k_m(x_0, 0)$.

In the following we will do an analysis of the equilibrium states of the system for the non-stationary flow conditions.

6.2.1 Structure of Equilibrium States

Since in this case the steady state density distribution is non-uniform, $f_m(x - \bar{V}_m t)$, whereas the speed distribution, $\bar{V}_m$ is constant, the equilibrium states, for time headway policy,

consist of the following set:

$$\mathcal{E} = \{\bar{V}_m, (0, \bar{K}_m]\}\,,\ \bar{K}_m = \frac{1}{h\bar{V}_m + l}. \tag{61}$$

In this case the set of desired equilibrium states is:

$$\mathcal{E}_d = \mathcal{E}|_{\bar{V}_m = V_m}\,. \tag{62}$$

Hence the effect of non-stationary flow conditions at steady state is to enlarge the set of desired equilibrium states. As expected, the set $\mathcal{E}_d = \{V_m, (0, K_m]\}$ given in (62) reduces to a single point $\{V_m, K_m\}$ for homogeneous density. In this case the same kind of arguments can be used to show that the region of attraction is:

$$k_m(x,t) \leq K_m. \tag{63}$$

Similarly, the results given for fixed distance headway policy, in the case of stationary flow conditions, hold for non-stationary flow, which proves proposition 6.1. It can be easily shown that the same kind of congestion recovery characteristics exist for this case too, which extends the proof of proposition 6.2 for non-stationary flow. As discussed before, an extension of this region, in the case of time headway policy, can be achieved with the help of cooperative control laws.

Till now we have assumed that it is possible for the system to attain a uniform speed profile. It is not true in general, that the system can reach the steady state with a constant speed V_m. In the following we will discuss a situation in which a locally steady traffic approaches to a somewhat different operating conditions downstream. We will show that this potentially discontinuous situation, in some cases, may result in shock waves.

6.3 Shock Waves

In the previous section we have shown that for non-stationary flow conditions, the density distribution at steady state is a wave traveling to the right with a constant speed $\bar{V}_m$. The implicit assumption of obtaining continuous solution in (60) is that there is no obstruction for this wave, i.e., all the sections downstream section m are operating at the same (or higher) constant velocity. However, this may not be true in general. If the wave (60) happens to come across another wave generated by the density fluctuations in some other section which is operating at a speed different than $\bar{V}_m$ then there will be some interaction between these two waves. This interaction may cause a shock wave in an attempt to match the conditions at the interface of these two waves. Without loss of generality, we can assume the two sections to be $m = 1$ and 2, with the density waves as:

$$k_1(x,t) = f_1(x - \bar{V}_1 t), \tag{64}$$

$$k_2(x,t) = f_2(x - \bar{V}_2 t). \tag{65}$$

Since k is constant along the characteristic line which is a function of the initial condition ξ, two waves will meet at a point (x_s, t_s), where:

$$\begin{aligned} & x_s = \bar{V}_1 t_s + \xi_1 = \bar{V}_2 t_s + \xi_2, \\ \Rightarrow \qquad & t_s = \frac{\xi_2 - \xi_1}{\bar{V}_1 - \bar{V}_2}, \end{aligned} \tag{66}$$

where $\xi_2 > \xi_1, \Rightarrow t_s > 0$ if $\bar{V}_2 < \bar{V}_1$. Hence the waves (64) and (65) meet at a positive time given by (66). In this case the continuous solutions given in (64) and (65) fail to exist beyond the time t_s. Furthermore, the assumption of constant speeds $\bar{V}_1$ and $\bar{V}_2$ is no longer valid near the interface of two waves. Hence (59) no longer holds around the discontinuity. But, in general, law of conservation of vehicles always holds, i.e.,

$$\frac{\partial k}{\partial t} + \frac{\partial q}{\partial x} = 0 \tag{67}$$

where k and q are the density and flow rate around the region of discontinuity. We will rewrite (67) in a form which is similar to (59) but permits the speed to be discontinuous. If we denote the curve of discontinuity to be $x = \phi(t)$ and since $q(k) = kv$, we can write:

$$\begin{aligned} & \frac{\partial k}{\partial t} + \frac{\partial q(k)}{\partial x} = 0 \\ \Rightarrow \qquad & \frac{\partial k}{\partial t} + \frac{dq}{dk}\frac{\partial k}{\partial x} = 0. \end{aligned} \tag{68}$$

We propose that (68) can be written as:

$$\frac{\partial k}{\partial t} + v\frac{\partial k}{\partial x} = 0 \tag{69}$$

where $v(x,t)$ is the speed in the region of discontinuity and is given as:

$$v(x,t) = \begin{cases} \bar{V}_1 = \frac{dq}{dk} & \text{for } x < \phi(t) \\ \bar{V}_2 = \frac{dq}{dk} & \text{for } x > \phi(t). \end{cases} \tag{70}$$

However, $\frac{dq}{dk}$ fails to exist at the curve of discontinuity, $x = \phi(t)$, due to jump in the values of q and k caused by the discontinuity in v. As given in (70), $v(x,t)$ has limits from below and above, i.e.,

$$\lim_{x \uparrow \phi} v = \bar{V}_1 \text{ and } \lim_{x \downarrow \phi} v = \bar{V}_2.$$

Now we can use the technique given in [12] to derive the relationship between the speed at the discontinuity and the jump in the values of k and q. Since, in the case of time headway policy, k and q are functions of speed, we can rewrite (67) as:

$$\frac{\partial k(v(x,t))}{\partial t} + \frac{\partial q(v(x,t))}{\partial x} = 0. \tag{71}$$

If we assume the discontinuity to be contained in the region $[a, b]$, then integrating (71) over this region we get:

$$\int_a^b \frac{\partial k(v(x,t))}{\partial t} dx + \int_a^b \frac{\partial q(v(x,t))}{\partial x} dx = 0,$$

$$\Rightarrow \quad \frac{d}{dt} \int_a^b k(v(x,t)) dx + [q(v(b,t)) - q(v(a,t))] = 0. \tag{72}$$

Since by construction, $a < \phi(t) < b$, and v goes from $\bar{V}_1$ to $\bar{V}_2$ across the curve $\phi(t)$, we can rewrite (72) as:

$$\frac{d}{dt} \left[\int_a^{\phi} k(v(x,t)) dx + \int_{\phi}^b k(v(x,t)) dx \right] + [q(v(b,t)) - q(v(a,t))] = 0. \tag{73}$$

Using Liebnitz rule and replacing $\frac{\partial k(v)}{\partial t}$ with $-\frac{\partial q(v)}{\partial x}$, we get:

$$\left[k(\bar{V}_1)\dot{\phi} - \int_a^{\phi} \frac{\partial q(v)}{\partial x} dx \right] - \left[\int_{\phi}^b \frac{\partial q(v)}{\partial x} dx + k(\bar{V}_2)\dot{\phi} \right] + [q(v(b,t)) - q(v(a,t))] = 0,$$

$$-\dot{\phi} \left[k(\bar{V}_2) - k(\bar{V}_1) \right] + \left[q(\bar{V}_2) - q(\bar{V}_1) \right] = 0, \tag{74}$$

where $\dot{\phi} = \frac{d\phi}{dt}$ and is given as:

$$\frac{d\phi}{dt} = \frac{[q(\bar{V}_2) - q(\bar{V}_1)]}{[k(\bar{V}_2) - k(\bar{V}_1)]}. \tag{75}$$

Hence the speed of propagation of the discontinuity or shock, $\frac{d\phi}{dt}$, is equal to $\frac{\Delta q}{\Delta k}$, where Δq and Δk are jump in the values of q and k across the discontinuity. It should be noted that the shock wave $\phi(t)$ can travel upstream or downstream depending on the signs of Δq and Δk.

The analysis given above is valid only for time headway policy, as the assumption in (71) that k is a function of speed $v(x,t)$ is not true for fixed distance headway policy. At this time it is not clear whether a similar analysis can be extended for fixed distance headway policy. However, some intuitive arguments can be used to show the possibility of existence of shock waves under fixed distance headway policy.

Under fixed distance headway policy and stationary flow conditions, if the disturbance causes the speed to drop below its desired value, then to preserve the density, the discontinuity in speed at the point of disturbance will instantaneously travel upstream. The impact of this discontinuity can be dissipated by an instantaneous reduction in speed at the lane boundary, which may or may not be possible. This argument can be strengthened by the analysis of fundamental diagrams for the two headway policies.

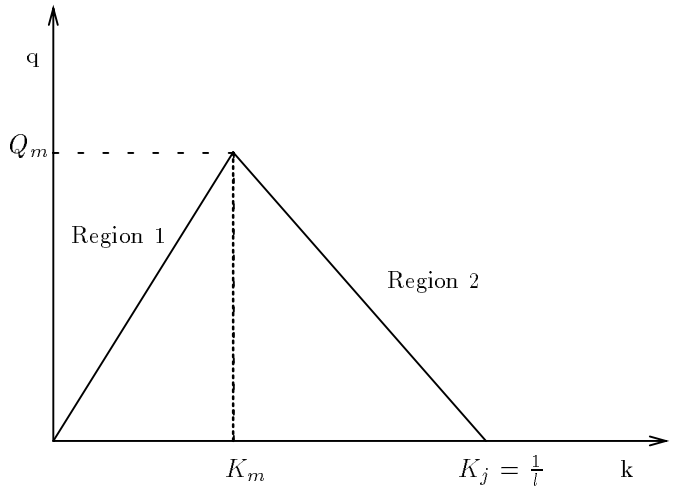

Figure 10: Fundamental diagram for automated traffic flow under time headway policy.

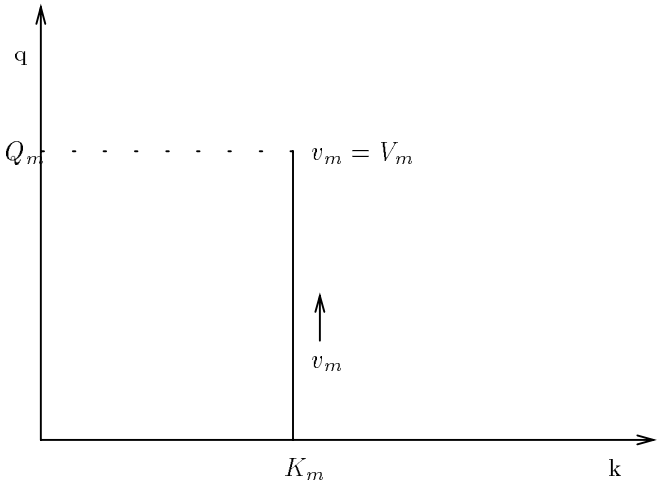

Figure 11: Fundamental diagram for automated traffic flow under fixed distance headway policy.

The fundamental diagrams showing the relationship between the steady state flow rate and density for the two headway policies are shown in Figures 10 and 11. The region 1 shown in Figure 10 corresponds to the region of attraction of the desired equilibrium state, when $k_m < K_m$. In this region the speed is constant at V_m and flow increases to Q_m as the density increases to its maximum permissible value K_m. The region 2 in Figure 10 results from congested traffic when $k_m > K_m$. The time headway policy has $q - k$ characteristics which are very similar to those of human driving, where the variations of $\frac{\Delta q}{\Delta k}$ give rise to shock waves. On the other hand, as shown in Figure 11, for fixed distance headway policy the density is constant at all operating speeds. The shape of $q - k$ characteristics in this case has an inherent discontinuity in the speed due to the requirement of density preservation. These arguments and the analysis given above are sufficient to prove proposition 6.3.

At this point we will make the following remarks.

Remarks

- As we have seen above, there are situations in which the undesirable phenomena observed on current highways such as congestion and shock waves will show up for some automatic vehicle following concepts. Hence the modes of operation of AHS which require less cooperation between vehicles and infrastructure, such as ICC and autonomous individual vehicles, have a restricted range of operation in which the required traffic throughput can be achieved. However, as shown above, some of these undesirable effects can be sufficiently attenuated with the help of macroscopic control laws.

- The major difference in the time and fixed distance headway policies lies in the recovery characteristics. In the case of fixed distance headway policy, if the disturbance, causing a reduction in speed, is removed the system can recover to its normal speed without an outbreak of shock waves. During recovery stage in the case of time headway policy, the increasing speeds of downstream vehicles will result in reduction in relative spacings of upstream vehicles, causing cyclic reductions in speed and hence shock waves.

In the next section we will simulate the model proposed in section 4.

7 Simulation of Model

In this section we will validate the macroscopic properties of automated traffic flow predicted by the analysis of the model in section 6. Since no macroscopic data from automated traffic flow is available to do this job, we will use simulation results only. In particular we will simulate the situations in which the undesirable effects outlined in propositions 6.1-6.3 can be visualized.

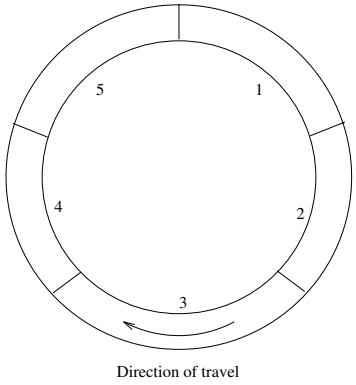

Figure 12: A single lane circular highway used for simulation.

For simplicity we have assumed a single lane circular highway shown in Figure 12. The highway is subdivided into five sections, $M = 5$, each with a length of 500 meters. The vehicles are assumed to be traveling in platoons of uniform size, $n_i = 5$. We assume a known initial distribution of platoons in each section. The subsequent distribution is then dynamically updated by using the kinematic equations (5) and (6). Different scenarios used for simulations are described below.

7.1 Scenario 1

In this scenario we will demonstrate the existence of shock waves for automated traffic flow, when vehicles are traveling under time headway policy. The transfer functions $W_1(s)$ and $W_2(s)$ are selected from the longitudinal vehicle following control design in [8]. The nominal highway speed is assumed to be 20 m/s with a constant time headway of 0.5 seconds.

For this scenario we assume that a disturbance exists in section 3, which causes the vehicles in that section to decelerate to a speed of 10 m/s. The rest of the sections are operating at their nominal speed. This disturbance is removed after 10 seconds so that the disturbed vehicles can resume their normal speed. The plots of the speed and density distribution functions are shown in Figures 13 and 14.

The speed distribution function in Figure 13 shows that, even though the disturbance is removed, the system was not able to return to its desired equilibrium point. The density distribution in Figure 14 indicates the presence of shock waves. These waves are generated as the system is trying to recover to its normal state. The vehicles at the point of disturbance with open space in front of them are returning to their normal speed, which causes a reduction in the relative spacings of the upstream vehicles. These vehicles then have to reduce their speed again, this cyclic variations is speed results in a shock wave. In this case this wave is traveling upstream with an approximate speed of 10 m/s which is exactly as predicted by the analysis of the model.

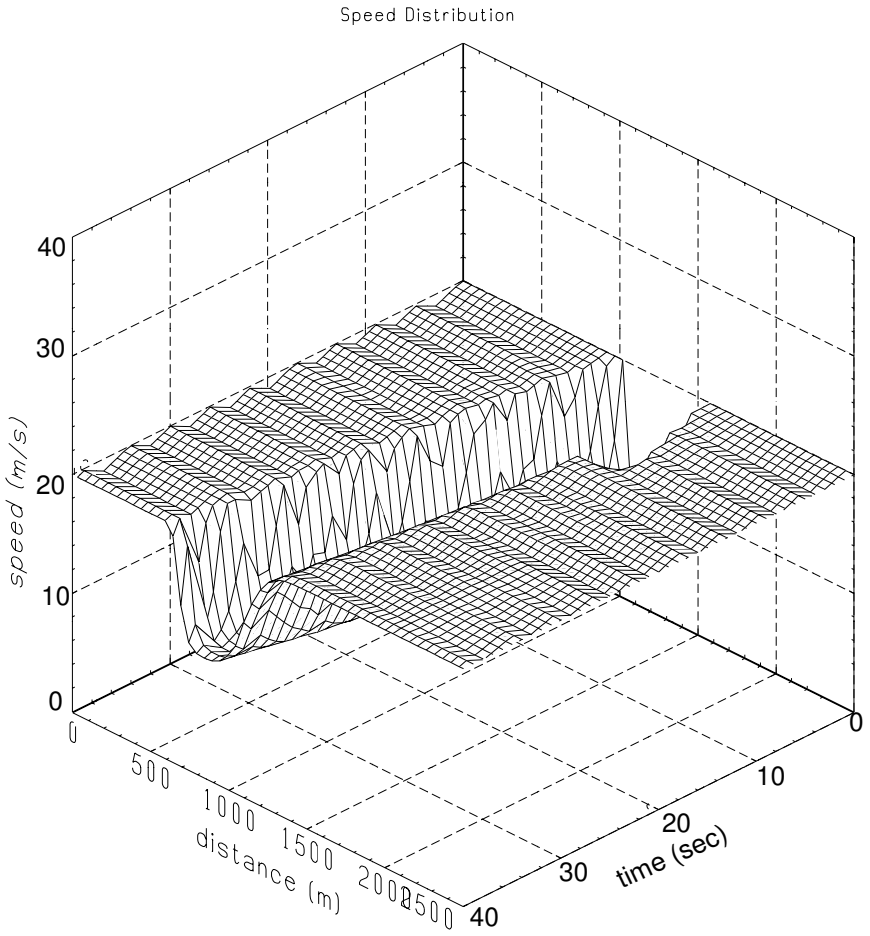

Figure 13: Speed distribution function for time headway policy. The system is disturbed from $t = 0$ to $t = 10$ seconds, after the disturbance is removed the system is not able to recover even after $t = 40$ seconds.

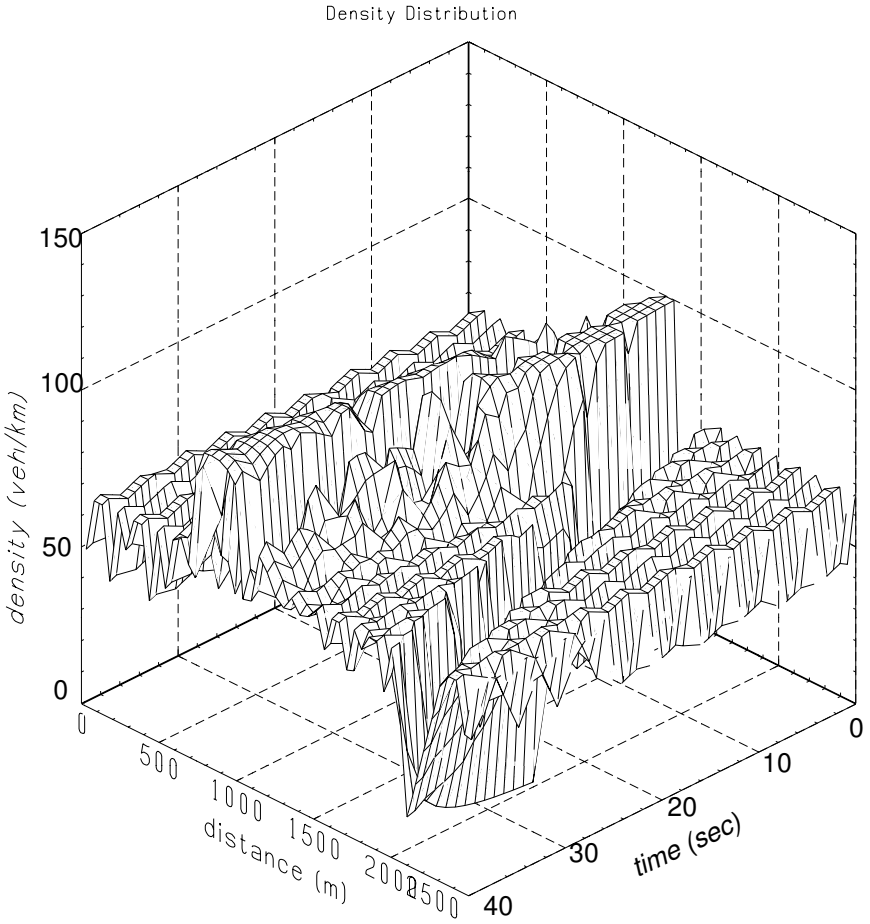

Figure 14: Density distribution function for time headway policy. The plot shows that shock waves are generated as the system is recovering to its normal state.

7.2 Scenario 2

In this scenario, we have selected the same kind of operating conditions as were created for scenario 1. The only difference in this case is that the vehicles are traveling under fixed distance headway policy with a constant headway of 10 meters. The transfer functions $W_1(s)$ and $W_2(s)$ are selected from the longitudinal vehicle following control design in [9].

The plots of the speed and density distributions are shown in Figures 15 and 16. The speed distribution function in Figure 15 indicates that the system returns to its normal operating point within few seconds after the disturbance is removed. The density distribution function in Figure 16 shows that no shock waves are created in this case.

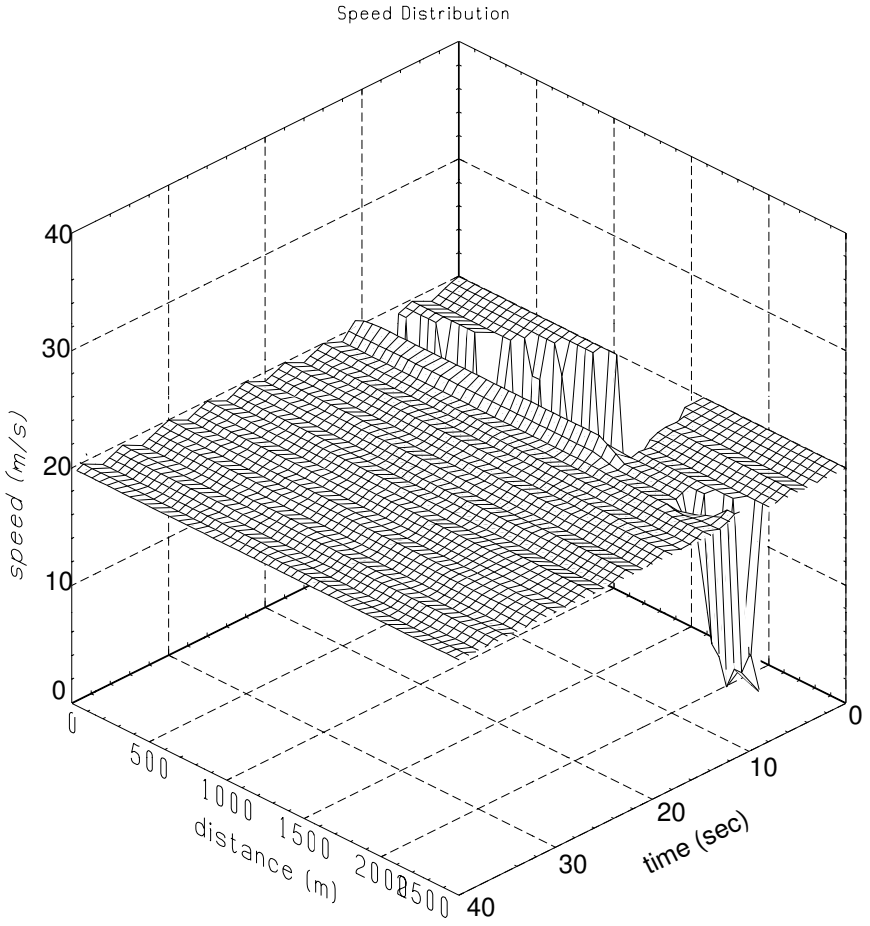

Figure 15: Speed distribution function for fixed distance headway policy. The system is disturbed from $t = 0$ to $t = 10$ seconds, after the disturbance is removed the system returns to its desired equilibrium state.

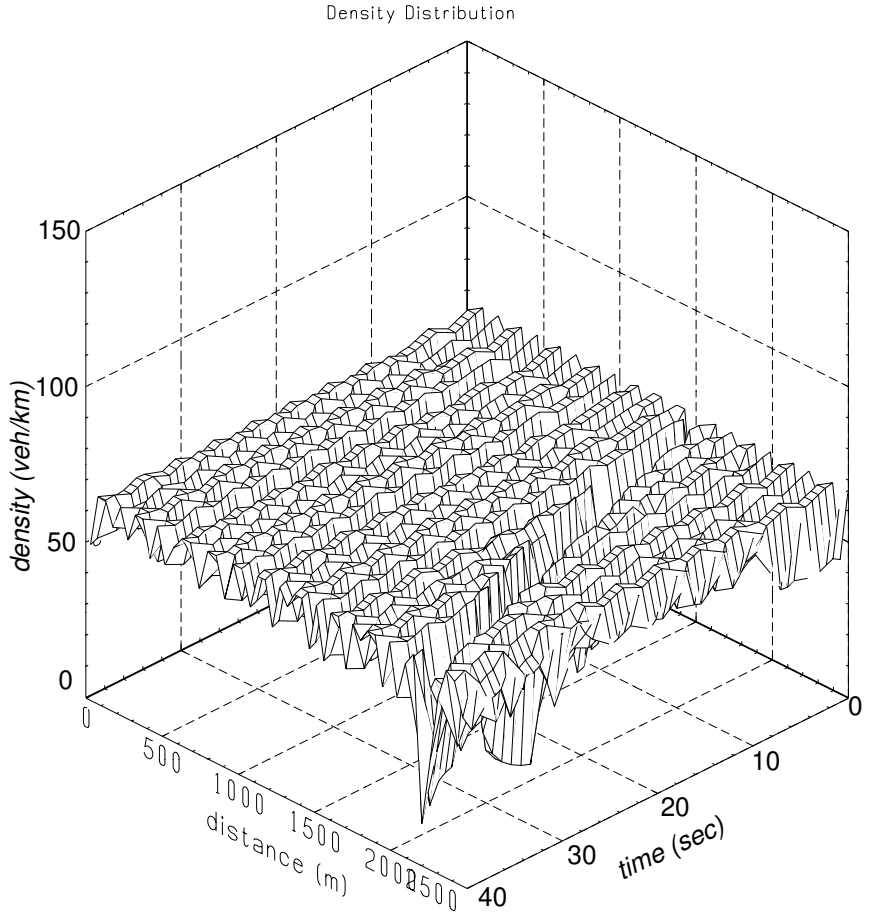

Figure 16: Density distribution function for fixed distance headway policy. The plot shows that no shock waves are generated as the system is recovering.

8 Conclusion

In this paper we have developed a model that describes the macroscopic behavior of automated traffic flow in terms of the kinematics of individual vehicles. The model captures the details of microscopic control laws, which are deterministic in nature, in a form which can be used for analysis and design of control laws to improve system level performance. We have given enough structure to the modeling task so that the model is independent of the implementation details of the system, hence can be applied to a variety of automated vehicle following concepts including the proposed modes of AHS. The model is then used to analyze the macroscopic properties of automated traffic flow for different operating conditions. In particular we have compared the convergence characteristics of equilibrium states of time and fixed distance headway policies. The analysis indicates differences in the congestion recovery characteristics of these headway policies. The automated traffic flow is shown to be susceptible to congestion and shock waves in some situations. It is shown that these undesirable phenomena can be eliminated with the help of cooperative control laws. Finally some of the undesirable phenomena predicted by the analysis of the model were also shown through the simulation of the model.

References

[1] J. J. Lighthill and G. B. Witham, "On Kinematic Waves II: A Theory of Traffic Flow on Long Crowded Roads", *Proc. of the Royal Society of London*, Series A 229, pp. 317-345, 1955.

[2] H. J. Payne, "Models of Freeway Traffic and Control", *Mathematical Models of Public Systems*, Simulation Council Proceedings, pp. 51-61, 1971.

[3] M. Cremer and A. D. May, "An Extended Traffic Model for Freeway Traffic Control", California PATH Research Report, UCB-ITS-PR-85-7, 1985.

[4] M. Papageorgiou, "Macroscopic Modeling of Traffic Flow on the Boulevard Périphérique in Paris", *Transportation Research*, -B, vol. 23B, no. 1, pp. 29-47, 1989.

[5] U. Karaaslan, P. Varaiya and J. Warland, "Two Proposals to Improve Freeway Traffic-Flow", Preprint 1990.

[6] C. C. Chien, Y. Zhang, A. Stotsky, S. R. Dharmasena, P. Ioannou, "Macroscopic Roadway Traffic Controller Design", California PATH Research Report, UCB-ITS-PRR-95-28.

[7] H. Raza, P. Ioannou, "Vehicle Following Control Design for Automated Highway Systems," *IEEE Control Systems*, vol. 16, no.6, pp. 43-60, December 1996.

[8] P. Ioannou, Z. Xu, "Throttle and Brake Control System for Automatic Vehicle Following", *IVHS Journal*, vol. 1(4), pp. 345-377, 1994.

[9] J. K. Hedrick, D. H. McMahon, D. Swaroop, "Vehicle Modeling and Control for Automated Highway Systems," PATH Technical Report, UCB-ITS-PRR-93-24, 1993.

[10] A. Kanaris, P. Ioannou, "Spacing and Capacity Evaluations of different AHS Concepts," *Automated Highway Systems*, Ed. P. Ioannou, Plennum Publishing Corporation, New York, pp. 125-171, 1996.

[11] P. Varaiya, "Smart Cars on Smart Roads: Problems of Control", *IEEE Transactions on Automatic Control*, vol. 38, no. 2, pp. 195-207, Feb. 1993.

[12] F. John, *Partial Differential Equations*, 4th edition, Springer-Verlag, New York, 1982.

Roadway Controller Design using Spatio-Temporal Control Technique*

H. Raza and P. Ioannou
Dept. of Electrical Engineering-Systems
University of Southern California
Los Angeles, CA 90089-2562

Abstract

The analysis of macroscopic model of automated traffic flow [1], indicates that there are operating conditions in which such a system can end up in undesirable steady states and that these undesirable effects can be sufficiently attenuated by introducing some kind of cooperation between vehicles. This analysis strongly suggests the presence of a high level controller, called roadway controller, to provide the necessary coordination between the automated vehicles. In this paper the design of a roadway controller is presented to guarantee global asymptotic convergence of the system states to the desired ones. The design is based on a spatio-temporal control (STC) technique. This particular choice is dictated by the macroscopic traffic flow model, which describes its states in spatial and temporal coordinates. The control input is derived by feedback linearizing the model with the help of a two dimensional virtual control input. The actual control input is obtained in the second step by inverting the dynamics related between the virtual and actual control input. The control design guarantees closed loop stability and achieves the desired performance.

1 Introduction

The analysis of the automated traffic flow, using the macroscopic model developed in [1], indicates that under some operating conditions, system will end up in undesirable states leading to congestion or shock waves. It has been argued in [1] that the recovery from these undesirable states can be expedited by introducing active feedback at the roadway level.

*This work is supported by the California Department of Transportation through PATH of the University of California. The contents of this paper reflect the views of the authors who are responsible for the facts and accuracy of the data presented herein. The contents do not necessarily reflect the official views or policies of the State of California or the Federal Highway Administration. This paper does not constitute a standard, specification or regulation.

In this paper we will present the design of a roadway controller to achieve its objective. This objective outlines that the roadway controller should be able to track the desired density and/or speed profiles provided to it by a higher level controller which is part of the network layer. The network controller selects the desired profiles by analyzing the existing traffic flow conditions and the projected demand on the network. In this study we will not consider the explicit process by which these profiles are selected, but will assume that they are available for the roadway controller to use.

In this study we will develop a spatio-temporal control technique to achieve the objectives of link layer controller. In this technique the partial derivatives of the speed distribution function are separately adjusted to track the desired density and speed profiles. The rationale for this distribution in control follows from the fact that the acceleration at any point, which is composed of spatial and temporal components, can be used as a two degree of freedom virtual control. The actual control input, the desired speed command, is obtained by inverting the dynamics associated with this virtual and the actual control. The resulting control input guarantees tracking of the desired speed and density profiles. In addition, other requirements, such as controller bandwidth and tracking response can be selected through appropriate filters.

The paper is organized as follows: A brief summary of the macroscopic traffic flow model used in the controller design is given in section 3. The control objectives are explained in section 4. The design of the roadway controller based on STC is presented in section 5. The controllability issues of such a design are discussed in section 6. In section 7, the simulation results for the scenarios discussed in the controller design are presented. The paper ends with the main results summarized in the conclusion section.

2 Macroscopic Traffic Flow Model

Before describing the control design it is worthwhile to summarize the macroscopic traffic flow model used. For details of this model the readers are referred to [1].

The macroscopic traffic flow model given in [1] derives its states from the microscopic dynamics of vehicles following automatically under the given control law. The model capitalizes on the deterministic closed loop dynamics of vehicles under automatic control. Such dynamics can be represented in terms of appropriate transfer functions $W_1(s)$, $W_2(s)$, which are known functions of the control law being implemented on the vehicles. With an assumption that the closed loop dynamics are identical, the speed v and relative distance X_r between any two vehicles in a platoon may be represented as:

$$v(x_{ij},t) = [W_1(s)]^j V(x_{i1},t) \tag{1}$$

$$X_r(x_{ij},t) = W_2(s)[W_1(s)]^{j-1} V(x_{i1},t) \qquad j = 1,\ldots,n_i,\ i = 1,\ldots,p. \tag{2}$$

where j represents the vehicle in a platoon, i represents the platoons in a section, n_i is the

size of the platoon i, p is the total number of platoons in a section m and $V(x_{i1},t)$ is the desired speed for platoon i.

Assuming that the traffic flow is above a certain threshold, such that the flow can be approximated as continuous fluid flow, from macroscopic point of view, the speed and density distribution functions, $v(x,t)$, $k(x,t)$, can be defined in terms of these individual vehicle dynamics (1)-(2) and are represented as:

$$v(x,t) \triangleq v(x_{ij},t) + \Big[v(x_{i(j-1)},t) - v(x_{ij},t)\Big]\left[\frac{x - x_{ij}}{X_r(x_{ij},t)+l}\right] \tag{3}$$

$$k(x,t) \triangleq k(x_{ij},t) + \Big[k(x_{i(j-1)},t) - k(x_{ij},t)\Big]\left[\frac{x - x_{ij}}{X_r(x_{ij},t)+l}\right] \tag{4}$$

$$x_{ij} \le x \le x_{i(j-1)};\ j = 1,\ldots,n_i,\ i = 1,\ldots,p$$

where:

$$k(x_{ij},t) \triangleq \frac{1}{X_r(x_{ij},t)+l} \tag{5}$$

where l is the length of the vehicle, assumed to be the same for all vehicles, x_{ij} is the location of any particular vehicle and is given as:

$$x_{ij} = L - \left[\sum_{\alpha=1}^{i-1}\sum_{\beta=1}^{n_\alpha}(X_r(x_{\alpha\beta},t)+l) + \sum_{\beta=1}^{j} X_r(x_{i\beta},t) + \sum_{\beta=1}^{j-1} l\right],\ j = 1,\ldots,n_i,\ i = 1,\ldots,p \tag{6}$$

where L is the length of the section m. Now by using the law of conservation of vehicles and the expression for the acceleration of an observer moving with the traffic stream, we can derive the state update laws as:

$$\dot{v}(x,t) = \frac{\partial}{\partial t}v(x,t) + v(x,t)\frac{\partial}{\partial x}v(x,t), \tag{7}$$

$$\dot{k}(x,t) = -k(x,t)\frac{\partial}{\partial x}v(x,t). \tag{8}$$

By using appropriate boundary and initial conditions, different sections in a lane can be connected to represent traffic flow in a single highway lane. This traffic flow model for a single highway lane can be extended to that for a multi-lane highway system by using the modifications introduced in [1] to account for changes in the states of the system caused by lane changes and on-ramp/off-ramp traffic flow. The complete macroscopic model that represents traffic flow in a multi-lane highway system is summarized below:

$$\dot{v}_{ym}(x,t) = \frac{\partial}{\partial t}v_{ym}(x,t) + v_{ym}(x,t)\frac{\partial}{\partial x}v_{ym}(x,t) \tag{9}$$

$$\dot{k}_{ym}(x,t) = \begin{cases} -k_{ym}(x_t,t_t)\frac{\partial}{\partial x}v_{ym}(x_t,t_t) + \phi_{ym}(x_t,t_t) & \text{for } x = x_t,\ t = t_t \\ -k_{ym}(x_o,t_o)\frac{\partial}{\partial x}v_{ym}(x_o,t_o) - \phi_{ym}(x_o,t_o) & \text{for } x = x_o,\ t = t_o \\ -k_{ym}(x,t)\frac{\partial}{\partial x}v_{ym}(x,t) & \text{else} \end{cases}$$

$$q_{ym}(x,t) = k_{ym}(x,t)v_{ym}(x,t)$$

$$v_{ym}(x,t_0) = g_{ym}(x),\ k_{ym}(x,t_0) = f_{ym}(x)$$

$$y = 1,\ldots,Y,\ m = 1,\ldots,M$$

$$v_{y1}(0,t) = v_{y0}(t),\ q_{y1}(0,t) = q_{y0}(t)$$

$$v_{ym}(0,t) = v_{y(m-1)}(L_{y(m-1)},t),\ q_{ym}(0,t) = q_{y(m-1)}(L_{y(m-1)},t),$$

$$y = 1,\ldots,Y,\ m = 2,\ldots,M$$

$$x_{ij} \le x \le x_{i(j-1)},\ j = 1,\ldots,n_i,\ i = 1,\ldots,p$$

$$x_{ij} = L_{ym} - \left[\sum_{\alpha=1}^{i-1}\sum_{\beta=1}^{n_\alpha}(X_{r_{ym}}(x_{\alpha\beta},t) + l) + \sum_{\beta=1}^{j} X_{r_{ym}}(x_{i\beta},t) + \sum_{\beta=1}^{j-1} l\right]$$

$$k_{ym}(x_{ij},t) = \frac{1}{X_{r_{ym}}(x_{ij},t) + l}$$

$$v_{ym}(x_{ij},t) = [W_1(s,h_{ym})]^j V_{ym}(x_{i1},t)$$

$$X_{r_{ym}}(x_{ij},t) = W_2(s,h_{ym})[W_1(s,h_{ym})]^{j-1} V_{ym}(x_{i1},t)$$

In (9) y refers to a particular lane within the given highway system. We will use the model (9) in section 4 to design a controller that can guarantee that the speed and density profiles in a section of the highway remain close to the desired ones. However, before presenting the control design, in the next section we will formally state the objectives of such a controller.

3 Control Objectives

Within the hierarchical control structure proposed for automated highway system [2], the objectives defined for the roadway or link layer controller are:

$$k_m(x,t) \to k_{d_m}(x,t)$$
$$v_m(x,t) \to v_{d_m}(x,t)$$

where $v_m(x,t)$, $k_m(x,t)$ are the speed and density distribution functions for section m of the highway and $v_{d_m}(x,t)$, $k_{d_m}(x,t)$ are the desired speed and density for that section. The desired profile $\{v_{d_m}, k_{d_m}\}$ is provided by the network layer controller. The network layer calculates these values by analyzing the real time measurements and predicting the future demand. For this study we assume that these values are available for the roadway controller to use. The exact mechanism of selecting these desired profiles will be addressed in

the subsequent part of this study.

The analysis of the model (9) in [1] indicates that the region of attraction associated with a set of equilibrium states is only local, which means that there are initial conditions which will not result in convergence of the system states to the desired ones. Hence the main objective of the design of roadway controller in this paper is to guarantee the global attractiveness of the equilibrium states.

As is obvious from the macroscopic model (9) that both the speed and density distributions are functions of the speed command issued to vehicles, $V_{ym}(x,t)$. The density is a function of headway command also, however, for the current study we will assume the headway to be constant and hence the speed command $V_{ym}(x,t)$ will be used as the only control input. Hence the control objectives can be met by using the speed command to track the desired speed and density profiles. Furthermore, for comfortable ride, the desired speed command should be band limited, i.e., the maximum allowable acceleration should not be violated by the speed command.

In the following, we will explain the spatio-temporal control (STC) technique for the design of a roadway controller. We will assume stationary and non-stationary flow conditions as two cases of interest and derive the control input for each case separately.

4 Spatio-Temporal Control (STC) Design

For simplicity, we will assume a single lane of the given highway system with no lateral traffic flow. Then as described in [1], the macroscopic model (9) given for a multi-lane highway system with lateral traffic flow reduces to:

$$\dot{v}_m(x,t) = \frac{\partial}{\partial t} v_m(x,t) + v_m(x,t) \frac{\partial}{\partial x} v_m(x,t) \tag{10}$$

$$\dot{k}_m(x,t) = -k_m(x,t) \frac{\partial}{\partial x} v_m(x,t). \tag{11}$$

Where we have used a general form for the acceleration and the rate of change of density at any point x within a given section of the lane. As pointed out, as a result of analysis of this model in [1], that the system has a non-unique set of equilibrium states and that the convergence properties of the desired equilibrium point can be enhanced by introducing an active feedback through the roadway controller. Since the objective of the roadway controller is to track the desired trajectory $\{v_d, k_d\}$, this objective can be achieved by issuing the desired speed command to vehicles in a section as a control input. In this study, we will develop a new technique to derive this control input, that will be denoted as spatio-temporal control (STC) technique.

Using STC we will derive the control input in two steps: In the first step the partial derivatives of the speed distribution function, $u_x = \frac{\partial v_m}{\partial x}$ and $u_t = \frac{\partial v_m}{\partial t}$ will be used as

fictitious control inputs to feedback linearize the model [3]. The linearizing inputs u_x and u_t can be selected so that the linearized model will have the desired tracking properties. In the next step the actual control input $V_m(x,t)$ will be obtained by inverting the dynamics related between the speed command V_m and these fictitious control inputs. During this inversion process we can impose different constraints, in terms of filters, so that the resulting control input has the desired properties.

In the following, we will explain this technique by considering stationary and non-stationary flow conditions as two special cases of interest, with varying degree of restrictions imposed on the desired trajectory $\{v_d, k_d\}$.

4.1 Case 1: Constant v_d, k_d

For the simplest case we assume the desired trajectory to be a constant value, $\{v_d, k_d\}$, i.e. the desired flow is stationary. In this case, from (11) we have:

$$\dot{\tilde{k}}_m = -k_m(x,t)\frac{\partial}{\partial x}v_m(x,t) \tag{12}$$

where $\tilde{k}_m = k_m - k_d$ is the density tracking error. With the assumption that $k_m(x,t) > 0$, $\forall x$, t, we can set the first part of fictitious control input, $u_x = \frac{\partial v_m}{\partial x}$, as:

$$u_x = H(s)\left[1 - \frac{k_d}{k_m(x,t)}\right] \tag{13}$$

where $H(s)$ is any stable, minimum phase and proper transfer function chosen to achieve the tracking objective within the desired bandwidth. One particular choice is $H(s) = W_1(s)H_1(s)$, where $W_1(s)$ is as defined in the macroscopic model (9) and $H_1(s)$ is any stable strictly proper transfer function. With this choice of $u_x(x,t)$, (11) becomes:

$$\dot{\tilde{k}}_m(x,t) = -H(s)\tilde{k}_m(x,t) \tag{14}$$

Similarly, by substituting (13) in (10), we get:

$$\dot{\tilde{v}}_m(x,t) = \frac{\partial v_m}{\partial t} + H(s)\left[1 - \frac{k_d}{k_m(x,t)}\right]v_m(x,t), \tag{15}$$

where $\tilde{v}_m = v_m - v_d$ is the speed tracking error. Now we can choose the second part of fictitious control input, i.e., $u_t = \frac{\partial v_m}{\partial t}$ as:

$$u_1(x,t) \le u_t(x,t) \le u_2(x,t) \tag{16}$$
$$u_\alpha(x,t) = -(c_\alpha + 1)H(s)v_m(x,t) + c_\alpha H(s)v_d + H(s)\frac{k_d}{k_m(x,t)}v_m(x,t),\ \alpha = 1,2$$

where $c_1 > c_2 > 0$ are design constants and are chosen to limit the bandwidth of the speed command. With this choice of u_t, (15) becomes:

$$-c_1 H(s)\tilde{v}_m(x,t) \le \dot{\tilde{v}}_m(x,t) \le -c_2 H(s)\tilde{v}_m(x,t). \tag{17}$$

It should be noted that in (16), instead of constants c_1 and c_2, we can choose some appropriate filters to make the closed loop response of the speed tracking different than that for density tracking. Hence using these fictitious inputs u_x and u_t, which are nothing but functions of the state of the system, speed distribution v_m in this case, we can achieve the control objective of tracking the desired trajectory $\{v_d, k_d\}$

Since the macroscopic model (10)-(11) derives its states $[v_m, k_m]^\top$ from the microscopic dynamics, these states and their functions, u_x and u_t in this case, can be explicitly represented in terms of these microscopic dynamics. It should be noted that the actual control input $V_m(x,t)$ exists at the microscopic level. In the next step we will derive the control input $V_m(x,t)$ by inverting the dynamics from this external control input to the functions u_x and u_t of the state $v_m(x,t)$ of the system. From the definition of the state $v_m(x,t)$, we can explicitly solve for $\frac{\partial v_m}{\partial x}$ as:

$$v_m(x,t) = v_m(x_{ij},t) + \left[v_m(x_{i(j-1)},t) - v_m(x_{ij},t)\right]\left[\frac{x - x_{ij}}{X_r(x_{ij},t) + l}\right]$$

$$\Rightarrow \qquad \frac{\partial v_m(x,t)}{\partial x} = k_m(x_{ij},t)[v_m(x_{i(j-1)},t) - v_m(x_{ij},t)]. \tag{18}$$

Since we are assuming that vehicles are grouped together in platoons of appropriate sizes, the speed command is directed only to the platoon leaders. Let x_{i1}, $i = 1, \ldots, p$ be the location of platoon leaders within the section m then:

$$u_x(x_{i2},t) = \frac{\partial v_m(x_{i2},t)}{\partial x} = k_m(x_{i2},t)\left[v_m(x_{i1},t) - v_m(x_{i2},t)\right] \tag{19}$$

Now by equating (13) and (19), we get:

$$H(s)\left[1 - \frac{k_d}{k_m(x_{i2},t)}\right] = k_m(x_{i2},t)W_1(s)(1 - W_1(s))V_m(x_{i1},t) \tag{20}$$

where we have used the definition, $v_m(x_{ij},t) = [W_1(s)]^{j-1}V_m(x_{i1},t)$, $j = 1, \ldots, n_i$. Now by imposing additional constraint on transfer function $W_1(s)$ that:

- $(1 - W_1(s))$ is minimum phase

and by choosing $H(s) = W_1(s)H_1(s)$, we can filter both sides of (20) with $\frac{1}{1-W_1(s)}$ to get:

$$V_m(x_{i1},t) = \frac{H_1(s)}{1 - W_1(s)}\left(1 - \frac{k_d}{k_m(x_{i2},t)}\right)\frac{1}{k_m(x_{i2},t)} \tag{21}$$

Now we can use the definition of $\frac{\partial v_m}{\partial t}$, we get:

$$u_t(x_{i2},t) = \frac{\partial v_m(x_{i2},t)}{\partial t} = [W_1(s)]^2\dot{V}_m(x_{i1},t) \tag{22}$$

From (16) and (22) we get:

$$\frac{H_1(s)}{W_1(s)}\left[\frac{k_d}{k_m(x_{i2},t)}-(c_1+1)\right]v_m(x_{i2},t)+c_1\frac{H_1(s)}{W_1(s)}v_d \le \dot{V}_m(x_{i1},t)$$
$$\le \frac{H_1(s)}{W_1(s)}\left[\frac{k_d}{k_m(x_{i2},t)}-(c_2+1)\right]v_m(x_{i2},t)+c_2\frac{H_1(s)}{W_1(s)}v_d \qquad (23)$$

The following theorem outlines the stability and performance of the closed loop system.

Theorem 4.1 *With the assumption that $k_m(x,t) > 0$ and $(1 - W_1(s))$ is minimum phase, the control law (21) and (23) has the following properties:*
(a) V_m, $\dot{V}_m \in \mathcal{L}_\infty$,
(b) $v_m \to v_d$, $k_m \to k_d$ (exponentially).

In the next section, we will extend the control input derived for the stationary flow case to the non-stationary one.

4.2 Case 2: Constant v_d, Arbitrary k_d

In this case we assume that v_d is constant, whereas k_d is arbitrary, which corresponds to non-stationary flow conditions. Furthermore, it is required that the desired trajectory, $\{v_d, k_d(x,t)\}$, follows the vehicle conservation law, i.e.,

$$\frac{\partial k_d(x,t)}{\partial t}+\frac{\partial(k_d(x,t)v_d)}{\partial x}=0 \qquad (24)$$
$$\Rightarrow \quad \dot{k}_d(x,t)=0$$

Hence in this case $\dot{\hat{k}}_m(x,t)=\dot{k}_m(x,t)$ and $\dot{\hat{v}}_m(x,t)=\dot{v}_m(x,t)$, i.e., the control law (21) and (23) holds for this case too. However, the desired density is not constant any more, i.e.,

$$V_m(x_{i1},t)=\frac{H_1(s)}{1-W_1(s)}\left(1-\frac{k_d(x_{i2},t)}{k_m(x_{i2},t)}\right)\frac{1}{k_m(x_{i2},t)} \qquad (25)$$
$$\frac{H_1(s)}{W_1(s)}\left[\frac{k_d(x_{i2},t)}{k_m(x_{i2},t)}-(c_1+1)\right]v_m(x_{i2},t)+c_1\frac{H_1(s)}{W_1(s)}v_d \le \dot{V}_m(x_{i1},t)$$
$$\le \frac{H_1(s)}{W_1(s)}\left[\frac{k_d(x_{i2},t)}{k_m(x_{i2},t)}-(c_2+1)\right]v_m(x_{i2},t)+c_2\frac{H_1(s)}{W_1(s)}v_d \qquad (26)$$

The stability properties of the control law (25) and (26) are given by theorem 4.1.

5 Controllability Issues

In the previous section we have assumed the desired density profile to be completely arbitrary. It is worthwhile to note that few restrictions, however, exist. These restrictions are imposed by the control objectives microscopic controllers have to follow. These control

objectives are outlined by the concept of the particular vehicle following scenario. For example if the vehicles are traveling in platoons with the fixed distance headway policy, then the vehicle following controllers will maintain that constant distance despite any variations in speed command. This constant inter-vehicle distance corresponds to a uniform density for the span of the platoon.

Hence due to these spatial restrictions imposed by the microscopic controllers, system is not controllable in strict sense, i.e., there exist trajectories in the state space $[v_d(x,t), k_d(x,t)]^\top$ which cannot be reached by the control input $V_m(x,t)$ given in (25) and (26). However, this loss of controllability can be avoided by restricting the desired density to be within a subset of the whole permissible space. This subset is a function of the characteristics of the microscopic controllers being used. For the roadway controller to have the tracking properties outlined in theorem 4.1, it is required that the desired density profile be appropriately modified through a pseudo-filter. This pre-filtering process ensures that the desired density provided to the roadway controller is compatible with the concept of automatic vehicle following being used. For example for platooning environment, the required modification is:

$$k_d^*(x,t) = \begin{cases} k_d(x_{i1},t) & \text{if } x \in S_i \\ k_d(x,t) & \text{else,} \end{cases} \tag{27}$$

where k_d^* is the density actually provided to the roadway controller, S_i is the span of the platoon i within a section. Similarly if the time headway policy is being used then the desired density and speed has to satisfy the following relation:

$$k_d^*(x,t) = \frac{1}{hv_d(x,t) + l}. \tag{28}$$

Hence for this study we assume that the desired density $k_d(x,t)$ is appropriately adjusted through a pre-filter which guarantees that all of the spatial restrictions are satisfied, i.e., the system is controllable. The design of such a filter is possible due to the knowledge of deterministic microscopic dynamics. Hence the properties outlined by theorem 4.1 hold for the modified desired trajectory $\{v_d, k_d^*\}$.

6 Simulation Results

In this section we will simulate the controller designed in section 4. The complete roadway/vehicle closed loop system simulated here can be used to measure the performance of the designed controller.

For simplicity we have assumed a single lane circular highway shown in Figure 1. The highway is subdivided into five sections, $M = 5$, each with a length of 500 meters. The vehicles are assumed to be traveling in platoons of uniform size, $n_i = 5$, under time headway

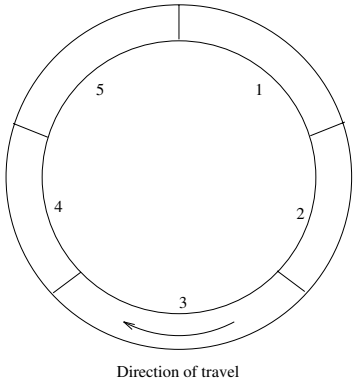

Figure 1: A single lane circular highway used for simulation.

policy with a constant time headway of 0.5 seconds. It is assumed that some incident has occurred in section 3 of the highway, giving rise to the initial density distribution shown in Figure 2. It is further assumed that the desired intention of the network layer is to clear the impact of this incident without causing significant slowing down of the vehicles upstream the incident.

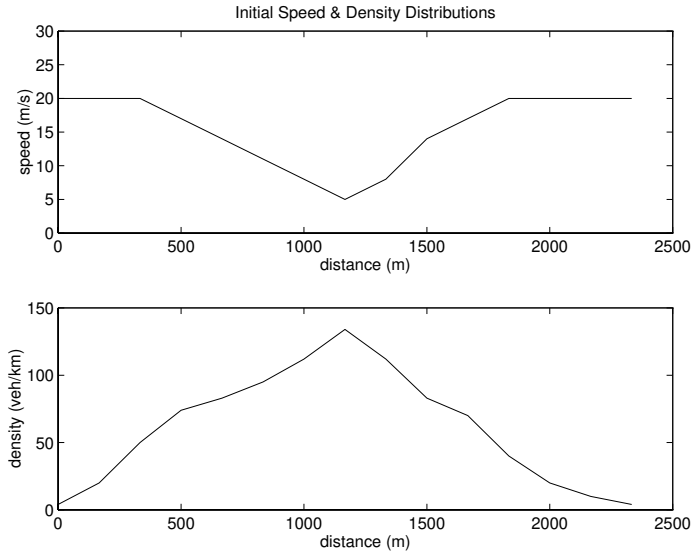

Figure 2: Initial speed and density distribution resulting due to incident in section 3 of the highway.

For this purpose we have assumed the desired profile to be stationary with the desired values $v_d = 20\ m/s$ and $k_d = 67\ veh/km$. The choice of the filters $W_1(s) = \frac{2}{s+2}$ and $H_1(s) = \frac{0.5}{s+0.5}$ results in the control input and states of the system shown in Figures 3-

5. The simulation results in Figures 3-5 are supportive of the claims given in theorem 4.1. Hence the roadway controller designed in this paper can be used to meet the control objectives outlined in section 3.

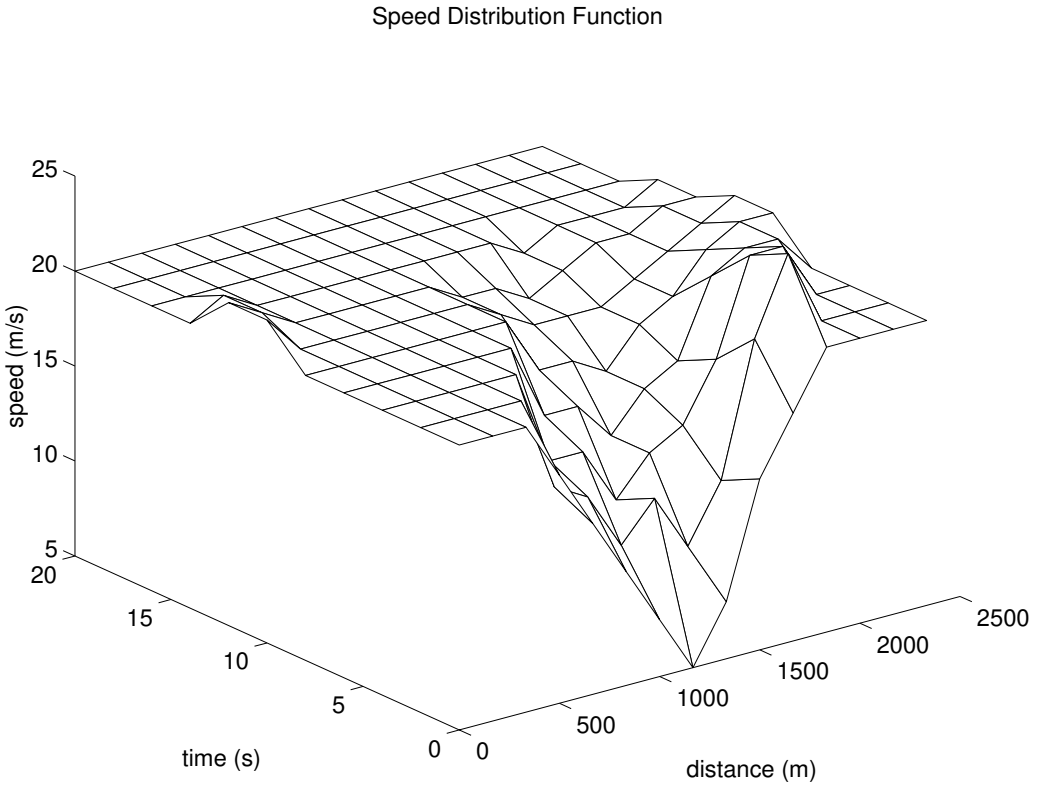

Figure 3: Speed distribution function of the closed loop system.

7 Conclusion

In this paper we have developed a spatio-temporal control technique based on feedback linearization. This technique is used to design a roadway controller with objectives as defined in section 3. We have derived the control input for two different cases of flow conditions. The designed controller in each case guarantees closed loop stability and performance. Finally, we have proposed that the desired density, provided by the network controller, has to be appropriately adjusted before it can be used by the roadway controller.

References

[1] H. Raza, P. Ioannou, "Macroscopic Traffic Flow Modeling of Automated Highway Systems" *Proc. of The 5th IEEE Mediterranean Conference on Control and Systems*, July

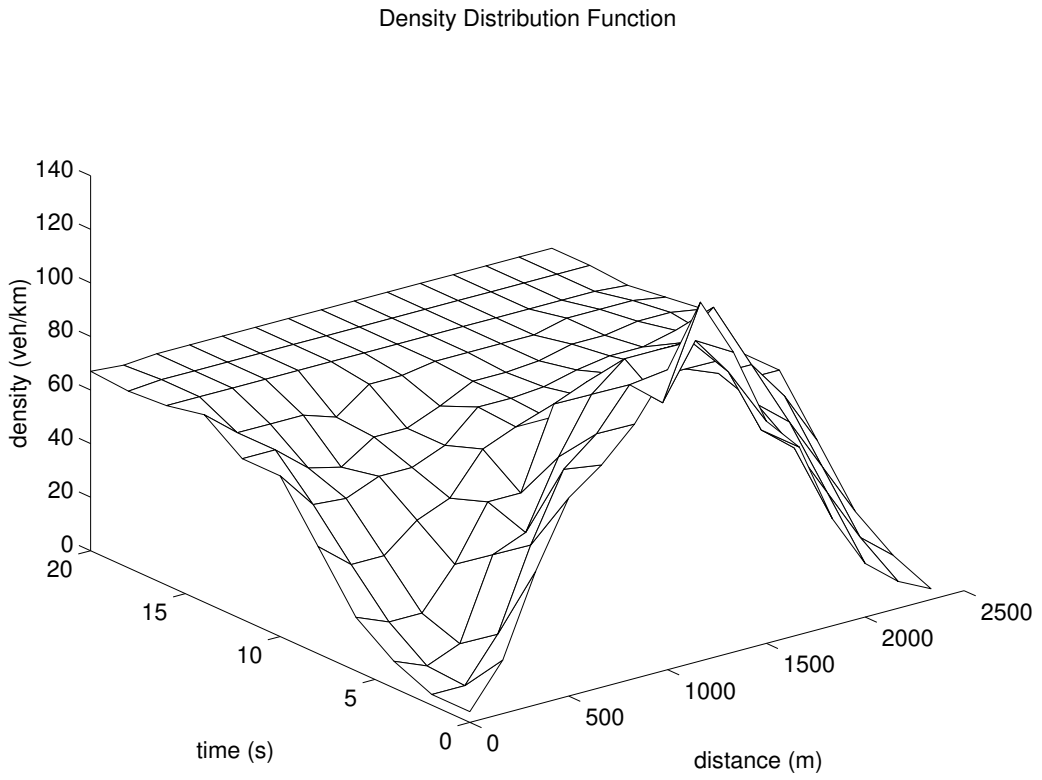

Figure 4: Density distribution function of the closed loop system.

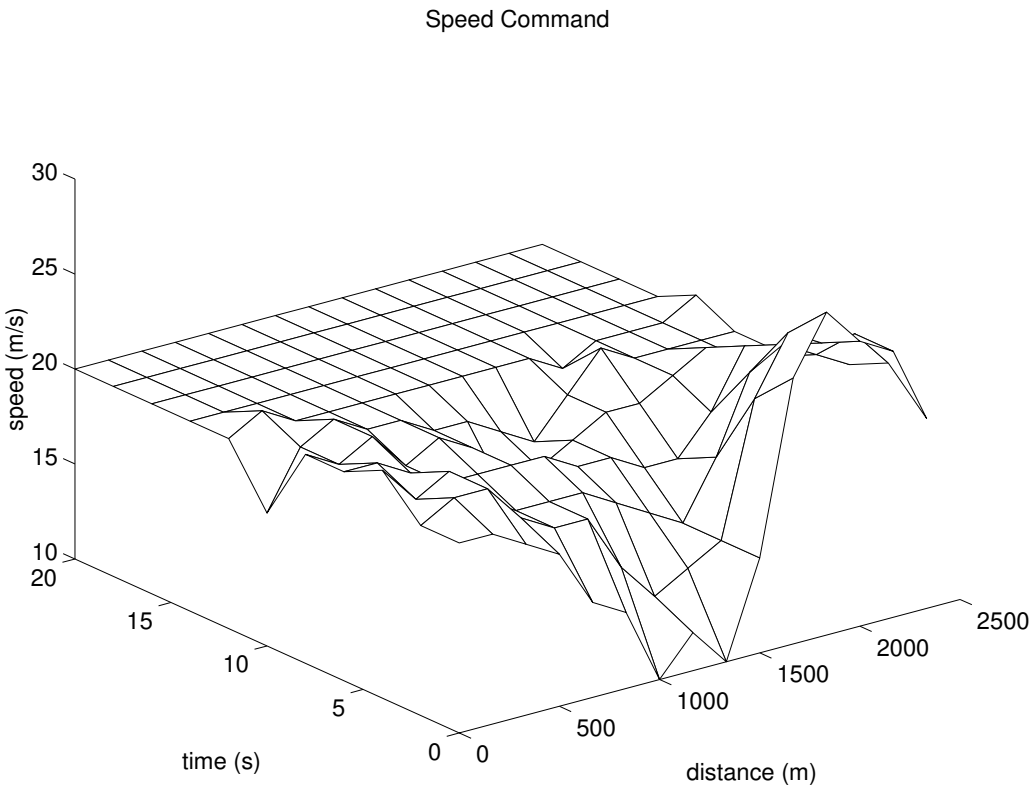

Figure 5: Speed command issued by the roadway controller.

1997.

[2] P. Varaiya, "Smart Cars on Smart Roads: Problems of Control", *IEEE Transactions on Automatic Control*, vol. 38, no. 2, pp. 195-207, Feb. 1993.

[3] J. E. Slotine, W. Li, *Applied Nonlinear Control*, Prentice Hall, Englewood Cliffs, NJ, 1991.